Do virus-encoded suppressors of RNA silencing reduce plant eIF2α kinase activity and thereby increase susceptibility to infection?

Kate Olliver

A thesis submitted to
Auckland University of Technology
In partial fulfilment of the requirements for the degree of Master of Applied Science (MAppSc)

2014

School of Applied Science

Supervisors: Dr. Colleen Higgins and Dr. Robin MacDiarmid

Abstract

Plant cells inhibit viral infection using a process which targets double stranded RNA (dsRNA), a necessary intermediate in viral infection. This process is known as RNA silencing. Many plant viruses, and some animal viruses, encode a suppressor of RNA silencing (a VSR) which interferes with this process, thereby allowing infection to occur. In animals, cells also protect themselves against viral infection by shutdown of protein production in the invaded host cell. The production of viral dsRNA in vertebrate cells activates Protein Kinase R (PKR), which phosphorylates the alpha subunit of eukaryotic translation initiation factor 2 (eIF2α). Phosphorylation of eIF2α interferes with protein production by the host cell, and consequently viral replication.

It has been found that certain vertebrate-infecting viruses encode inhibitors of PKR activity which function in a number of ways, one of which is the activation of Inhibitor of Protein Kinase R (IPK), a host-encoded inhibitor of PKR. By inhibiting the ability of PKR to phosphorylate eIF2α, virus replication can proceed. Recently, some inhibitors of PKR were also shown to be VSRs. It is unknown if VSRs encoded by plant viruses can also affect phosphorylation of eIF2α.

This research had two aims; firstly to determine whether or not eIF2α phosphorylation is triggered upon infection of *Arabidopsis thaliana* with the viruses *Turnip vein clearing virus* (TVCV) and *Turnip yellow mosaic virus* (TYMV), and if IPK activity alters this potential kinase activity. To determine this, wild-type *A. thaliana* and *A. thaliana* mutants lacking a functional IPK gene were infected with TVCV and TYMV and sampled over a time period of two weeks. Total plant protein was extracted from the sampled tissue and phosphorylated eIF2α detected via western blot. No eIF2α phosphorylation was seen in wild-type or mutant *A. thaliana* upon infection with either TVCV or TYMV.

Secondly, to determine whether or not plant VSRs can also inhibit eIF2α phosphorylation by suppressing the function of plant eIF2α kinases. VSRs were transiently expressed in *Nicotiana benthamiana* plants, eIF2α phosphorylation by the eIF2α kinase GCN2 (general control nonrepressible 2) was triggered by amino acid starvation, and the quantity of phosphorylated eIF2α present measured via western blot to determine whether or not VSRs directly inhibit eIF2α kinase activity. No decrease in eIF2α phosphorylation levels was seen in plant tissue expressing any of the VSRs used, although expression of the p19 gene from *Tomato bushy stunt virus* (TBSV) appeared to cause an increase in eIF2α phosphorylation upon amino acid starvation.

From this, it was concluded that neither infection with the viruses TVCV or TYMV or expression of the VSRs used in this study altered eIF2α kinase activity, with the exception of the VSR p19 from TBSV, which when expressed in *N. benthamiana* appears to increase eIF2α phosphorylation upon glyphosate treatment of the plant. The fact that no other VSR caused an increase in eIF2α phosphorylation upon glyphosate treatment suggests that the effect of p19 on eIF2α phosphorylation is not due to its ability to function as a VSR, and plant viruses have not developed a mechanism of inhibiting the phosphorylation of eIF2α. The lack of phosphorylation of eIF2α in *A. thaliana* upon infection with the viruses TVCV and TYMV suggests that eIF2α phosphorylation is not an antiviral mechanism utilised in plants, although further research in this area is required to determine if this is representative of all *A. thaliana* ecotypes.

Table of Contents

List of Figures

List of Tables

List of Abbreviations

Attestation of Authorship

Acknowledgements

Chapter 1: An Introduction to Virus-Host Interactions 20

1.1. Viruses are reliant on host systems to replicate 21

1.1.1. Viruses are obligate intracellular parasites 21

1.1.2. Viruses have a range of different replication methods 22

1.2. Eukaryotic cells have a variety of mechanisms to inhibit viral infection 25

1.2.1. RNA interference is an antiviral defence mechanism which viruses have evolved to counter 26

1.2.1.1. RNAi is common to all eukaryotic life 27

1.2.1.2. RNAi is necessary for the development and maintenance of life 28

1.2.1.3. RNAi recognises dsRNA and establishes a sequence-specific mRNA degradation or translation inhibition pathway 28

1.2.1.4. Viruses code for inhibitors of RNAi 32

1.2.2. eIF2α kinases are part of an antiviral defence which viruses have evolved to counter 35

1.2.2.1. eIF2α kinases are triggered by stresses on the host eukaryotic organism and mitigate adverse effects 35

1.2.2.2. eIF2α kinases are part of an antiviral defence mechanism 38

1.2.2.3. IPK is an inhibitor of an unknown eIF2α kinase in plants 39

1.2.2.4. Viruses have evolved ways of inhibiting eIF2α phosphorylation 40

1.3. Some viral suppressors of RNA silencing also inhibit eIF2α phosphorylation 44

1.4. Research questions and aims of this research 46

1.4.1. Aim 1: To determine if eIF2α kinase activity is altered in plants upon virus infection 46

1.4.2. Aim 2: To determine if VSRs affect eIF2α kinases independently of viral infection 47

Chapter 2: Is eIF2α kinase activity altered in plants upon virus infection? Methods and Materials 48

2.1. Plants 49

2.2. Viral infection 49

2.2.1. Inoculation 49

2.2.2. Sampling of inoculated leaves for protein extraction 51

2.2.3. Confirmation of viral infection via Agdia Immunostrip® 51

2.2.4. Detection of TVCV infection via ELISA 52

2.2.5. Detection of CaMV and CMV via two-step RT-PCR 54

2.2.5.1. Total RNA extraction 54

2.2.5.2. Two-step RT-PCR for detection of viral RNA 56

2.2.5.3. Agarose gel electrophoresis 57

2.3. Extraction of total plant protein 58

2.4. Concentration of plant protein via precipitation 58

2.5. Quantification of total plant protein 59

2.5.1. Bradford Assay 59

2.5.2. Qubit ® fluorometric quantitation 60

2.6. Western blot 61

2.6.1. Gel electrophoresis 61

2.6.2. Transfer 61
2.6.3. Antibody incubation using the phosphorylated eIF2α specific primary antibody 62
2.6.4. Antibody incubation using the generic eIF2α primary antibody 63
2.6.5. Exposure of western membranes 63
2.6.6. Removing antibodies from *post-exposure* membranes 64
2.7. Coomassie blue staining of SDS-PAGE gels 64
2.8. Quantification of eIF2α in positive control 64
2.8.1. Phosphorylation and serial dilution of eIF2α 64
2.8.2. Creation of eIF2α positive control 65
Chapter 3: Is eIF2α kinase activity altered in plants upon virus infection? Results 66
3.1. Virus inoculation 67
3.2. Evaluation of protein extraction methods 69
3.2.1. Protein extraction method A 69
3.2.2. Protein extraction method B 73
3.3. Optimisation of primary antibodies 75
3.3.1. Phosphorylated eIF2α specific antibody 76
3.3.2. Generic eIF2α antibody 78
3.4. Quantification of phosphorylated eIF2α present in extracted *A. thaliana* protein for use as a positive control 84
3.5. Detection of phosphorylated eIF2α in time-point sampled TVCV and TYMV inoculated *A. Thaliana* 94
3.5.1. Inoculation and confirmation of infection of *A. thaliana* with the virus TVCV 94

3.5.2. Quantification of phosphorylated eIF2α present in TVCV infected *A. thaliana* tissue 95
3.5.3. Inoculation and confirmation of infection of *A. thaliana* with the virus TYMV 97
3.5.4. Quantification of phosphorylated eIF2α present in TYMV infected *A. thaliana* tissue 98
3.6. Summary of results **100**
3.7. Discussion of results **100**
3.7.1. Quantification of phosphorylated eIF2α in positive control *A. thaliana* protein 100
3.7.2. Detection of Tobamovirus infection in mock-inoculated *A. thaliana* 102

Chapter 4: Can VSRs affect eIF2α kinases outside of viral infection? Methods and Materials **104**

4.1. Plants **105**
4.2. Glyphosate treatment methods **105**
4.3. Transformation of *A. tumefaciens* **106**
4.3.1. Growth and maintenance of *A. tumefaciens* 106
4.3.2. Plasmids 106
4.3.2.1. Transformation of *Escherichia coli* 108
4.3.2.2. Plasmid extraction 108
4.3.2.3. Confirmation of plasmid insert via sequencing 109
4.3.2.4. Confirmation of plasmid insert via enzymatic digestion of plasmid 111
4.3.3. Transformation of *A. tumefaciens* 111

4.3.4. Primer design 112
4.3.5. Confirmation of successful transformation via colony PCR 112
4.4. Infiltration of *N. benthamiana* **114**
4.4.1. Preparation of *A. tumefaciens* 114
4.4.2. Infiltration of *N. benthamiana* 115
4.5. Confirmation of expression of gene of interest **116**
4.6. Protein extraction **118**
4.7. Quantification of phosphorylated eIF2α in infiltrated *N. benthamiana* **118**

Chapter 5: Can VSRs affect eIF2α kinases outside of viral infection? Results **119**
5.1. Induction of eIF2α phosphorylation in *N. benthamiana* **120**
5.2. Confirmation of the presence of plasmid inserts via sequencing **122**
5.2.1. Detection of the gene 2b in plasmid 2b207 125
5.2.2. Detection of the gene p6 in the plasmid p6p100 126
5.3. Confirmation of successful transformation of bacteria **127**
5.4. Infiltration of *N. benthamiana* in order to determine if VSR expression alters eIF2α kinase ability **129**
5.5. Detection of VSR mRNA in *N. benthamiana* **129**
5.5.1. Detection of VSR mRNA by RT-PCR 130
5.6. Detection of phosphorylated eIF2α in VSR expressing *N. benthamiana* **135**
5.7. Summary of results **141**
5.8. Discussion of results **143**
5.8.1. Variation in the amount of phosphorylated eIF2α detected in agroinfiltrated *N. benthamiana* 143
5.8.2. Expression of VSRs and IPK in agroinfiltrated *N. benthamiana* 144

5.8.3. Increased phosphorylation of eIF2α upon glyphosate treatment of p19 expressing *N. benthamiana* 144

Chapter 6: Discussion 147

6.1. Viruses and VSRs used in this research 148

6.2. Lack of phosphorylation of eIF2α upon infection or wounding of *A. thaliana* or *N. benthamiana* 149

6.3. Do virus-encoded suppressors of RNA silencing reduce plant eIF2α kinase activity and thereby increase susceptibility to infection? 152

List of Figures:

Chapter 1:

Figure 1.1: Methods of viral genome replication. Red indicates RNA and blue indicates DNA. A) dsDNA viruses such as *Cauliflower mosaic virus* replicate their genome by first passing through a positive ssRNA intermediate which often forms tertiary structures of dsRNA. The dsDNA is unwound and viral genes are transcribed (ii, iii), some of which are translated by host proteins (iv). The RNA is then transcribed to DNA by the virally encoded protein reverse transcriptase (RT) (v), and the second DNA strand synthesised by host proteins (vi). B) ssDNA viruses such as *Turnip curly top virus* contain a single strand of DNA (i), the complementary strand of which is synthesised by host proteins (ii, iii). The virally-encoded coat protein is transcribed (iv) and translated (v) by host proteins. The coat protein then unwinds the dsDNA (vi), and both strands act as templates for further DNA synthesis. C) In order to replicate, the two strands comprising the genome of dsRNA viruses (i) such as *Rice dwarf virus* are separated within the host (ii). One strand is translated (iii) to viral proteins including the enzyme RNA dependant RNA polymerase (RDRP) (iv), and the other serves as a template for synthesis of the complementary RNA strand by RDRP (v). D) Negative ssRNA viruses such as *Tomato spotted wilt virus* (i) cannot immediately be translated into proteins, and so contain a virus-encoded RDRP within the virion, which upon infection immediately starts transcription of the positive strand of RNA using the negative strand as a template (ii). The newly synthesised positive strand of RNA (iii) contains genes which are able to be translated, and also serves as a template for the synthesis of new negative strand RNA (iv). E) Positive ssRNA viruses such as *Tobacco mosaic virus* and *Cucumber mosaic virus* (i) can be immediately translated (ii) into proteins, including RDRP (iii). The positive RNA strand is then used as a template for synthesis of a negative RNA strand by RDRP (iv); the newly synthesised dsRNA (v) is split and the negative strand used as a template for multiple copies of a positive sense strand (vi). F) Viruses such as *Tomato spotted wilt virus* may contain one or multiple strands of ambisense RNA (i), each of which may be read in either direction in order to produce different proteins. Ambi-sense RNA virions also contain an RDRP (ii), which upon infection of a host cell synthesises dsRNA (iii) from whatever original RNA was present in the virion. Either or both of the RNA strands produced can be incorporated into the new virion. 23

Figure 1.2: In *A. thaliana,* viral or host dsRNA is cleaved into 21-26 nucleotide long fragments by DCL proteins 1-4. A single strand of the 21-26 nucleotide long ssRNA is incorporated into 31

the AGO protein, creating the RISC complex. RISC binds to and cleaves ssRNA complementary to the incorporated RNA fragment. Both viral and host RNA is degraded in this manner, although most viruses encode at least one method of suppressing the RNA silencing pathway.
Figure 1.3: In order for eIF2α to be phosphorylated in response to viral infection, first PKR be present in sufficient quantity in the cell, then be activated by dsRNA, dimerise and finally phosphorylate eIF2α. Viruses can encode products which interfere with this pathway at a variety of points, as illustrated in Table 1.2 (Gale Jr and Katze, 1998) 41

Chapter 3:

Figure 3.1: Comparison of glyphosate treated and untreated *A. thaliana* and *N. benthamiana* protein samples harvested on two dates. (A) Ponceau S stained image of total protein and (B) Chemiluminescent exposure of phosphorylated eIF2α proteins following detection using a phosphorylated eIF2α-specific antibody. Size of proteins (kDa) is indicated by the Bio-Rad Precision Plus All Blue Protein™ marker in lane 1. Lanes 2-9 contain total protein from plants treated and harvested as described above each lane. Lane 10 contains 2.6 µg of bacterially expressed in vitro phosphorylated eIF2α protein. 71
Figure 3.2: Protein concentrations of the *A. thaliana* protein samples shown in Figure 3.1 as measured via Qubit® and Bradford assays. The protein concentration of each sample was measured three times via Qubit® and Bradford assay and the average of the three readings is shown. 72
Figure 3.3: Comparison of protein extraction methods A and B. Panel A illustrates the increased thickness and intensity of protein bands on a Ponceau S stained membrane when protein is extracted using extraction method B (Lanes 2-5) than with protein extraction method A (Lanes 6-9). This is further illustrated by the increased detection of bands containing phosphorylated eIF2α at 37kDa on the exposure of the same membrane (Figure 3.3, panel B).The sample in the far right lane was protein extracted from glyphosate treated *A. thaliana* and provided by the New Zealand Institute of Plant and Food Research. Lane 1 contains 15 µl of Bio-Rad Precision Plus All Blue Protein™ marker, all other lanes contain 8µg of total *A. thaliana* protein. 74
Figure 3.4: The effect of phosphorylated eIF2α specific primary antibody concentration on signal detection. BEx is a contraction of phosphorylated bacterially expressed *A. thaliana* eIF2α. All *A. thaliana* samples were from the same protein extraction of glyphosate treated *A. thaliana* to eliminate variation between samples. Phosphorylated eIF2α is detected at 37 kDa in lanes 1 and 5, and at approximately 28 kDa in lanes 3 and 4. All other bands are due to non-specific binding of the primary antibody. All lanes were exposed for the same time. 77
Figure 3.5: Exposure of membranes containing bacterially expressed in vitro phosphorylated eIF2α and protein extracted from glyphosate treated *A. thaliana*. The membranes were incubated with varying dilutions of generic eIF2α primary antibody. BEx is a contraction of bacterially expressed eIF2α. As in Figure 3.4, the protein in lanes 2-4, 6-8 and 10-12 are from the extraction of a single sample of glyphosate treated A. thaliana, and phosphorylated eIF2α is detected at 37 kDa in lanes 1, 5 and 9, and at 28 kDa in lanes2- 4 and 10-12. Other bands are also visible which do not correspond with any known sizes of eIF2α, indicating binding of an antibody to nonspecific proteins. 79
Figure 3.6: Exposure of membrane treated with the generic eIF2α antibody. No eIF2α is visible at 37 kDa, despite the fact that this membrane has previously been shown to contain phosphorylated eIF2α in all samples which were both extracted using Method A and treated with glyphosate. Phosphorylated eIF2α had also previously been shown to be present in the 81

supplied *A. thaliana* protein sample in lane 9. Lane M contains 15 µl of Bio-Rad Precision Plus All Blue Protein™ marker, all other lanes contain 8µg of *A. thaliana* protein
Figure 3.7: A comparison of the effect of increase protein concentration on the detection of eIF2α in a membrane containing high concentrations of *A. thaliana* protein. The membrane was treated with generic (panel B) and phosphorylated specific (panel C) eIF2α antibodies in order to determine if the generic eIF2α antibody was detecting eIF2α at the same size at the phosphorylated-specific eIF2α antibody. Lane M contains 15 µl of Bio-Rad Precision Plus All Blue Protein™ marker. Lanes 1 and 3 contain 20 µg of protein from glyphosate treated (Lane 1) and untreated (Lane 3) *A. thaliana*, and Lanes 2 and 4 contain 50µg of precipitated protein from glyphosate treated (Lane 2) and untreated (Lane 4) *A. thaliana*. A) Ponceau S stain of a post-transfer membrane containing 20 and 50µg of protein from glyphosate treated and control *A. thaliana* plants. B) Exposure of the membrane in 7A after treatment with generic eIF2α antibody. C) Exposure of the membrane in panels A and B after the generic eIF2α antibody was removed and the membrane treated with the phosphorylated eIF2α specific antibody. 82
Figure 3.8: Ponceau S stain (A) and exposure of (B) a membrane comparing the amount of phosphorylated eIF2α present in protein extracted from glyphosate treated *A. thaliana* (Lanes 1-5) to serially diluted bacterially expressed in vitro phosphorylated eIF2α (BEx, lanes 6-14). The lane containing 7500ng of A. *thaliana* protein was inaccurately loaded, and is not a valid representation of 7500 ng of protein. Areas of red within band in panel B indicate overexposure of the membrane. Rubisco is visible at 50 kDa, and eIF2α at 37 kDa, as indicated by arrows on the left and right hand sides, respectively. Lane M contains 15µL of Bio-Rad Precision Plus All Blue Protein™ marker. 86
Figure 3.9: Relationship between concentration of phosphorylated eIF2α and chemiluminescence detected per band as seen in Figure 3.8 (panel B, lanes 8-12). Each datapoint is the amount of phosphorylated eIF2α present in a lane (x axis) plotted against the corresponding degree of exposure caused by that band (y axis). There is a strong linear relationship described by the equation y = 4.3695x – 14.5 between the amount of phosphorylated eIF2α present on the membrane and the amount of chemiluminescence produced between 0-20 ng eIF2α and 0-70 percent exposure, however at concentrations of higher that 20 ng phosphorylated eIF2α the relationship between the chemiluminescence produced and the amount of eIF2α present changes and the linear model deviates strongly from the observed results. 88
Figure 3.10: Relationship between concentration of phosphorylated eIF2α and amount of chemiluminescence detected in Figure 3.8, lanes 8-12. Each datapoint is log of the ng of phosphorylated eIF2α present in a lane (x axis) plotted against the corresponding degree of exposure caused by that band (y axis). The relationship describes an S curve, which only corresponds to a linear model (equation y = 79.505x - 39.239) at concentrations of phosphorylated eIF2α greater than 18.98 ng. 91
Figure 3.11: Western detection of phosphorylated eIF2α in wild-type (wt) and deficient (ΔIPK) *A. thaliana* either inoculated with TVCV or buffer (mock). Leaf samples were collected at 0 dpi, 3 and 9 hpi, and 1, 2, 3 and 7 dpi. 96
Figure 3.12: Detection of eIF2a phosphorylation in wild-type (wt) and ΔIPK mutant *A. thaliana* either inoculated with TYMV or buffer (mock) by western blot using a phosphorylated eIF2α specific antibody. Leaf samples were collected at 0 dpi, 3, 6 and 9 hpi, and 3, 5 and 7 dpi. 99

Chapter 5:

Figure 5.1: Western blot detection of phosphorylated eIF2α. Each lane contains 10 µg of total protein extracted from *N. benthamiana* leaves sprayed with varying concentrations of glyphosate. Three leaves, each taken from a different plant 24 hours after glyphosate treatment, were tested. Increasing glyphosate concentration does not appear to increase the amount or reliability of phosphorylated eIF2α present within the leaf tissue. 121

Figure 5.2: Detection of phosphorylated eIF2α in plant tissue by western blot. All lanes contain 10 µg of protein. Lane 1 contains positive control glyphosate sprayed *A. thaliana*. Lanes 2 – 10 show phosphorylation in *N. benthamiana infiltrated* with 150 µM glyphosate (lanes 2 and 3); sprayed with 150 µM glyphosate (lanes 4-7) and immersed in 150 µM glyphosate for one minute (lanes 8-10). All samples were collected 24 hours after treatment. Topical application of glyphosate produces weak and intermittent phosphorylation of eIF2α, whereas infiltration of glyphosate into the air gap within the leaf produces weak but consistent phosphorylation of eIF2α. 121

Figure 5.3: Western blot detection of phosphorylated eIF2α present in protein extracted from the tissue of emerging (leaf 1, unfolding (leaf 2) and expanded (leaf 3) leaves) from three individual plants, all of which were treated with 300 µM glyphosate. 122

Figure 5.4: PCR amplification of plasmid DNA using the 277F and 277R primers. Lane M: 1 Kb Plus DNA Ladder. Templates used were as follows: No template control (lane 1), empty pGD plasmid (lane 2), stock 2b207 plasmid (lane 3), sequenced 2b241 plasmid (lane 4) and *E. coli* transformed with stock 2b207 (lane 5). 125

Figure 5.5: Digestion of the plasmid p6p100 with *HindIII*. Two bands are visible, one at 2300 bp (lane 1), and one at greater than 12000 bp (lane 2). Lane M contain 1 Kb Plus DNA Ladder. Lane 1 contains an H2O control containing only ddH2O and *HindIII*. Lane 2 contains 300 ng of digested p6p100. 127

Figure 5.6: PCR products resulting from the amplification of transformed A. tumefaciens colonies. Lane M contain 1 Kb Plus DNA Ladder. Lane 1 contains no template. Lane 2 contains plasmid DNA amplified with the primer pairs 277F and 227R (Panels A, B, C and E) or 277F and NOS R (Panels D and F).Lanes 3, 4 and 5 contain transformed *A. tumefaciens* colonies amplified using the primer pairs 277F and 227R (Panels A, B, C and E) or 277F and NOS R (Panels D and F). Only the areas of each gel containing bands are shown. 128

Figure 5.7: RT-PCR products amplified from RNA extracted from *N. benthamiana* tissue infiltrated with wild-type or 2b241 transformed A. tumefaciens. Lane M contains 1 Kb Plus DNA Ladder. Lane 1 contains no template DNA. Lanes 2 and 3 contain RNA extracted from *N. benthamiana* infiltrated with wild-type A. *tumefaciens* and amplified using the NAD5 and CMV241-2b primer pairs respectively. Lanes 4 and 5 contain RNA extracted from *N. benthamiana* imfiltrated with 2b241 and amplified using the NAD5 and CMV241-2b primer pairs respectively. Lane 6 contains 2b241 plasmid DNA amplified using the CMV241-2b primer pair. 131

Figure 5.8: RT-PCR products amplified from RNA extracted from *N. benthamiana* tissue infiltrated with wild-type or 2b241 transformed *A. tumefaciens*. Lane M contains 1 Kb Plus DNA Ladder. Lane 1 contains no template with the NAD5 primers. Lane 2 contains p19wt plasmid DNA amplified with the p19 primer pair. Lanes 3 and 4 contain RNA extracted from *N. benthamiana* agroinfiltrated with p19wt and amplified using the p19 and NAD5 primer pairs respectively. Lane 6 contains the products of the amplification using the NAD5 primer pair on RNA from N. benthamiana infiltrated with wild-type A. tumefaciens. 132

Figure 5.9: PCR products resulting from the amplification of the plasmid HC-ProPVY (lane 2) and DNA extracted from *A. tumefaciens* transformed with the plasmid HC-ProPVY (lane 3) using the primer pair HC-ProGlias F and HC-ProGlias R. Lane M contains 1 Kb Plus DNA Ladder. Lane 1 contains no template. No bands are visible in either lane at the expected size of 1.8 kb. No bands of the same size are visible in either lane 2 or lane 3. 134
Figure 5.10: RT-PCR products amplified from RNA extracted from *N. benthamiana* tissue argoinfiltrated with HC-ProPVY or wild-type *A. tumefaciens*. Lane M contains 1 Kb Plus DNA Ladder. Lane 1 contains no template. Lanes 2 and 3 contain RNA extracted from wild-type *A. tumefaciens* infiltrated *N. benthamiana* amplified using the NAD5 and HC-ProOlliver1 primers respectively. Lanes 4 and 5 contain RNA extracted from N. *benthamiana agroinfiltrated* with HC-ProPVY and amplified using the NAD5 and HC-ProOlliver1 primer pairs respectively. Lane 6 contains the PCR product of the HC-ProPVY plasmid amplified with the HC-ProOlliver1 primer pair. 134
Figure 5.11: Detection of phosphorylated eIF2α in VSR and/or IPK expressing *N. benthamiana* tissue by western blot using a phosphorylated eIF2α specific antibody. All positive control lanes (At+) contain aliquots of the same positive control. Differences in the size and darkness of sample bands relative to the positive control is due to a difference in the amount of phosphorylated eIF2α present between the positive control and the sample. Detection of chemiluminescence was achieved using the BioRad ChemiDoc MP™ System and ImageLab™ Software. 136
Figure 5.12: A comparison of the average amount of phosphorylated eIF2α present per µg of total plant protein in glyphosate treated *N. benthamiana* expressing a VSR or a VSR+IPK. Error bars show the standard error of each sample group. 139

List of Tables:

Chapter 1:

Table 1.1: Examples of VSRs, the methods of action employed to suppress RNA silencing by viruses and the variety of hosts infected by VSR-encoding viruses. 34
Table 1.2: Virus encoded inhibitors of eIF2α kinases, the method of action, virus, host range and name of the inhibitor. 42
Table 1.3: The three viruses known to encode a protein which functions as both an inhibitor of PKR and a VSR, the method of RNAi suppression, and the method by which eIF2α phosphorylation is inhibited. 45

Chapter 2:

Table 2.1: Viruses used for A. thaliana inoculation in this experiment and their descriptors, hosts, symptoms, method of identification and VSR. 50
Table 2.2: Primers used to confirm presence of the infecting virus and the control gene NAD5. 57

Chapter 3:

Table 3.1: Symptom and infection rate in virus infected *A. thaliana* at 28dpi. 68

Chapter 4:

Table 4.1: Plasmids used for transformation of *A. tumefaciens* and subsequent agroinfiltration of *N. benthamiana*. 107
Table 4.2: Primers used for confirmation of successful transformation of *A. tumefaciens* and *E.coli* via PCR, including sequence, primer target and amplicon size. All primers anneal at 55ºC. 113
Table 4.3: Primers used for confirmation of expression of the gene of interest in infiltrated *N. benthamiana* tissue, including sequence, primer target, annealing temperature and amplicon size. 117

Chapter 5:

Table 5.1 Megablast results of trimmed sequences from plasmids extracted from transformed *E.coli.* 124
Table 5.2: The amount of phosphorylated eIF2α present in protein extracted from glyphosate treated *N. benthamiana* tissue expressing a variety of VSRs and/or IPK. Quantification of eIF2α was done by comparison to a control sample with a known concentration of phosphorylated eIF2α. 140

List of Abbreviations:

aa	amino acid
AGO	Argonaute
ARC1	acyl RNA complex 1
At	Arabidopsis thaliana
ATP	adenosine triphosphate
BEx	bacterially expressed
BLASTn	basic local alignment search tool
bp	base pairs
BSA	bovine serum albumin
CaMV	Cauliflower mosaic virus
cDNA	copy DNA
CMV	Cucumber mosaic virus
Col-0	Columbia-0
CYMK	cyan yellow magenta key
DCL	Dicer-like protein
ddH2O	double distilled H2O
DNA	deoxyribonucleic acid
DOC	Deoxychlorate
dpi	days post inoculation
dsDNA	double stranded DNA

dsRBM	double stranded RNA binding motif
dsRBP	double stranded RNA binding protein
dsRNA	double stranded RNA
DTT	Dithiothreitol
ECL	enhanced chemiluminescence
EDTA	ethylenediaminetetraacetic acid
eIF2	eukaryotic initiation factor 2
eIF2α	eukaryotic initiation factor 2 subunit α
eIF2β	eukaryotic initiation factor 2 subunit β
ELISA	enzyme-linked immunosorbent assay
FNY	Fast New York
GCN2	general control nonderepressible 2
GCN4	general control nonderepressible 4
GDP	guanosine diphosphate
GIMP	gnu image manipulation program
GTP	guanosine triphosphate
HC-Pro	helper component protease
HIV-1	human immunodeficiency virus 1
hpi	hours post inoculation
HRI	haem regulated eIF2α kinase
HRP	horseradish peroxidase
i.e.	id est
IFN	interferon
IgG	immunoglobulin G
IPK	inhibitor of PKR
kDa	kilodalton
LB	Luria broth
met-tRNA	methionine t-RNA
miRNA	micro RNA
MP	movement protein
mRNA	messenger RNA
NAD5	NADH dehydrogenase subunit 5
NaF	sodium fluoride
Nb	Nicotiana benthamiana
NCBI	National center for biotechnology information
NOS	nopaline synthase
nt	nucleotide
OCS	octopine synthase
OD	optical density
PAGE	poly-acrylamide gel electrophoresis
PCR	polymerase chain reaction

PERK	protein kinase RNA-like endoplasmic reticulum kinase
PKR	protein kinase R
pNPP	p-nitrophenyl phosphate
Poly I:C	polyinosinic:polycytidylic acid
PVDF	polyvinylidene fluoride
PVP	polyvinylpyrrolidone
PVX	Potato virus X
PVY	Potato virus Y
RDRP	RNA dependant RNA polymerase
RISC	RNA induced silencing complex
RLC	RNA loading complex
RNA	ribonucleic acid
RNAi	RNA interference
RT-PCR	reverse transcriptase PCR
RuBisCo	ribulose-1,5-biphosphate carboxylase oxygenase
S51	serine 51
SDS	sodium dodecyl sulfate
siRNA	small interfering RNA
ssDNA	single stranded DNA
TAE	Tris acetic acid EDTA
taq	Thermophilus aquaticus
TBS	Tris buffered saline
TBS-T	TBS-Tween
TBSV	Tomato bushy stunt virus
TCA	Trichloroacetic acid
TEMED	tetramethylethylenediamine
TMV	Tobacco mosaic virus
tRNA	transfer RNA
TSWV	Tomato spotted wilt virus
TuMV	Turnip mosaic virus
TVCV	Turnip vein clearing virus
TYMV	Turnip yellow mosaic virus
UV	ultraviolet
VSR	virus encoded suppressor of RNA silencing
wpi	weeks post inoculation
wt	wild type
ΔIPK	deleted IPK

Attestation of Authorship

I hereby declare that this submission is my own work and that, to the best of my knowledge and belief, it contains no material previously published or written by another person (except where explicitly defined in the acknowledgements), nor material which to a substantial extent has been submitted for the award of any other degree or diploma of a university or other institution of higher learning.

Kate Olliver

Acknowledgements

First and foremost, I would like to thank my supervisors Colleen Higgins and Robin Mac Diarmid for their invaluable assistance in supporting, planning, troubleshooting and documenting this research, and the Bio-Protection Research Centre for providing funding for materials and my stipend. I would also like to thank the New Zealand Institute for Plant & Food Research for the materials and conditions needed to complete this research. Special thanks to everyone in the PFR VLO team for your advice, information and supportive environment, and especially to Tracey Immanuel, Kieren Arthur, Gardette Valmont, Sonia Lilly and Samantha Edwards for your support and help throughout my research.

I'd also like to thank my family and friends who supported me throughout my masters; I could not have found the willpower to continue without all of you. Special thanks to my parents, Vik and Suz Olliver for help with troubleshooting and proofreading, my sister Tamara Olliver for lending a supportive shoulder and delicious baked goods, and my partner Ethan Kaminski, who provided significant emotional support and many late-night deliveries of hugs, food and caffeine.

Thanks also to Dylan Ryan for assistance with proof-reading, and to my cats for walking over the keyboard while I was trying to work.

Thank you to each and every one of you, I could not have done this without you.

Chapter 1

An introduction to virus-host interactions

1.1. Viruses are reliant on host systems to replicate

Viruses require the proteins and energy within host cells to replicate. The replication cycle of viruses varies depending on the type of virus, but all viruses produce double stranded RNA (dsRNA) of varying lengths at some point of their lifecycle. Long dsRNA provides a target for recognition and inhibition for the host cell.

1.1.1. Viruses are obligate intracellular parasites

Viruses are obligate intracellular parasites which infect a range of organisms covering all three domains of life (Rice et al., 2004).Viruses are one of the most basic microbes, with a genome consisting of either DNA or RNA which codes for the genes necessary for host infection and viral replication, a multi-protein capsid which protects the genome from damage while in transit between cells, and external epitopes which help in the transmission of the virus (Atreya et al., 1991, Vazquez et al., 2004). In some viruses, a lipid envelope provides further protection and helps the virus infect host cells (Gergerich and Dolja, 2006). The fully assembled viral structure is known as a virion. Viruses only contain the barest essentials necessary for viral replication; replication proteins that are needed to transcribe the viral genome, structural proteins needed to form the coat proteins, proteins which make up the capsid, and movement proteins which allow the virus to move between cells. Therefore, in order to replicate viruses must utilise the systems within a host cell.

1.1.2. Viruses have a range of different replication methods

The nucleic acid inside the protein shell varies widely between virus types, with viruses either containing either single stranded (ss) or double stranded (ds) DNA or RNA, in linear or circular form, in one or many fragments. Viruses containing ssRNA are further divided into those with positive sense RNA; which is directly translated, negative sense RNA which must first be transcribed into positive sense RNA before being translated; and ambi-sense viruses, which contain a mixture of both positive and negative sense RNAs. The type of nuclear material within a virus determines the method of replication, giving a total of six ways in which viruses replicate based on the type of genetic material they contain, all of which include or produce dsRNA as part of the replication cycle (Matthews, 1992), as shown in Figure 1.1.

Regardless of the replication method required, the newly synthesised viral genome is incorporated into the assembled viral coat proteins, which form a protective shell around the vulnerable genetic material. The new virions then exit through openings in the cell wall of the plant cell, with some species of virus forming a lipid envelope from the plant cell membrane, or are ingested with the cell contents by a feeding insect, which then transmits the virus to the next plant it feeds upon.

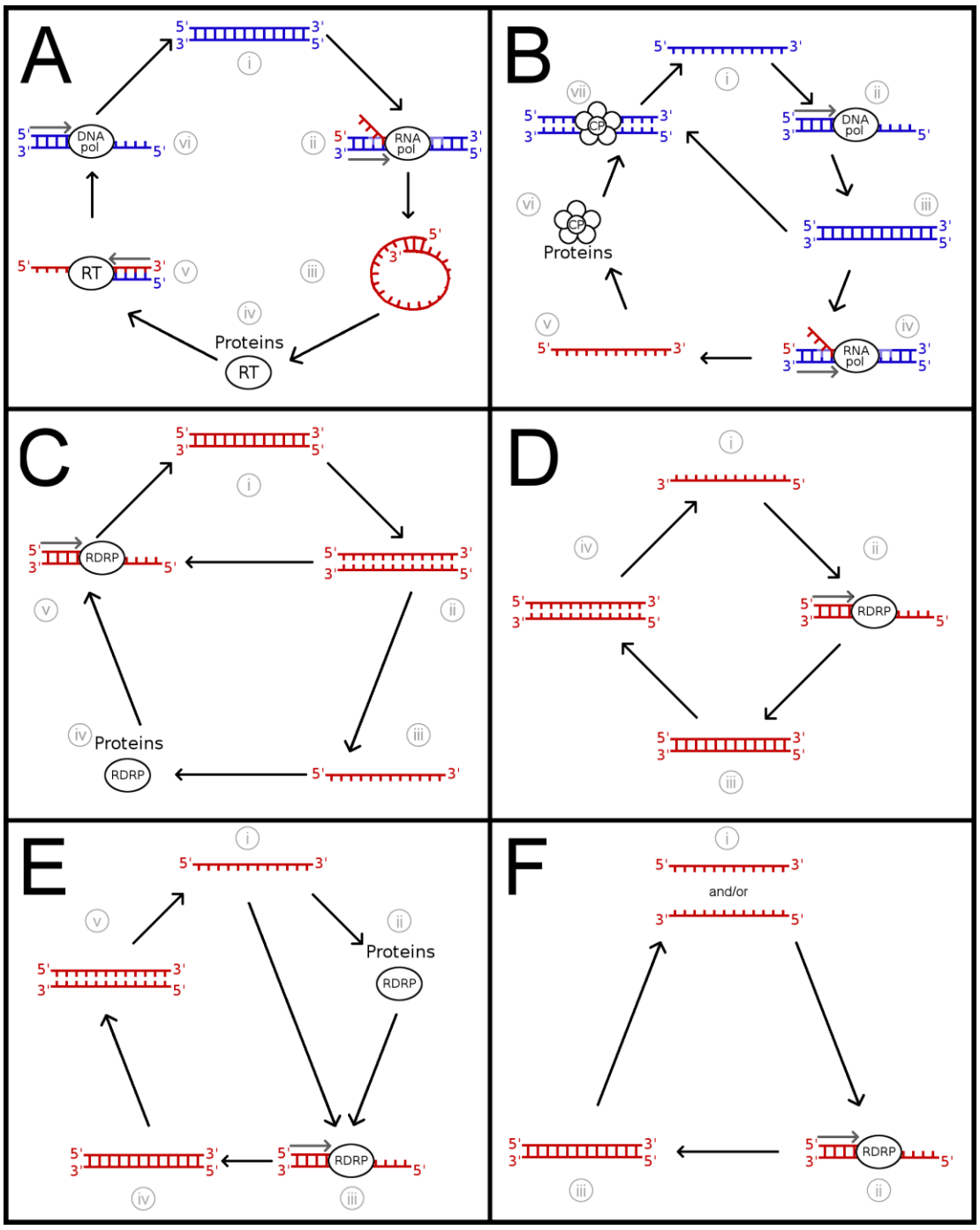

Figure 1.1: Methods of viral genome replication. Red indicates RNA and blue indicates DNA.

A) dsDNA viruses such as Cauliflower mosaic virus *replicate their genome by first passing through a positive ssRNA intermediate which often forms tertiary structures of dsRNA. The dsDNA is unwound and viral genes are transcribed (ii, iii), some of which are translated by host proteins (iv). The RNA is then transcribed to DNA by the virally encoded protein reverse transcriptase (RT) (v), and the second DNA strand synthesised by host proteins (vi). DNA viruses such as CaMV often encode RNA which form secondary, double stranded structures which are sufficient to trigger RNA silencing (Ryabova and Hohn, 2000)*

B) ssDNA viruses such as Turnip curly top virus *contain a single strand of DNA (i), the complementary strand of which is synthesised by host proteins (ii, iii). The virally-encoded coat protein is transcribed (iv) and translated (v) by host proteins. The coat protein then unwinds the dsDNA (vi), and both strands act as templates for further DNA synthesis.*

C) In order to replicate, the two strands comprising the genome of dsRNA viruses (i) such as Rice dwarf virus *are separated within the host (ii). One strand is translated (iii) to viral proteins including the enzyme RNA dependant RNA polymerase (RDRP) (iv), and the other serves as a template for synthesis of the complementary RNA strand by RDRP (v).*

D) Negative ssRNA viruses such as Tomato spotted wilt virus *(i) cannot immediately be translated into proteins, and so contain a virus-encoded RDRP within the virion, which upon infection immediately starts transcription of the positive strand of RNA using the negative strand as a template (ii). The newly synthesised positive strand of RNA (iii) contains genes which are able to be translated, and also serves as a template for the synthesis of new negative strand RNA (iv).*

E) Positive ssRNA viruses such as Tobacco mosaic virus *and* Cucumber mosaic virus *(i) can be immediately translated (ii) into proteins, including RDRP (iii). The positive RNA strand is then used as a template for synthesis of a negative RNA strand by RDRP (iv); the newly synthesised dsRNA (v) is split and the negative strand used as a template for multiple copies of a positive sense strand (vi).*

F) Viruses such as Tomato spotted wilt virus *may contain one or multiple strands of ambisense RNA (i), each of which may be read in either direction in order to produce different proteins. Ambi-sense RNA virions also contain an RDRP (ii), which upon infection of a host cell synthesises dsRNA (iii) from whatever original RNA was present in the virion. Either or both of the RNA strands produced can be incorporated into the new virion.*

1.2. Eukaryotic cells have a variety of mechanisms to inhibit viral infection

Eukaryotic cells have a number of ways of responding to viral infection (Balachandran et al., 2000, Banchereau and Steinman, 1998, Vance and Vaucheret, 2001).When a eukaryotic cell is infected with a virus it must first recognise it has been infected, and then prevent the virus from replicating. One of the proteins found to detect dsRNA in animal cells is Protein Kinase R (PKR), which when bound to dsRNA, phosphorylates the alpha subunit of eukaryotic initiation factor 2 (eIF2α)(Meurs et al, 1990). This prevents the eukaryotic initiation factor 2 (eIF2) from initiating protein synthesis, and thereby prevents viral replication.

In some cases the phosphorylation of eIF2α has been seen to lead to cell death (Balachandran et al., 1998) but the advantages to the organism in preventing the spread of the virus usually outweigh the disadvantages of losing the cell. However, in cases where a significant number of cells are infected, the death of all infected cells would be lethal to the organism. Thus, there are other less extreme measures that eukaryotic organisms can utilise, such as recognising dsRNA and destroying it directly, a process known as RNA silencing. As discussed earlier, most viruses pass through a dsRNA stage during replication (Figure 1.1), and the remaining viruses produce long dsRNA through other methods. As dsRNA is not naturally present within eukaryotic cells except as part of the RNA interference (RNAi) pathway (Hutvágner and Zamore, 2002), it is easily recognised and is an efficient trigger for an immune response.

1.2.1. RNA interference is an antiviral defence mechanism which viruses have evolved to counter

RNAi is a biochemical pathway common to all eukaryotic life. RNAi serves a number of functions, one of which is the protection of cells against viral infection (Ratcliff et al., 1997). It does this by responding dsRNA and destroying cognate RNA in a sequence-specific manner, thus reducing the ability for viral replication to occur (Lindbo et al., 1993). In order to combat this antiviral mechanism, viruses have evolved a variety of methods of either preventing RNAi from being activated or suppressing the RNAi process (Csorba et al., 2007, Diaz-Pendon et al., 2007, Ding et al., 2004, Haas et al., 2008, Kasschau and Carrington, 1998, Love et al., 2007, Takeda et al., 2002). Each virus-encoded suppressor of RNA silencing (VSR) interferes at single or multiple points within the RNAi pathway, and some viruses also encode multiple VSRs (Cañizares et al., 2008, Lu et al., 2004). In this manner viruses can neutralise the effects of RNAi on the viral replication process, thus allowing viral infection to occur to high titre within the host.

1.2.1.1. RNAi is common to all eukaryotic life

The RNAi pathway is strongly conserved amongst eukaryotes, and is present in plants, fungi, invertebrates and vertebrates (Rice et al., 2004). RNAi is used to down-regulate endogenous genes in a sequence specific manner, and in plants it also acts as a crucial antiviral mechanism (Ratcliff et al., 1997). Until recently, it was thought that somatic mammalian cells had lost the ability to use RNAi as an antiviral pathway (Cullen, 2011), and instead dsRNA triggers the phosphorylation of eIF2α, resulting in the inhibition of protein translation as an alternative antiviral pathway, as detailed in section 1.2.2. However, recently research has been published suggesting that mammalian cells may utilise both RNA silencing and eIF2α phosphorylation as antiviral defences (Maillard et al., 2013, Li et al., 2013).

The initial discovery of RNAi was in plant models, with the creation of transgenic plants carrying an extra copy of a gene which coded for chalcone synthase, an enzyme responsible for the purple pigmentation in petunia flowers. Instead of being more purple, the resulting flower produced little to no pigment (Napoli et al., 1990), as the mRNA from the chalcone synthase transgene formed a dsRNA. The RNAi pathway degraded the dsRNA, all chalcone synthase mRNAs were targeted and destroyed by RNAi, and the resulting flowers were partially or entirely white. RNAi has subsequently been discovered in all plants studied, as well as in fungi, invertebrates and vertebrates (Fire et al., 1991, Romano and Macino, 1992, Wargelius et al., 1999).

1.2.1.2. RNAi is necessary for the development and maintenance of life

The mechanism of RNAi includes post-transcriptional down regulation of genes, protection against viral infection in plants and possibly animals, post-transcriptional gene silencing and control over the developmental stages of growth. A number of disorders are associated with both the underexpression and overexpression of silencing (Chapnik et al., 2011, Fénelon et al., 2011, Gatto et al., 2000).

Although this thesis focuses on the forms of RNAi used as antiviral defence mechanisms, RNAi is a vital part of normal cell function, and the effects of disruption of the RNAi pathway on cell development and regulation should be noted.

1.2.1.3. RNAi recognises dsRNA and establishes a sequence-specific mRNA degradation or translation inhibition pathway

RNAi destroys viral RNA in both single and double-stranded forms, using fragmented dsRNA as a template for targeting the specific sequence of ssRNA for degradation (Ratcliff et al., 1997). A summary of the process is illustrated in Figure 1.2. The RNA silencing pathway begins with the recognition and cleavage of dsRNA into small dsRNA fragments 21-26 nucleotides long (Zamore et al., 2000). The target dsRNA may have been produced as part of the viral genome replication cycle, which upon cleavage produces small interfering RNA (siRNA), (Ratcliff et al., 1999), or it may have been encoded by the host cell as part of the gene regulation function of RNAi (Lagos-Quintana et al., 2001, Lau et al., 2001, Lee and Ambros, 2001), which upon cleavage produces micro RNA (miRNA). In this thesis, the focus is on the virally-encoded dsRNA.

The cleavage of the dsRNA into smaller fragments is non-sequence specific and is performed in animals by the enzyme Dicer, and in plants by a number of Dicer-Like proteins (DCL) (Bernstein et al., 2001). Animal genomes code for a single Dicer protein which cleaves dsRNA for a variety of purposes, in response to a range of stresses (Chan et al., 2004, Li et al., 2002, Lee et al., 1993). In contrast, plant genomes code for a larger number of DCL proteins which are present in all plant cells (Tang et al., 2003), although the quantity and type of DCL present within a plant cell varies depending on the developmental stage of the plant tissue and outside factors, such as drought, cold, osmotic pressure and disease. This allows the RNAi pathway to respond specifically to each stress (Fujii et al., 2005).

In both animals and plants, the resulting dsRNA fragments have a two nucleotide long overhang at the 3′ end, and are phosphorylated at the 5′ end. The 3′ overhang of some types of dsRNA are phosphorylated in plants in order to increase stability of the RNA fragment (Ebhardt et al., 2005).

Before cleaving the dsRNA into fragments, the DCL protein forms a complex called an RISC loading complex (RLC) with a dsRNA binding protein (dsRBP), the structure of which varies between species of plants (Tomari et al., 2004). After DCL cleaves the dsRNA, the RLC asymmetrically loads the 21-26 nt dsRNA fragment into an Argonaute (AGO) protein, where the less stable of the two RNA strands is cleaved by AGO. The more stable strand of the small RNA is incorporated into the AGO protein to form an RNA-induced silencing complex, or RISC (Hammond et al., 2000). Although RISC complexes can vary in composition, they always contain a member of the Argonaute family of

nucleases, and a guiding strand of ssRNA 21-26 nucleotides in length to guide the complex to a complementary ssRNA via Watson-Crick bonding. Upon complementary binding of the guide strand to the target sequence, the AGO protein then cleaves the complementary strand.

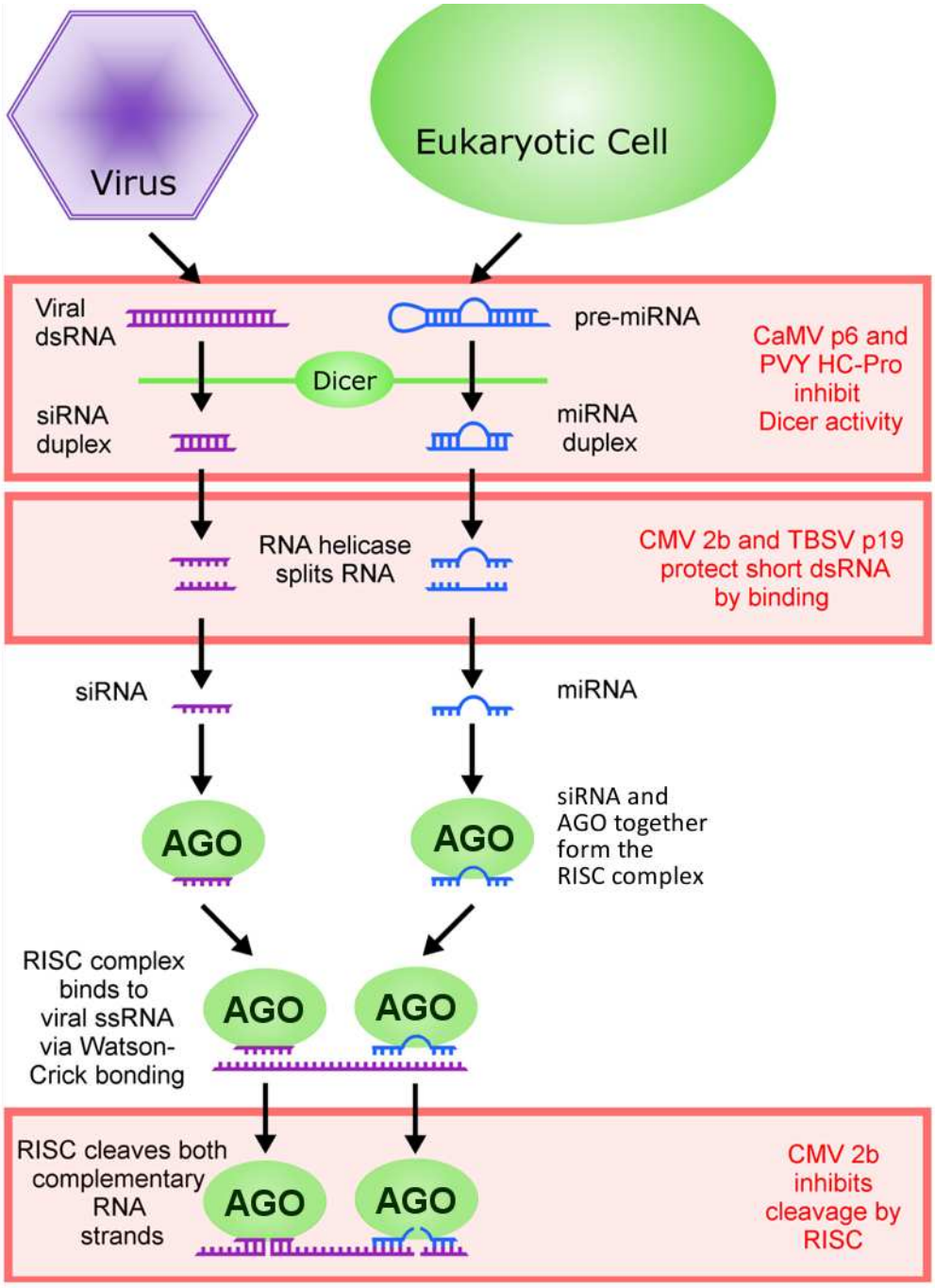

Figure 1.2: In A. thaliana, *viral or host dsRNA is cleaved into 21-26 nucleotide long fragments by DCL proteins 1-4. A single strand of the 21-26 nucleotide long ssRNA is incorporated into the AGO protein, creating the RISC complex. RISC binds to and cleaves ssRNA complementary to the incorporated RNA fragment. Both viral and host RNA is degraded in this manner, although most viruses encode at least one method of suppressing the RNA silencing pathway.*

1.2.1.4. Viruses code for inhibitors of RNAi

RNA is vital to all viral replication. All viruses produce dsRNA at some point during replication, as described in section 1.1.2. Therefore, viruses are susceptible to RNAi, which many organisms use to prevent viral replication and spread (Lindbo et al., 1993, Ratcliff et al., 1997, Li et al., 2013, Maillard et al., 2013). Without a virus-encoded counter-defence mechanism, RNAi has the potential to clear viral RNA entirely from infected cells.

In order for the virus to successfully infect, replicate and spread throughout the host organism, it is necessary for the virus to overcome, to some extent, the RNA silencing mechanism (Kasschau and Carrington, 2001, Liu et al., 2002, Qiu et al., 2002, Voinnet et al., 1999, Voinnet et al., 2000, Yelina et al., 2002). Viruses encode a range of products which suppress silencing within the host cell, with each virus typically encoding between one to three VSRs. VSRs have been found to be encoded in viruses which infect plants, fungi, invertebrates and vertebrates (Li and Ding, 2006). As most VSRs seem to be structurally unrelated and act within different steps of the RNAi pathway they have to be identified empirically through a demonstration of suppression of RNAi. Therefore, many more VSRs are likely to be discovered. If a virus shut down all RNA silencing in a host, the host would quickly die and therefore the virus, as an obligate parasite, would be unable to reproduce. In order for a virus to be successful, it must infect the host and spread to other hosts. Often, the longer an infected host survives, the more opportunity a virus has to infect other hosts, although this is dependent on the method of vectoring between hosts. Therefore, VSRs do not suppress all silencing, and are instead usually targeted to interfere with a specific step in the host's RNA silencing response (Voinnet, 2001).

Like many biochemical mechanisms, VSRs were known long before they were named and the mechanism understood. The initial discovery of a VSR occurred when it was discovered that when *Potato virus X* infected a host plant, the infected plant was more susceptible to infection by a range of other viruses (Pruss et al., 1997). This synergy of infection was due to the presence of HC-Pro, a potyvirus-encoded VSR which binds to dsRNA and prevents Dicer from forming siRNA which are necessary for RISC function (Kasschau et al., 2003).

Since then, a large number of VSRs have been discovered, with many other mechanisms of activity such as RNAi amplification (Blevins et al, 2011), RNAi signalling (Voinnet, Lederer & Baulcombe, 2000) and DNA methylation (Duan et al, 2012). Table 1.1 displays a selection of VSRs found in plant and animal infecting viruses. The mechanisms of these VSRs fall into three categories; those that affect Dicer or DCL proteins, those that bind to siRNAs, and those that bind to long dsRNAs (Figure 1.2).

Table 1.1: Examples of VSRs, the methods of action employed to suppress RNA silencing by viruses and the variety of hosts infected by VSR-encoding viruses.

	VSR	Method of action	Virus	Host Range	Reference
Plant Viruses	P6	Prevents Dicer and DCL from being triggered	*Cauliflower mosaic virus*	Cruciferae	(Haas et al., 2008)
	126 kDa protein	Binds to small dsRNA	*Tobacco mosaic virus*	Wide plant host range	(Ding et al., 2004, Vogler et al., 2007)
	P19		*Tomato bushy stunt virus*	Wide plant host range	(Qiu et al., 2002, Silhavy et al., 2002a, Ye et al., 2003)
	2b	Binds to short and long dsRNA	*Cucumber mosaic virus*	Wide plant host range	(Diaz-Pendon et al., 2007)
	NSs		*Tomato spotted wilt virus*	Wide plant host range	(Takeda et al., 2002)
	HC-Pro	Protects dsRNA from Dicer	*Potato virus X*	Solanaceae	(Kasschau et al., 2003)
			Turnip mosaic virus	Wide plant host range	(Kasschau et al., 2003)
Animal and Plant Viruses	σ3	Binds to long dsRNA	*Reovirus*	Animals, plants	(Denzler and Jacobs, 1994)
Animal Viruses	Tat	Binds to Dicer to prevent formation of siRNA	*Human immunodeficiency virus*	Humans	Bannasser et al, 2005
	E3L	Binds to short and long dsRNA	*Vaccinia virus*	Mammals	(Chang et al., 1992)
	NS1	Binds to short dsRNA	Influenza viruses types A, B and C	Mammals, poultry	(Chang et al., 1992)

1.2.2. eIF2α kinases are part of an antiviral defence which viruses have evolved to counter

eIF2α kinases are a group of proteins present in eukaryotic cells which are triggered when the cell is under stress and respond by phosphorylating the alpha unit of eIF2. eIF2 is a eukaryotic initiation factor which is required to initiate protein synthesis (Matts and London, 1984). When eIF2α is phosphorylated, protein synthesis is inhibited within the cell, with a small number of genes preferentially translated (Dever et al., 1992, Farrell et al., 1977). The phosphorylation of eIF2α prevents both viral and host genes from being translated, and so prevents the spread of viral infection. An inhibitor of eIF2α kinases, IPK, has been shown to inhibit an unknown eIF2α kinase in plants which would otherwise react to viral infection (Bilgin et al., 2003). As eIF2α phosphorylation by an eIF2α kinase is an effective antiviral mechanism, viruses have evolved a number of ways of inhibiting the function of eIF2α kinases (Figure 1.3, **Error! Reference source not found.**).

1.2.2.1. eIF2α kinases are triggered by stresses on the host eukaryotic organism and mitigate adverse effects

The protein eIF2 is a heterotrimer consisting of an alpha, beta and gamma subunit, and is responsible for the initiation of protein synthesis. eIF2 forms a complex with guanosine triphosphate (GTP) and the methionine-transfer RNA (met-tRNA), the first t-RNA needed for any eukaryotic protein synthesis. Once eIF2, GTP and the met-tRNA are associated, the ternary complex binds to the 40S ribosomal subunit, followed by the 60S ribosomal subunit and the mRNA to be translated. GTP is hydrolysed to guanosine diphosphate GDP and protein synthesis is initiated (Safer et al., 1975).

The gamma subunit of eIF2 binds to either GTP or GDP, the energy depleted form of GTP. To initiate translation, eIF2β must be bound to GTP, as the energy needed to start translation is provided when GTP loses a phosphate group and becomes GDP. In order to initiate protein synthesis again, the GDP must be swapped for GTP in an exchange catalysed by eIF2β, an exchange which can only occur while eIF2α is unphosphorylated (Gonsky et al., 1990, Yang and Hinnebusch, 1996).

Finally, the alpha subunit provides regulation sites which control the activity of eIF2. In humans, when the phosphorylation site on serine 51 is phosphorylated, the exchange of GDP for GTP is prevented. In this way, the phosphorylation of eIF2α inhibits protein synthesis within a cell.

There are four well documented eIF2α kinases currently known, with each responding to a different stress either within or external to the cell:

1. Protein Kinase R (PKR) is an eIF2α kinase which is activated by dsRNA, and has so far only been found in animals. As dsRNA is an integral part of the viral replication cycle, PKR acts as an antiviral defence mechanism, which will be discussed in greater detail in section 1.2.2.2

2. Protein-kinase-like Endoplasmic Reticulum Kinase (PERK) phosphorylates eIF2α in response to the accumulation of incorrectly folded proteins in the endoplasmic reticulum, and has only been discovered so far in animals (Harding et al., 1999). When viral infection is successful within a cell, a large number of unfolded or mis-

folded viral proteins are produced. This can trigger PERK to phosphorylate eIF2α, slowing down protein synthesis and easing the stress on the ER. This may or may not be of benefit to the virus as while protein synthesis is slowed, the host cell becomes more effective at producing correctly-folded proteins.

3. Haem Regulated eIF2α kinase (HRI) phosphorylates eIF2α in response to iron (haem) deficiency in animals. Haem is necessary for the creation of red blood cells, binding to α- and β-globin to form haemoglobin. When haem levels drop, α- and β-globins accumulate in the RBC, forming haem-free aggregations. This causes hyperplasia and anaemia in the host, as well as decreasing the availability of precursor red blood cells in bone marrow and the spleen. In order to prevent the accumulation of α- and β-globins, HRI responds to low haem levels by phosphorylating eIF2α, slowing down protein synthesis and preventing a build-up of harmful proteins (Han et al., 2001).
4. GCN2, which has been shown to have homologues in plants, yeast and invertebrates (Olsen et al., 1998), phosphorylates eIF2α in response to wounding, UV damage, cold shock or amino acid shortages within a cell (Jiang and Wek, 2005, Jiang et al., 2003, Lageix et al., 2008, Hofmann et al., 2012). The slow speed of translation while eIF2α is phosphorylated causes other genes to be preferentially translated. For example, when plants experience nutrient limitation, uncharged t-RNAs accumulate in the cell, binding to GCN2 and triggering it to phosphorylate eIF2α, allowing the gene GCN4 to be preferentially translated, which in turn stimulates the production of enzymes involved in amino acid biosynthesis (Dever et al., 1992).

In addition to these well documented eIF2α kinases, studies by Bilgin et al in 2006 suggested that another eIF2α kinase may be present in plants, but is usually suppressed by IPK, a plant encoded inhibitor of eIF2α kinases. This protein reacts to viral infection, causing over-phosphorylation of eIF2α resulting in a lethal reduction in protein synthesis.

1.2.2.2. eIF2α kinases are part of an antiviral defence which viruses have evolved to counter

Currently only two eIF2α kinases, PKR and GCN2, have well documented responses to viral infection, with a third unknown kinase in plants found to be active only when IPK is knocked out. This third kinase will be discussed in greater detail in section 1.2.2.3, while this section focuses on the two better known eIF2α kinases, PKR and GCN2. PKR is part of the interferon (IFN) response, and is usually suppressed within a cell by IPK. Upon viral infection, PKR binds to dsRNA of greater than 30 bp in length via two dsRNA binding motifs at the N terminus, causing PKR to dimerise and thereby become capable of phosphorylating eIF2α (Wu and Kaufman, 1997). PKR can bind to dsRNA of at least 15bp, but requires at least 30bp to achieve dimerisation and hence eIF2α phosphorylation. As dsRNA is an integral part of the viral replication cycle, without inhibition PKR is an effective antiviral mechanism.

Although PKR is the most well-known eIF2α kinase to respond to viral infection, it is only present in animals. GCN2 is found in yeast, with orthologues present in plants and animals. GCN2 has been shown to respond to Sindbis virus infection by phosphorylating eIF2α (Berlanga et al., 2006), but most commonly phosphorylates eIF2α in response to nutrient limitation. GCN2 contains a histidyl-tRNA synthatase-like domain near its C-terminal which binds to uncharged t-RNAs. When bound to an uncharged tRNA, GCN2 dimerises and becomes capable of phosphorylating eIF2α (Qiu et al., 2001).

1.2.2.3. IPK is an inhibitor of an unknown eIF2α kinase in plants

IPK is found in plants, animals and yeast, and functions as an inhibitor of PKR in animals by binding directly to PKR amino acids (aa) 244 to296, a region necessary for the dimerisation of PKR (Tan et al., 1998). IPK also acts as an inhibitor for an unknown eIF2α kinase in plants. This unknown eIF2α kinase is triggered by viral infection, and, in the absence of IPK, causes over-phosphorylation of eIF2α. Over phosphorylation of eIF2α in plants inhibits protein translation to such an extent that the infected leaf will die within 12 days of infection, and the entire plant within 21 days (Bilgin et al, 2004). As the unknown eIF2α kinase is both repressed by IPK and triggered by viral infection, it is possible that the unknown kinase is a functional homologue to PKR.

1.2.2.4. Viruses have evolved ways of inhibiting eIF2α phosphorylation

The phosphorylation of eIF2α is a vital host defence against viral infection, preventing translation of viral proteins and rendering the cell machinery unusable to the virus. Many viruses such as Epstein-Barr virus, adenovirus, Poliovirus, vaccinia virus, human immunodeficiency virus type one (HIV-1), influenza virus and Reovirus encode inhibitors of eIF2α kinases. As this is a crucial step in successful viral infection, being able to suppress the eIF2α pathway provides viruses with a great advantage. Consequently, a number of viruses have independently evolved different mechanisms of inhibition. Most viruses encode at least one inhibitor, with some viruses encoding multiple inhibitors, as shown in Table 1.2. For example, vaccina and influenza viruses both produce at least two PKR inhibitors (Davies et al, 1993). Methods of inhibition vary widely, including such techniques as decoy dsRNA, destruction or inhibition of eIF2α kinases, the protection or concealment of virus RNA, or preventing dimerisation of PKR. Figure 1.3 illustrates the pathway by which PKR phosphorylates eIF2α, while Table 1.2 lists known ways in which virus-encoded inhibitors of eIF2α kinases interrupt this pathway.

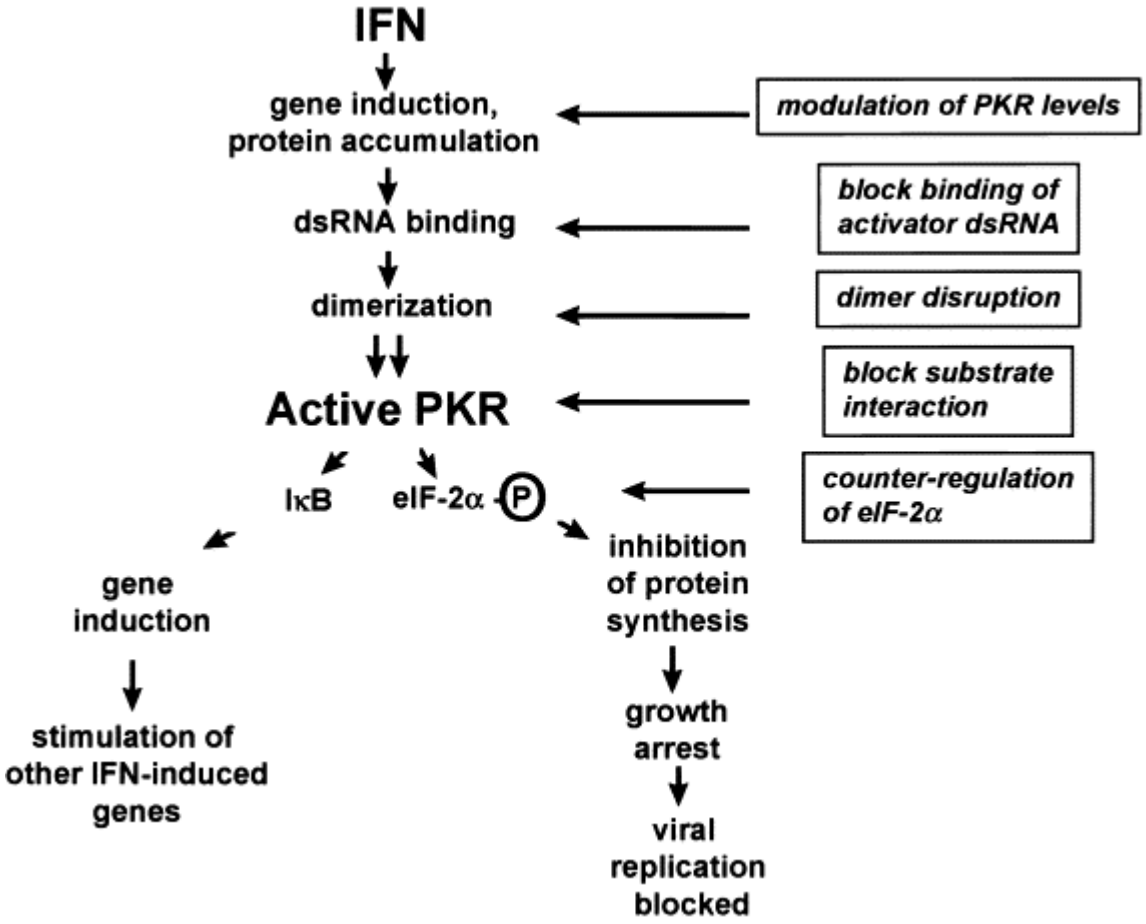

Figure 1.3: In order for eIF2α to be phosphorylated in response to viral infection, first PKR be present in sufficient quantity in the cell, then be activated by dsRNA, dimerise and finally phosphorylate eIF2α. Viruses can encode products which interfere with this pathway at a variety of points, as illustrated in Table 1.2 (Gale Jr and Katze, 1998)

Table 1.2: Virus encoded inhibitors of eIF2α kinases, the method of action, virus, host range and name of the inhibitor.

Method	Virus	Host Range	Inhibitor	Reference
Decoy dsRNA	*Epstein-Barr virus*	Humans	EBER1	Clarke, Sharp & Clemens, 1996
	Adenovirus	Animals	VA1	Thimmappaya et al 1982
PKR degradation	*Poliovirus*	Humans	$2A^{Pro}$	Black et al, 1989
Protect or hide viral dsRNA	*Reovirus*	Plants and Animals	σ3	Schiff et al, 1988
	Vaccina virus	Mammals	E3L	Chang & Jacobs, 1993
	Influenza virus	Poultry and Mammals	NS1	Lu et al, 1995
Pseudo-substrate	*Vaccina virus*	Mammals (including humans)	K3L	(Sharp et al., 1997)
	Human Immuno-deficiency Virus 1 (HIV-1)	Humans	Tat	(Endo-Munoz et al., 2005)

Decoy dsRNA such as that encoded by adenovirus and Epstein-Barr virus were discovered to be inhibitors of PKR function in the early 1980s (Thimmappaya et al., 1982) and were later discovered to function by binding to PKR in the same dsRNA binding zone that would usually trigger eIF2α phosphorylation. However, no inhibition of protein synthesis is observed, suggesting that the abundant decoy dsRNA produced by adenovirus and Epstein-Barr virus do not activate PKR. This is likely due to the complex secondary structures in EBER1 and VA1 RNA (Clarke et al., 1990).

One of the most direct methods of preventing phosphorylation of eIF2α in response to viral infection is the degradation of PKR. The $2A^{Pro}$ protease encoded by Poliovirus appears to cleave PKR (O'Neill and Racaniello, 1989), although this is disputed, with studies suggesting that the reduced translation of viral in proteins in $2A^{Pro}$ mutants is due to the ability of $2A^{Pro}$ to allow protein synthesis to occur independently of eIF2α phosphorylation (Redondo et al., 2011, O'Neill and Racaniello, 1989). However this does not explain the findings of Black et al, who in 1989 found high levels of degraded PKR in Polio virus infected cells.

The protection of dsRNA by virally encoded proteins prevents PKR from activation, as it cannot dimerise without binding to dsRNA. The virally encoded proteins E3L, NS1 and σ3 from Vaccina, Influenza and Reovirus, respectively, all bind to dsRNA, resulting in low levels of eIF2α phosphorylation. Each of these viral proteins contain dsRNA binding motifs (dsRBM), areas of highly conserved protein sequences which have been shown to bind to dsRNA regardless of the RNA sequence. dsRBMs are found in proteins from viruses, bacteria and both lower and higher eukaryotes (Fierro-Monti and Mathews, 2000). A potential mechanism of action for the dsRBM can be found in the tertiary structure of σ3, as it has been found that when σ3 forms a homodimer, a long negatively charged area which has been proposed to interact with dsRNA is created (Olland et al., 2001).

The final method of PKR inhibition mentioned in Table 1.2 is that of the formation of pseudosubstrates, proteins which bind to PKR in the same area as eIF2α, blocking the eIF2α-binding site of PKR and thereby preventing the phosphorylation of eIF2α. Both the K3L protein encoded by *vaccina* virus (Sharp et al., 1997) and the Tat protein encoded by

HIV-1 bind to PKR at the eIF2α binding site, but with different results. K3L provides competitive inhibition by physically blocking eIF2α from PKR, whereas Tat both competes with eIF2α as a substrate for PKR, and uses the subsequent phosphorylation of Tat by PKR as an advantage. Tat functions as an elongation factor, binding to the TAR region of viral dsRNA to begin translation. Phosphorylation of Tat by PKR allows faster, stronger and greater binding of Tat to TAR RNA (Endo-Munoz et al., 2005), initiating translation. TAR has also been shown to activate PKR, causing increased levels of phosphorylation of Tat. In this way, HIV-1 both activates PKR and prevents eIF2α phosphorylation.

1.3. Some viral suppressors of RNA silencing also inhibit eIF2α phosphorylation

With the establishment of standardised methods of establishing whether or not a virally-virally-encoded protein has VSR activity (Roth et al., 2004), a number of PKR-inhibiting proteins are now being tested for VSR activity (Lichner, Silhavy & Burgyan 2002, Hasse et al, 2005). Some proteins have been found to function not only as PKR inhibitors, but also as VSRs. For example, the viral proteins σ3, E3L and NS1 are featured in both

Table 1.1 , which lists suppressors of RNA silencing, and Table 1.2, which lists PKR inhibitors.

Table 1.3 compares the two, demonstrating that, so far, these proteins function in both cases by binding to dsRNA - a key component in the activation of eIF2α kinases and DCL. This demonstrates that inhibitors of RNA silencing can have effects ranging far beyond gene repression, effecting other pathways entirely. As RNA and DNA are the foundations upon which all life is built, any suppression of gene expression can have a long-reaching effect, which we are only just beginning to understand.

So far, no plant viruses have been investigated to determine if plant VSRs can also function as inhibitors of eIF2α kinases. To date, research has focused primarily on the animal kinase, PKR, excluding other eIF2α kinases such as GCN2, which not only has been shown to respond to a virus infection but also can be found in yeasts, plants and animals. Study of the interactions between plant VSRs and inhibitors of eIF2α kinases would allow research currently limited by ethical and practical considerations surrounding animal cell culture to be more freely investigated.

Table 1.3: The three viruses known to encode a protein which functions as both an inhibitor of PKR and a VSR, the method of RNAi suppression, and the method by which eIF2α phosphorylation is inhibited.

Virus	**Host Range**	**VSR/PKR inhibitor**	**Method of RNAi suppression**	**Method of PKR inhibition**
Reovirus	Animals, plants	σ3	Binds to long dsRNA	Protects or hides viral dsRNA
Vaccina virus	Mammals	E3L	Binds to short and long dsRNA	Protects or hides viral dsRNA
Influenza viruses types A, B and C	Mammals, poultry	NS1	Binds to short dsRNA	Protects or hide viral dsRNA

1.4. Research questions and aims of this research

1.4.1. Aim 1: To determine if eIF2α kinase activity is altered in plants upon virus infection

The first aim of this project was to identify whether or not virus infected *A. thaliana* have altered eIF2α phosphorylation activity upon viral infection, and if eIF2α phosphorylation upon viral infection is inhibited by the presence of the host-encoded protein kinase inhibitor IPK. In order to do this, the four objectives described below were met. The methods and materials required for the completion of the following objectives is described in Chapter 2, while findings are described in Chapter 3.

1. Wild-type and Arabidopsis plants with a non-functional IPK gene were infected with *Turnip vein clearing virus* (TVCV) and *Turnip yellow mosaic virus* (TYMV). Virus infection was confirmed by symptomology, enzyme-linked immunosorbent assay (ELISA) or Agdia® Immunostrip.
2. Samples were taken from inoculated leaf tissue at 0, 3, 6, 9 and 24 hours, 3, 5 and 7 days and 2 weeks post inoculation, and the total protein extracted and quantified.
3. The amount of phosphorylated eIF2α present in a control sample of *A. thaliana* tissue was quantified via western blot.
4. The amount of phosphorylated eIF2α present in leaf tissue was determined by western blot, using the control sample from Objective 3 as a reference.

1.4.2. <u>Aim 2:</u> To determine if VSRs affect eIF2α kinases independently of viral infection

The second aim of this project was to determine if the expression of a VSR in plant tissue inhibits the ability of the host plant to phosphorylate eIF2α by the protein kinase GCN2. In order to achieve this, the six objectives described below were met. The methods and materials for this aim are described in Chapter 4, while the findings are described in Chapter 5. The projects as a whole is discussed and final perspectives are provided in Chapter 6.

1. The bacteria *Agrobacterium tumefaciens* was transformed to contain a binary vector one of a number of VSRs or the eIF2α kinase inhibitor IPK.
2. The VSR transformed *A. tumefaciens* were introduced into the leaf cavity of *Nicotiana benthamiana* plants through agroinfiltration, either in isolation or together with IPK-transformed *A. tumefaciens*.
3. Total RNA was isolated from agroinfiltrated *N. benthamiana* and the presence of RNA matching the introduced VSR was confirmed via RT-PCR.
4. Half of each sample group of agroinfiltrated *N. benthamiana* plants were sprayed with glyphosate to induce eIF2α phosphorylation.
5. The total protein was extracted from agroinfiltrated leaves of both glyphosate treated and untreated agroinfiltrated *N. benthamiana.*
6. The amount of phosphorylated eIF2α present in the plant tissue expressing the VSR was quantified via western blot, using the control sample from Aim 1, Objective 3 as a positive control for a known amount of phosphorylated eIF2α.

Chapter 2

Is eIF2α kinase activity altered in plants upon virus infection?

Methods and Materials

Plants

Seeds from wild-type *Arabidopsis thaliana*, ecotype Columbia 0 and the mutant IPK knockout line SALK_103659 (Yamamoto et al., 2008) were grown in Daltons Premium Seed Mix® and maintained at 22°C under 16 hours light and eight hours dark for the duration of the experiment. Seeds were initially sown in bulk and seedlings were planted into individual pots at three weeks for inoculation with TVCV, or five weeks for inoculation with CaMV, CMV, TMV or TYMV, and then allowed to mature for a further week before inoculation.

2.2. Viral infection

2.2.1. Inoculation

Leaves from the inoculum source (Table 2.1) were homogenised with inoculation buffer (K_2HPO_4 pH 7.4 in double distilled H_2O (ddH_2O), with 0.1% w/v Na_2SO_3 added before use) at a ratio of roughly 1 mL inoculation buffer per 2.5 cm square of leaf material. The resulting homogenate was then mixed with 5% w/v powdered carborundum of an unknown mesh size and applied to the upper surface of 3-4 fully expanded leaves with a cotton bud while the leaf was supported from below. For each virus tested, 48 wild-type *A. thaliana* and 48 IPK knockout mutant *A. thaliana* plants were inoculated as described above. As a control, the same number of wild-type and mutant plants were mock-inoculated with inoculation buffer mixed with 5% w/v carborundum.

Table 2.1: Viruses used for A. thaliana *inoculation in this experiment and their descriptors, hosts, symptoms, method of identification and VSR.*

Virus	Family	Genome	Host	Symptoms	Test	VSR
CMV	*Bromoviridae*	Positive sense ssRNA	>1200 species	Young leaves appear narrow and the entire plant to be stunted.	RT-PCR/Agdia Immunostrip®	2b
CaMV	*Caulimoviridae*	dsDNA	Brassica & Solanaceae	Variety of systemic symptoms such as mosaic, necrotic lesions on leaf surfaces, stunted growth, and deformation of the overall plant structure	RT-PCR	P6
TMV	*Virgaviridae*	Positive sense ssRNA	Solanaceae	The infection causes characteristic patterns, such as "mosaic"-like mottling and discoloration on the leaves	Agdia Immunostrip®/ELISA	126kDa protein
TVCV	*Virgaviridae*	Positive sense ssRNA	Brassica	Vein-clearing, mosaic, symptomless, other.	Agdia Immunostrip®/ELISA	Replicase small subunit
TYMV	*Tymoviridae*	Positive sense ssRNA	Brassica	Bright yellow mosaic disease showing vein clearing and moulting of plant tissues	RT-PCR	P69, V2

2.2.2. Sampling of inoculated leaves for protein extraction

For time points up to and including one week, two to three inoculated leaves were removed from the plant at the base of the petiole and frozen at -80°C. Samples taken at two and three weeks were of approximately 1 cm^2 of leaf tissue cut by a scalpel from one or two symptomatic leaves, which were also stored at -80°C.

2.2.3. Confirmation of viral infection via Agdia Immunostrip®

Agdia Immunostrip® (Agdia, Elkhart, IN, USA) testing kits were used to confirm infection of *A. thaliana* with CMV, TMV or TVCV as described in section 2.2.1. Approximately 2.5 cm square of leaf tissue from 28 days post inoculation was placed in the bag provided with the sample kit with the provided extraction buffer (Agdia SEB). Mechanical force was applied via the blunt end of a pen over the bag, disintegrating the sample tissue and dispersing the cell contents into the extraction buffer. The lower portion of the immunostrip was then immersed in the resulting homogenate for five to ten minutes. A single line on the immunostrip confirmed the efficiency of the test, and two lines indicated the samples were positive for CMV, TMV or TVCV, depending on the immunostrip used. TMV immunostrips were used for detection of both TMV and TVCV.

2.2.4. Detection of TVCV infection via ELISA

Metal punches 8 mm in diameter were used to remove circles of leaf tissue from four week old inoculated plants for testing, as well as a positive control (TVCV infected *N. benthamiana*) and negative control (uninoculated *A. thaliana*). Leaf discs from *A. thaliana* samples were homogenised in 1 mL extraction buffer (0.16%, Na_2CO_3, 0.294% $NaHCO_3$, 2% polyvinylpyrrolidone (PVP), 0.02% NaN_3, pH 9.6) and 200 µL of the resulting homogenate was loaded into a C96 MaxiSorp™ Nunc ELISA plate, which was covered with the lid and left to incubate for four hours at 30°C.

The positive control was prepared in the same manner as the *A. thaliana* samples. 100 µL of the resulting homogenate was loaded into two wells. To one of these, 100 µL of extraction buffer was added and pipetted up and down to mix. This solution (100 µL) was loaded into the next well over along with 100 µL extraction buffer, and in this manner serial dilutions to 1/126 homogenate to buffer were loaded onto the plate.

The primary antibody used for TVCV detection was Bioreba DAS-ELISA TMV primary antibody, which although designed for used against TMV worked reliably for TVCV detection. Due to the cross-reactive nature of the primary antibody, the antibody was first incubated with plant extract from healthy tissue of the same species as the sample. Plant tissue was crushed in conjugate buffer (2% PVP, 0.2% Bovine Serum Albumin, 5% PBS Tween® 20, pH 7.4) at a concentration of 10 µg/mL. The homogenate was centrifuged at 5000 rcf for ten minutes at room temperature, and the primary antibody added to the supernatant at a dilution of 1 µL/mL (1:1000). This solution was left to incubate at room temperature for three hours.

After incubation, the plate was washed four times in ddH_2O and once in 1X PBS-Tween® (16% NaCl, 0.4% KH_2PO_4, 2.3% Na_2HPO_4, 0.4% KCl, 0.4% NaN_3, 1% Tween-20, pH 7.4). The plate was tapped upside-down on an absorbent surface to remove excess moisture, and 200 µL of the primary antibody solution described above added to each well. The plate was then covered and incubated overnight at 4°C.

Conjugate antibody was prepared by diluting anti-mouse antibody (Anti-Mouse IgG Alkaline Phosphatase conjugate, Sigma Aldrich, St Louis, MO, USA) 0.1 µl/mL (1:10000) in conjugate buffer (recipe on previous page). After incubation, the plate was rinsed four times in ddH_2O and tapped dry. Conjugate antibody (200 µL) was loaded into each well, and the plate covered and incubated at 30°C for four hours.

After incubation, the plate was rinsed seven times in ddH_2O and vigorously tapped dry. To each well 200 µL of 1 mg/mL p-nitrophenyl phosphate (pNPP) in substrate buffer (10.68% diethanolamine, 0.02% NaN_3 and HCl to pH 9.8) was added and left to incubate at room temperature for two minutes. The plate was then scanned by a Multiskan EX ELISA plate reader (Thermo-Fisher Scientific, Waltham, MA, USA). For each reading the scanner took two optical density (OD) measurements; firstly at an absorbance of 405 nm and ten seconds later at an absorbance of 490 nm. Readings were taken every half hour for two and a half hours, and the final optical density (OD) used to determine the rate of colour development. The formula below was used to determine the overall OD/min for each well.

Reaction rate (OD/min) = (OD2 – OD1) / (t2 – t1)

Where, OD_2 is the optical density at time point 2 (OD)

OD_1 is the optical density at time point 1 (OD)

t_2 is the time when the optical density reading 2 (OD_2) was taken (min)

t_1 is the time when the optical density reading 1 (OD_1) was taken (min)

Final OD/min readings were arranged in order of largest to smallest and any OD/min lower than the third lowest positive dilution (1/32) was considered to be negative (Dan Cohen, personal communication). Borderline and unexpected results were tested using Agdia TMV ImmunoStrips®.

2.2.5. Detection of TYMV and CMV via two-step RT-PCR

2.2.5.1. Total RNA extraction

Total plant RNA was extracted from approximately 100 mg of plant tissue, sampled 3 weeks post inoculation and stored at -80°C. RNA was extracted using a Sigma Spectrum Plant Total RNA Kit (Sigma-Aldrich, St Louis, MO, USA), following the manufacturer's instructions, which were as follows: plant tissue was ground in liquid nitrogen to a fine powder using a mortar and pestle, and 250 µL lysis solution containing 10µL/mL of β-mercaptoethanol was added directly to the ground tissue, then mixed thoroughly with the pestle.

The mixture was then incubated for five minutes at 56°C, and then centrifuged at maximum speed at room temperature for three minutes to pellet cellular debris. The supernatant was then filtered through the provided column filter at 16,000 rcf for 1 minute to remove remaining cellular debris. Binding solution (250 µl) was then added to the lysate, the solution mixed immediately and transferred to the provided binding column. In cases where less than 100 mg of plant tissue was harvested, 500 µL of binding solution was added. This was allowed to sit for one minute, and then centrifuged at 16,000 rcf for a further minute. The resulting filtrate was discarded, and the column washed once with Wash Solution 1 and twice with Wash Solution 2, centrifuging in between each wash and after the final wash for 30 seconds at 16,000 rcf. The RNA was then eluted from the column using 30 µL of elution solution instead of the recommended 50 µL, as this provided a more concentrated sample.

The quality and concentration of the RNA was measured using a Nanodrop 1000 (Thermo-Fisher, Waltham, MA, USA) at 260/280 and 260/230 nm, and the RNA stored at -80°C until use.

2.2.5.2. RT-PCR for detection of viral RNA

Single strand cDNA was synthesised from the sample using SuperScript III Reverse Transcriptase kit (Life Technologies, Carlsbad, CA, USA). The sample RNA (approx 100ng) was added to 0.1 µM reverse primer (see Table 2.2), 0.5 µM dNTPs and sufficient nuclease free water to bring the total volume to 13 µL. The solution was then heated at 65°C for 5 minutes, then chilled on ice for a further 2 minutes. To the chilled solution was added 1 x RT buffer (50 mM Tris-HCl [pH 8.3], 75 mM KCl; 3 mM $MgCl_{2)}$, 5 mM $MgCl_2$, 10 mM dithiothreitol (DTT), 100 U SuperScript III, 20 U RNase OUT and sufficient ddH_2O to bring the volume to 20 µL. The solution was heated at 50°C for 50 minutes, then 85°C for 5 minutes. The resulting cDNA was then stored at -20°C until needed, or used immediately for PCR.

PCR was performed using native *Taq* DNA polymerase (Life Technologies, Carlsbad, CA, USA) and accompanying buffers (Life Technologies, Carlsbad, CA, USA). The cDNA (1 µL) was mixed with 0.1 µM each of forward and reverse primer (see Table 2.2), 0.25 µM dNTPs, 1 x PCR buffer (10 mM Tris-HCl, 50 mM KCl [pH 6.8]), 1.25 mM $MgCl_2$ and 1 U native *Taq* polymerase (Life Technologies, Carlsbad, CA, USA). Each plant sample was also tested with NAD5 primers as an internal control to confirm viability of RNA and RT-PCR (Ecke et al., 1990, Menzel et al., 2002)

Table 2.2: Primers used to confirm presence of the infecting virus and the control gene NAD5.

Primer	Primer Sequence (5´ -3´)	Expected product size	Annealing temp. (°C)
CaMV-P35S-F	CACGCTGAAATCACCAGTCTC	118 bp	64.0
CaMV-P35S-R	AACACGTGAGCGAAACCCTA		63.8
TYMV-MP- F	CACCATCCATCCTACCTTGC	247 bp	58.8
TYMV-MP- R	CGGTGATGGAGATGAGGAGT		58.5
NAD5 F	GATGCTTCTTGGGGCTTCTTGTT	181 bp	63.6
NAD5 R	CTCCAGTCACCAACATTGGCATAA		63.8

2.2.5.3. Agarose gel electrophoresis

Agarose gel electrophoresis was performed using 2% agarose in 1x TAE (40mM Tris-HCl [pH 8.4], 0.11% glacial acetic acid, 1mM ethylenediaminetetraacetic acid (EDTA)). PCR product (8 µL) was mixed with 0.8 µl 10x Loading Buffer (30% v/v glycerol, 0.25% w/v bromphenol blue, 0.25% w/v xylene cyanol (Wood, 1992) and from this 8 µL total was loaded into each well. One lane per gel contained 8-10 µL 1 Kb Plus DNA Ladder (Life Technologies, Carlsbad, CA, USA). Electrophoresis was performed at 90 V for 60 minutes. The gel was then immersed in 0.01% ethidium bromide in 1x TAE for 20 minutes, after which it was examined under UV light using a Bio-Rad GelDoc™ 1000 imager.

2.3. Extraction of total plant protein

Two methods of protein extraction were used in this thesis. Protein extraction method A involved grinding approximately 100 mg of plant tissue into a fine powder in liquid nitrogen. To this, 200 µL of extraction buffer A (25mM Tris-HCl [pH 7.6], 85mM NaCl, 15mM $MgCl_2$, 15mM EDTA, 0.05% sodium dodecyl sulphate (SDS), 2.5 mM NaF, 10µL/mL Sigma Protease Inhibitor Cocktail, 5mM DTT) was added and mixed thoroughly. Protein extraction method B was performed by mechanical homogenisation of 100 mg plant tissue in 100 µL extraction buffer B (20mM 4-(2-hydroxyethyl)-1-piperazineethanesulfonic acid (HEPES), 0.1M KCl, 10% glycerol, 5mM $MgCl_2$, 5mM $MgSO_4$, with 10 µL/mL of Sigma Protease Inhibitor Cocktail and 10µL/mL β-mercaptoethanol added directly before use) on ice. Protein concentration was then measured (see section 2.5.1) and the protein aliquoted to a total of 10µg protein per tube. These were then frozen at -80°C until use.

2.4. Concentration of plant protein via precipitation

In order to increase the quantity of total plant protein which could be loaded into each well of an SDS-PAGE gel, plant protein was precipitated using the tricholoroacetic acid (TCA) -acetone method.

After protein extraction using protein extraction method B (section 2.2.5.3), the extracted protein was mixed with 100% TCA-DOC (100 g/mL TCA, 0.1% w/w sodium deoxychlorate in ddH_2O) in a 4:1 ratio plant protein to TCA-DOC. This was then incubated on ice for 30 minutes, after which the resulting suspension was centrifuged at 16 000 rcf at 4°C for 15 minutes. The supernatant was discarded and the pellet resuspended in 0.5 mL acetone kept at -20°C. The suspension was then centrifuged again at 16 000 rcf for 10 minutes at 4°C. Excess acetone was removed, and the pellet air-dried until no liquid was visible in the tube. Without allowing the pellet to dry further, 30 µL SDS loading buffer (section 2.6) and 1 µL 1 M Tris-HCl was added to the pellet and the mixture left under gentle agitation at 4°C overnight. The solution was then spun down at 5000 rcf for one minute at 4°C and any remaining solid material discarded. The supernatant contained the total plant protein, which was then quantified.

2.5. Quantification of total plant protein

Protein was quantified either by Bradford assay or Qubit® fluorometry.

2.5.1. Bradford assay

The dye reagent used was Bio-Rad Protein Assay Dye Reagent Concentrate (Bio-Rad Laboratories Inc., Hercules. CA, USA) diluted one part concentrate to three parts ddH_2O, then filtered through a Whatman #1 filter. Bovine Serine Albumin (BSA) standards were prepared by reconstituting 0.1 g BSA (Sigma Aldrich, St Louis, MO, USA) in 10mL ddH_2O. From this, dilutions of 300, 500, 750 and 1000 µg/mL were made and used as standards.

A 20µL aliquot of sample or standard was placed into an Eppendorf tube and 0.5mL diluted Bradford reagent added. Samples were mixed thoroughly and left to incubate for 5 minutes at room temperature. Absorbance was then measured at 595 nm using a Thermo-Fisher Nanodrop 1000 according to manufacturer's instructions.

2.5.2. Qubit ® fluorometric quantitation

For the majority of protein measurements, Qubit® 2.0 Fluorometer (Life Technologies, Carlsbad, CA, USA) was used to determine protein concentration. Qubit® Working Solution was prepared by diluting Qubit® Protein Reagent 1:200 in Qubit® Protein Buffer. For each sample, 198 µL Qubit® Working Solution was added to 2 µL of protein extract. This was vortexed immediately and left to incubate for 15-20 minutes. For each sample, 2 µL of the batch of extraction buffer (see section 2.2.5.3) used for sample preparation was also measured. All readings were performed in duplicate. After 15-20 minutes, the samples were read using the Qubit® 2.0 Fluorometer, which automatically calculates the protein concentration in the sample.

2.6. Western blot

2.6.1. Gel electrophoresis

Equal weights of protein as determined by step 2.5.1 were loaded into an Eppendorf test tube and the total volume made up to 22µL with SDS loading buffer (1% SDS, 10 mM Tris-HCl [pH 6.8], 1 mM EDTA and 80 mM DTT). To this 3µL of loading dye (0.5 mg/mL bromophenol blue in glycerol) was added and the solution mixed by pipetting up and down. The sample was heated in a sealed tube at 85°C for 5 minutes, then cooled at room temperature for 5-10 minutes. The samples were then centrifuged to return evaporated water on the sides and lid to the bottom of the tube.

Samples were loaded into SDS-polyacrylamide gel electrophoresis (PAGE) gel (Loading gel: 15% acrylamide, 375 mM Tris-HCl [pH 8.8], 2% SDS, 2% ammonium persulfate, 0.2% tetramethylethylenediamine (TEMED). Running gel: 10% acrylamide, 375 mM Tris-HCl [pH 8.8], 0.1% SDS, 0.1% ammonium persulfate, 0.125% TEMED) and run in SDS Running Buffer (1% SDS, 187 mM glycine, 25 mM Tris) at 90V for 120 minutes in a Mini-PROTEAN 2-D Cell gel electrophoresis tank (Bio-Rad, Hercules, CA, USA).

2.6.2. Transfer

Once electrophoresis was complete a 0.45 µm polyvinylidene difluoride (PVDF) Millipore Immobilon-P Membrane was briefly immersed in methanol and then left to rest for 2-5 minutes in Towbin Western Transfer Buffer (20% methanol, 192 mM glycine, 25 mM Tris-HCl (pH 8.3).

The SDS-PAGE gel was then placed on the membrane and filter paper on both sides. The gel-membrane sandwich was placed between transfer buffer-soaked sponges, and placed into the transfer apparatus, which was run at 90 amps for 16 hours. After transfer, the membrane was removed from the sandwich and incubated in Ponceau S stain (0.1% w/v Ponceau S, 5% acetic acid) for 5 minutes. The stain was then gently washed off by agitation of the membrane in ddH_2O. Presence of red bands confirmed protein transfers.

2.6.3. Antibody incubation using the phosphorylated eIF2α specific primary antibody

Prior to incubation with the primary antibody, the membrane was blocked by immersion in 3% BSA in Tris buffered saline with 0.1% Tween (TBS-T) (20mM Tris [pH 7.5], 150mM NaCl, 0.1% Tween 20). The BSA was first dissolved in TBS-T, then filtered through a sterile 0.2µM cellulose-acetate filter to remove undissolved crystals of BSA and large microbes. The membrane was then incubated in the 3% BSA TBS-T for 1 hour at room temperature with gentle agitation.

After blocking, the membrane was incubated in 1 µL/mL (1:1000) anti-eIF2A (phospho S51) primary antibody (Abcam, Cambridge, UK) diluted in 3% BSA TBS-T. Blocking occurred by immersion in the diluted antibody for 14 hours at 4ºC with gentle agitation. After incubation with primary antibody, the membrane was immersed in TBS-T and placed on a rocker for 5 minutes. The TBS-T was drained and replaced, and the membrane was rinsed in this manner seven times.

The secondary antibody used was horseradish peroxidase (HRP) conjugate of goat

anti-rabbit IgG (Life Technologies, Carlsbad, CA, USA) and was diluted directly before use to 0.1 µL/mL (1:10000) in filtered 3% BSA-TBS-T. The membrane was immersed in the diluted antibody for one hour at room temperature, while being gently agitated. The membrane was then washed in TBS-T as it was after incubation with primary antibody a further nine times.

2.6.4. Antibody incubation using the generic eIF2α primary antibody

Blocking of the membrane was performed as in section 2.6.2 using 3% BSA TBS-T. Concentrations of primary antibody varied from 2 (1:500) to 0.3 (1:3000) µL/mL and were diluted directly before use in 3% BSA TBS-T. The membrane was incubated and washed as in section 2.6.2. The secondary antibody used was HRP conjugate of goat anti-mouse IgG (Life Technologies, Carlsbad, CA, USA) and concentrations of 0.1 (1:10000) and 0.05 (1:20000) µL/mL antibody in 3% BSA TBS-T were used. Incubation and subsequent washing occurred as described in section 2.6.3.

2.6.5. Exposure of western membranes

PerkinElmer Western Lighting ECL Pro substrate (PerkinElmer Inc., Waltham, MA, USA) was mixed and 0.5 mL was applied equally to the entire membrane, then allowed to incubate for 2 minutes before the membrane was squeezed dry. Detection of the amount of position of the resulting chemiluminescence took place immediately after removal of the substrate, using the Bio-Rad ChemiDoc MP™ System and ImageLab™ Software. Exposure times varied from 30 seconds to an hour, depending on signal strength.

2.6.6. Removing antibodies from post-exposure membranes

In order to remove previous antibodies, membranes were immersed and gently agitated in 0.2 M glycine stripping buffer (200 mM glycine, 1% Tween-20, 0.1% SDS) for 20 minutes at room temperature. The membrane was then washed in TBS-T seven times as described in section 2.6.2. Addition of the new antibody then proceeded as described in sections 2.6.2 or 2.6.3.

2.7. Coomassie blue staining of SDS-PAGE gels

In order to determine if all protein has transferred from an SDS-PAGE gel to the western membrane, the gels were stained post transfer by immersion in Coomassie blue staining solution (methanol 50% v/v, glacial acetic acid 10% v/v, 0.1% Coomassie brilliant blue w/v) for one hour. After this, gels were left immersed in ddH_2O for 15 minutes three times, with the water changed in between each sock. The gel was then immersed in water and gently agitated overnight.

2.8. Quantification of eIF2α in positive control

2.8.1. Phosphorylation and serial dilution of eIF2α

In order to use pure phosphorylated eIF2α as a standard by which to quantify phosphorylated eIF2α in plant samples, bacterially expressed *A. thaliana* eIF2α was incubated with bacterially expressed human PKR and ATP as follows.

In order to phosphorylate eIF2α for quantification in section 3.4, 5.2 µg bacterially expressed eIF2α, 2.6 µg PKR and 1µg of Poly I:C were added to incubation buffer to a final volume of 40µL. After 30 minutes, 10µL of the solution was diluted in 150µL SDS loading buffer (see section 2.6) to create a solution with a final phosphorylated eIF2α content of 312 ng/µL. Of this, 20µl was added to 20µL of SDS loading buffer and mixed to create a 1:2 dilution with a phosphorylated eIF2α concentration of 156 ng/µL. From the 1:2 dilution, 20µl was again mixed with 20µL of SDS buffer to create a 1:4 dilution, and so on down to a final dilution of 1:2048, with a phosphorylated eIF2α concentration of 0.1523 ng/µL. The dilutions were stored at -80ºC until use, where 20µL of each dilution was mixed with a further 2 µL of SDS loading buffer and 3 µL loading dye, then heated to 85ºC for 5 minutes and loaded as in section 2.6.

2.8.2. Creation of eIF2α positive control

In order to quantify the amount of eIF2α present in glyphosate-sprayed *A. thaliana*, approximately 20 *A. thaliana* seedlings were sprayed four weeks after germination with 150 µM glyphosate until the droplets ran off the leaves. After 24 hours, all leaves from all seedlings were harvested and 2 mL of extraction buffer B (see section 2.3) was added. The mixture was mechanically homogenised on ice, the protein concentration measured via Qubit® fluorometry and subsequently aliquoted into tubes each containing a total of 10 µg of plant protein. These were then frozen at -80ºC until needed.

Chapter 3

Is eIF2α kinase activity altered in plants upon virus infection?

Results

3.1. Virus inoculation

In order to determine whether or not viral infection would alter the phosphorylation status of eIF2α *in planta*, it was first necessary to determine which viruses would infect *A. thaliana* efficiently. Initial attempts to infect *A. thaliana* with the viruses *Cauliflower mosaic virus* (CaMV), *Cucumber mosaic virus* (CMV), *Tobacco mosaic virus* (TMV), *Turnip vein clearing virus* (TVCV) and *Turnip yellow mosaic virus* (TYMV) showed considerable variation in infection rate and visual symptoms for each virus. A large number of virus-infected plants was required to ensure sufficient biological replicates at each time point of the planned experiments. Therefore, it was preferable that the selected viruses were capable of a high infection rate on *A. thaliana*. Also, due to the large number of plants to be tested, a direct correlation between symptoms and virus infection would be useful instead of requiring immunological testing to confirm virus infection.

In order to test the infection rate and the correlation between symptom development and infection, sets of ten *A. thaliana* plants were each infected with one of the above viruses and observed for 28 dpi for symptom development. In addition, eight plants were mock inoculated as negative controls to compare symptom development. At 28 dpi, each plant was tested via Agdia Immunostrip® or RT-PCR (see sections 2.2.3 and 2.2.4 respectively for method) for the presence of the inoculated virus, with mock control plants tested for all viruses

Table 3.1: Symptom and infection rate in virus infected A. thaliana *at 28dpi.*

Inoculum	Number of plant with symptoms			Tested for infection via	Percentage of infected plants
	No visible symptoms	Mild	Severe		
CaMV	10/10	0/10	0/10	RT-PCR	0
CMV	4/10	6/10*	0/10	Immunostrip®	0
TMV	6/10	0/10	4/10	Immunostrip®	100
TVCV	0/10	0/10	10/10	Immunostrip®	100
TYMV	0/10	0/10	10/10	Immunostrip®	100
Mock	7/10	1/10	0/10	Immunostrip®, RT-PCR	0

***** Symptoms were mild (slight yellowing of leaves) and due to inexperience were attributed to potential virus infection. This was likely due to nutrient deficiency, as this was an issue in other areas of the greenhouse.

Table 3.1 shows that TVCV and TYMV were suitable viruses for use in future experiments due to their strong visual symptoms (TYMV infection resulted in chlorosis, necrosis, stunting of leaves and inflorescences, and plant death, TVCV infection resulted in stunting and rounded leaves) and high infection rates. Although TMV had a high infection rate it did not give visual symptoms (a light mottling of leaves) on all infected plants. In addition, only a single member of the *Tobamovirus* genus was required; no significant additional data was likely to be provided by infecting *A. thaliana* with both TMV in addition to TVCV. Subsequent research used the *Tobamovirus* TVCV and the Tymovirus TYMV exclusively.

3.2. Evaluation of protein extraction methods

3.2.1. Protein extraction method A

As the phosphorylation status of eIF2α was to be compared between healthy and virus-infected plants by western blot, it was necessary to analyse protein of high quality. Any unextracted or degraded protein would result in inaccurate quantification, as they may be detected by protein quantification methods which detect small proteins, but not detected by the antibody. Initial protein extraction from glyphosate treated plants using protein extraction method A (see section 2.2.5.3) was of sufficient concentration to load 8 µg of total plant protein per well, as measured using the Qubit® Fluorometer. This amount of

total plant protein extracted and measured by the same method had been shown previously to be sufficient to detect phosphorylated eIF2α via western blot (Tracy Immanuel, personal communication).

In order to replicate the experiment described above, protein was extracted from single leaves taken from one *A. thaliana* and from one *N. benthamiana* plant, which were sprayed with 150 M glyphosate 24 hours before harvest, and from control plants of the same species which had not been sprayed with glyphosate. Protein was extracted from the leaf tissue immediately and stored for a week at -80ºC, and compared with protein extracted from leaf tissue from fresh plants under the same conditions one week later. The protein concentration of the samples was measured via Qubit® fluorometric quantitation, and 8 µg of protein from each sample was examined via western blot using the phosphorylated eIF2α specific primary antibody as described in section 2.6.2.

Upon Ponceau S staining of the post-transfer membrane (method described in section 2.6.1), samples appeared pale and inconsistent in concentration. The Ponceau S stain in Figure 3.1, panel A shows the total protein present on the membrane and illustrates that inconsistent amounts of protein were present in each lane despite equal loading of the gel. Staining of the gel post-transfer with Coomassie Blue (section 2.6.6) showed no protein remaining on the gel. Figure 3.1, panel B shows upon treatment of the western membrane with phosphorylated eIF2α specific antibody, phosphorylated eIF2α was not detected in the plant samples, but the 2.6 ng of bacterially expressed eIF2α used as a positive control was clearly visible. This suggested that there were issues with the quality

or quantity of protein extracted from the glyphosate treated plants resulting in the concentration of phosphorylated eIF2α on the membrane being too low to detect.

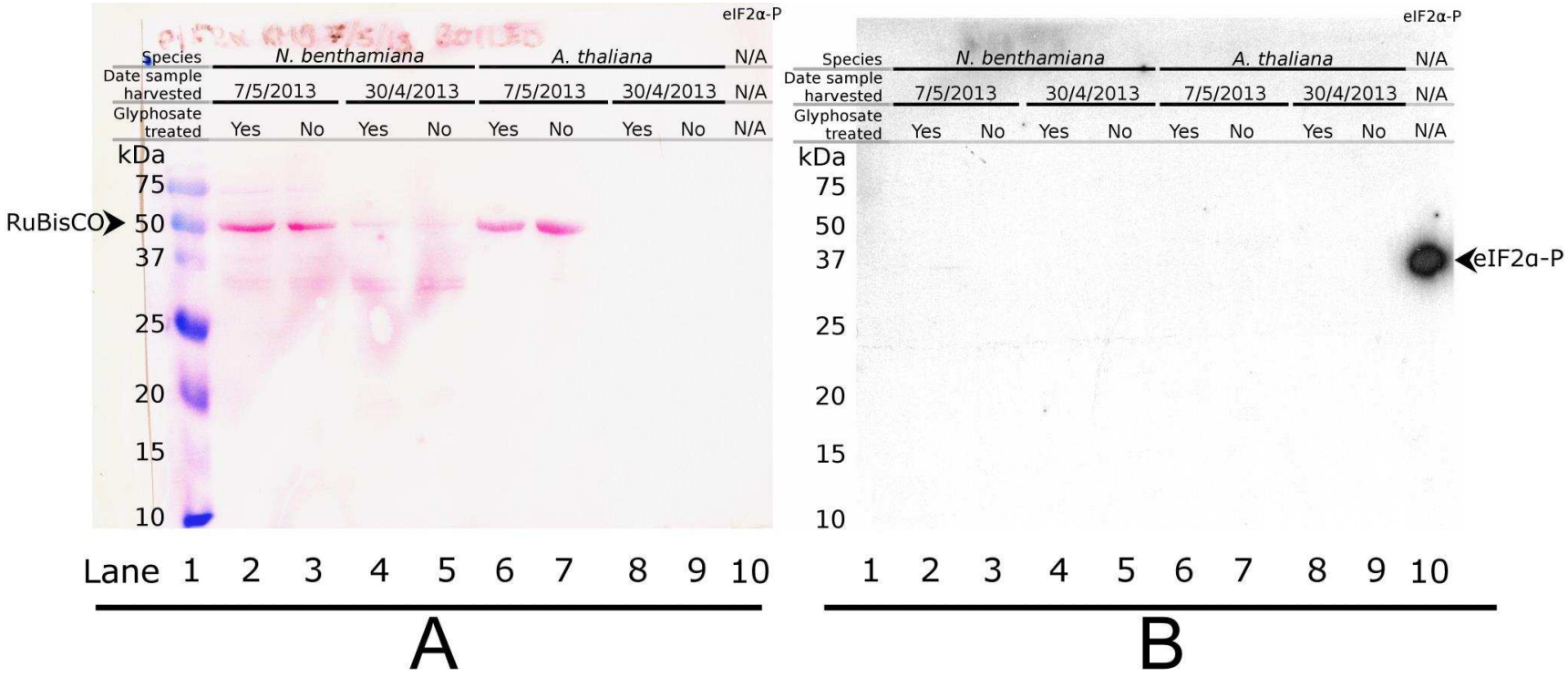

Figure 3.1: Comparison of glyphosate treated and untreated A. thaliana *and* N. benthamiana *protein samples harvested on two dates. (A) Ponceau S stained image of total protein and (B) Chemiluminescent exposure of phosphorylated eIF2α proteins following detection using a phosphorylated eIF2α-specific antibody. Size of proteins (kDa) is indicated by the Bio-Rad Precision Plus All Blue Protein™ marker in lane 1. Lanes 2-9 contain total protein from plants treated and harvested as described above each lane. Lane 10 contains 2.6 µg of bacterially expressed* in vitro *phosphorylated eIF2α protein.*

Since the total protein present in each lane of Figure 3.1, panel A was inconsistent, a possible cause of the lack of detection of phosphorylated eIF2α following treatment of plants with 150 µM glyphosate was the protein extraction method and resulting quality of total plant protein. It was also possible that the amount of protein present on the membrane was too low to be detected by the phosphorylated eIF2α specific primary antibody. To confirm that the readings obtained via Qubit® Fluorometer were accurate and at least 8 µg total protein was loaded into each lane of the gel, the total protein concentration from the samples shown in Figure 3.1was measured by both Qubit® fluorometry and Bradford assay.

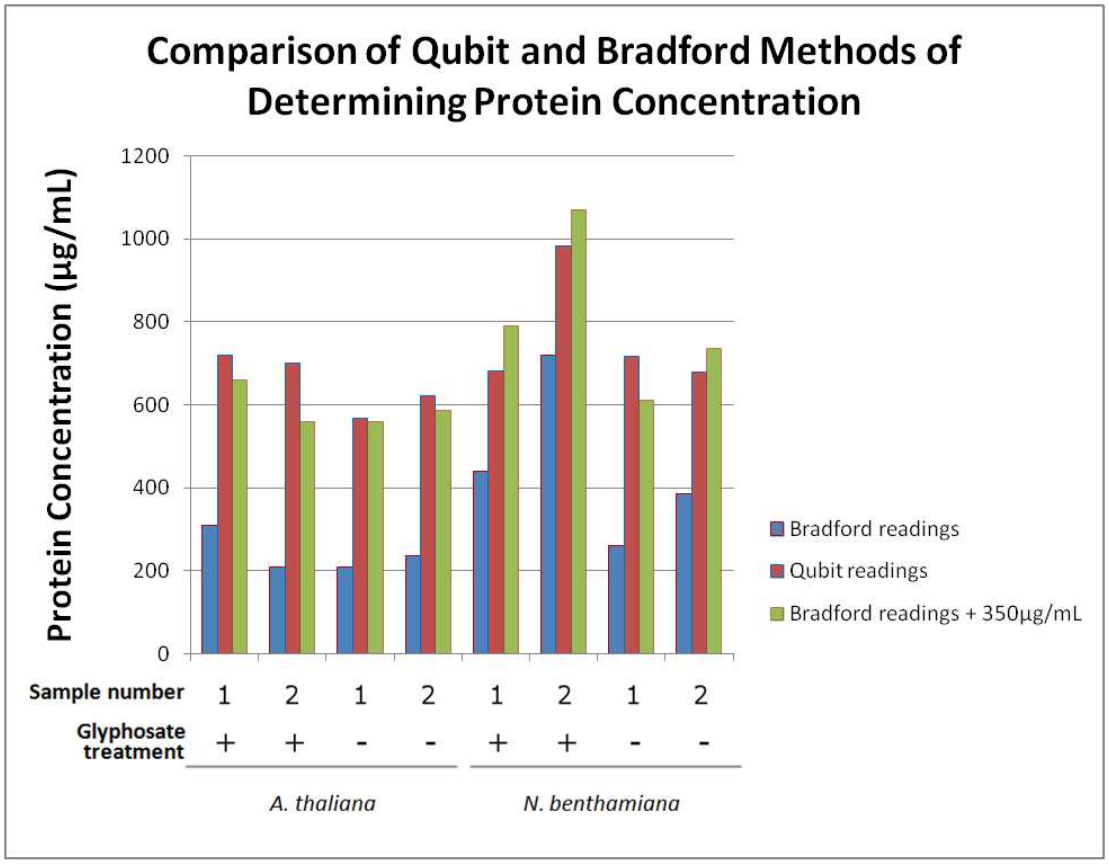

Figure 3.2: Protein concentrations of the A. thaliana *protein samples shown in Figure 3.1 as measured via Qubit® and Bradford assays. The protein concentration of each sample was measured three times via Qubit® and Bradford assay and the average of the three readings is shown.*

Figure 3.2 shows the Bradford method gave different protein readings to the Qubit® Fluorometer with an approximate reduction of 350 µg/mL in all samples. The consistently higher concentration of protein reported by the Qubit® Fluorometer may be due to the sensitivity of the method to SDS and NaF (Invitrogen, 2010), both of which are present in the extraction buffer used in protein extraction method A. This may have caused falsely high protein concentration readings, and therefore a lower amount of actual protein to be present per lane rather than the calculated 8µg total protein per lane required and previously used by another researcher in the laboratory. However, the co-worker also used protein extraction method A and measured protein concentration using Qubit® fluorometry.

This suggested that the inconsistent amount of protein in each lane was due to quality, and not quantity of protein. In order to test this hypothesis, an alternative method of protein extraction was trialled (Tang, 2006).

3.2.2. Protein extraction method B

As protein extraction method A resulted in protein of insufficient quality for phosphorylated eIF2α to be detected by the phosphorylated eIF2α specific primary antibody, an alternative method of protein extraction was trialled. The alternative method of protein extraction is described in section 2.2.5.3, and provided a significant increase in both quality and quantity of protein extracted (see Figure 3.3).

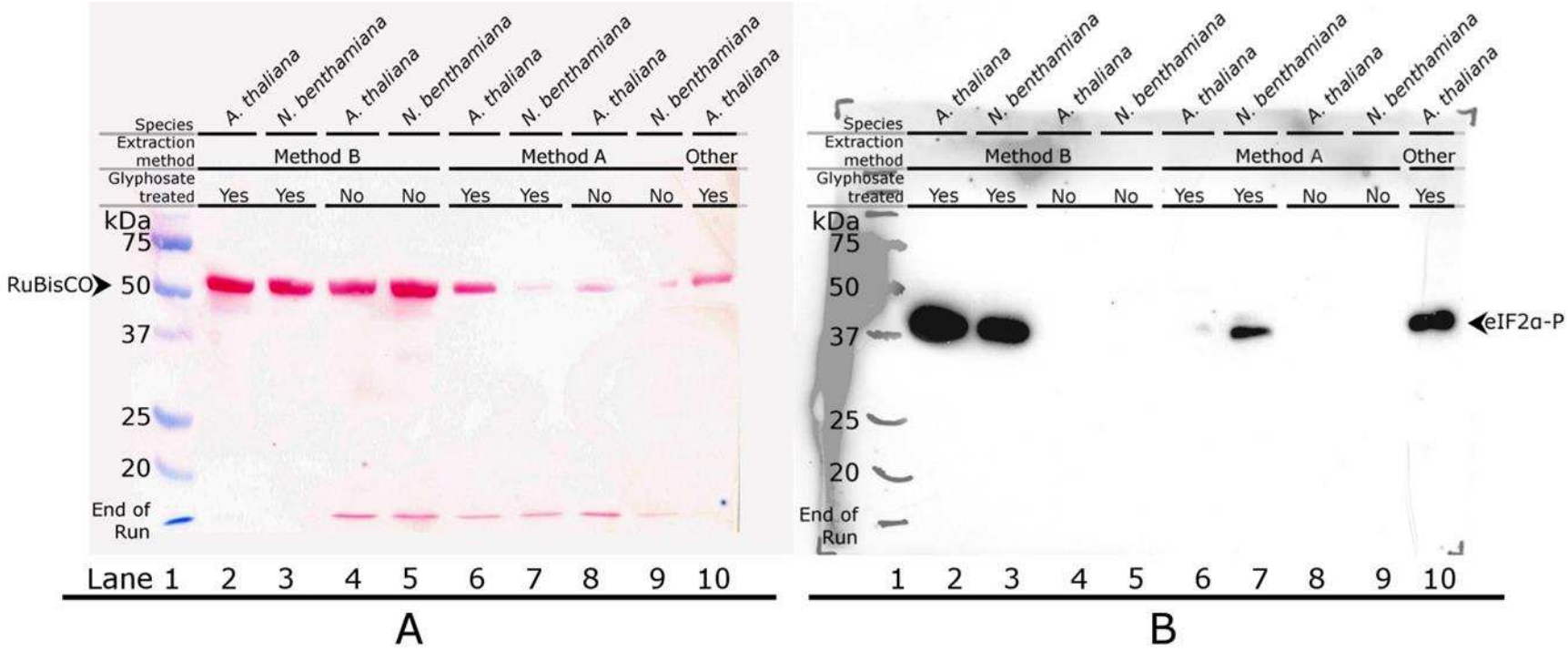

Figure 3.3: Comparison of protein extraction methods A and B. Panel A illustrates the increased thickness and intensity of protein bands on a Ponceau S stained membrane when protein is extracted using extraction method B (Lanes 2-5) than with protein extraction method A (Lanes 6-9). This is further illustrated by the increased detection of bands containing phosphorylated eIF2α at 37kDa on the exposure of the same membrane (Figure 3.3, panel B).The sample in the far right lane was protein extracted from glyphosate treated A. thaliana *and provided by the New Zealand Institute of Plant and Food Research. Lane 1 contains 15 µl of Bio-Rad Precision Plus All Blue Protein™ marker, all other lanes contain 8µg of total* A. thaliana *protein.*

As phosphorylated eIF2α was clearly detected in the glyphosate treated *A.* thaliana protein extracted using extraction method B (Figure 3.3, lanes 6 and 7), and only weakly detected in glyphosate treated *A.* thaliana protein extracted using protein extraction method A (Figure 3.3 lanes 2 and 3), it can be concluded that the use of protein extraction method B provides plant protein of sufficient quality and quantity as to allow the detection of phosphorylated eIF2α in glyphosate treated *A. thaliana* and *N. benthamiana*. In addition to providing a higher quality of protein, extraction method B can be performed without the use of liquid nitrogen, decreasing both risk of injury and cost of materials.

3.3. Optimisation of primary antibodies

In order to determine if a change in the overall ratio of phosphorylated to non-phosphorylated eIF2α occurs *in planta* upon infection with any of the viruses used in this research, a method of identifying both forms of eIF2α must first be validated. Antibodies are available for detection of either phosphorylated eIF2α or all eIF2α and therefore an attempt was made to optimise their use for western blots. Western blot allows the detection of specific proteins through antigen-antibody binding. As antibodies are expensive and the use of too much or too little antibody can result in failure of the western, optimal concentrations of primary and secondary antibody had to first be determined before further experimentation could occur.

3.3.1. Phosphorylated eIF2α specific antibody

In order to determine the optimal concentration of the antibody specific to the phosphorylated form of eIF2α, phosphorylated bacterially expressed eIF2α as well as three different quantities of total protein extracted from glyphosate treated *A. thaliana* were first run out on an SDS-PAGE gel in triplicate and transferred to a membrane as described in sections 2.6 and 2.6.1. The membrane was then cut into three equivalent portions, each portion treated with unfiltered 3% BSA TBS-T, then with phosphorylated eIF2α specific primary antibody diluted to either 1:1000, 1:2000 or 1:3000, followed by the secondary antibody, which was consistently diluted to 1:20000 according to manufacturer's instructions. All other methods were as described in section 2.6.2.

The *A. thaliana* total plant protein used in this experiment was kindly provided by the New Zealand Institute of Plant and Food Research, and was prepared using unknown extraction methods differing from those described in section 2.2.5.3. As such, it was not subject to earlier issues regarding protein quality.

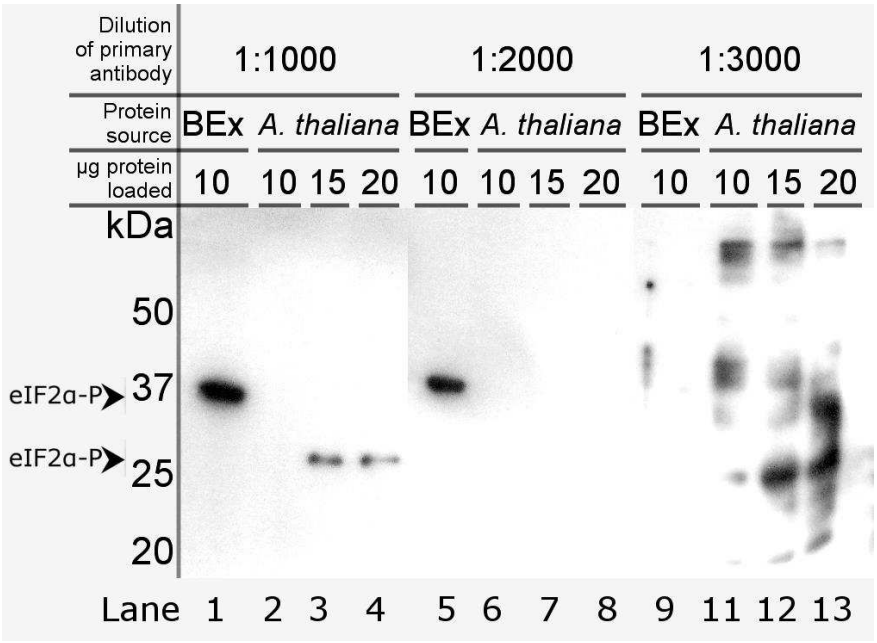

Figure 3.4: The effect of phosphorylated eIF2α specific primary antibody concentration on signal detection. BEx is a contraction of phosphorylated bacterially expressed A. thaliana *eIF2α. All* A. thaliana *samples were from the same protein extraction of glyphosate treated* A. thaliana *to eliminate variation between samples. Phosphorylated eIF2α is detected at 37 kDa in lanes 1 and 5, and at approximately 28 kDa in lanes 3 and 4. All other bands are due to non-specific binding of the primary antibody. All lanes were exposed for the same time.*

As shown in Figure 3.4, a dilution of 1:1000 primary antibody is sufficient to detect both bacterially expressed naturally phosphorylated eIF2α as well as phosphorylated eIF2α from glyphosate treated *A. thaliana*. Interestingly, the eIF2α from glyphosate treated *A. thaliana* is detected at just above 28 kDa, whereas the bacterially expressed and *in vitro* phosphorylated eIF2α is detected at the expected size of 37 kDa. The difference in size between the expected band at 37 kDa and the band seen at 28 kDa was not seen again, and may have been due to protein degradation due to repeated freeze-thaw cycles prior to the experiment. In all subsequent work, extracted plant protein was aliquoted into several portions directly after extraction to avoid any further freeze-thaw damage, and in all subsequent western blots *A. thaliana* phosphorylated eIF2α was seen at 37 kDa.

At the lower primary antibody concentration of 1:2000, only bacterially expressed phosphorylated eIF2α is detected. This is likely due to the fact that in lanes containing bacterially expressed eIF2α, 10µg of pure *in vitro* phosphorylated eIF2α is present, and in lanes containing eIF2α phosphorylated *in planta*, 10µg of total plant protein is loaded, only a fraction of which is phosphorylated eIF2α. Thus, there is much more of the target protein present in lanes 1, 5 and 10. At the lowest primary antibody concentration of 1:3000, nonspecific binding occurs and phosphorylated eIF2α cannot be reliably detected. Therefore, subsequent westerns used a 1:1000 dilution of phosphorylated eIF2α specific primary antibody.

3.3.2. Generic eIF2α antibody

Detection of total eIF2α present in a sample would allow the determination of the percentage of total eIF2α being phosphorylated, as well as allowing detection of any increase or decrease in total eIF2α occurring due to viral infection. The generic eIF2α antibody used for the following experiments apparently binds to all eIF2α, regardless of phosphorylation status. In order to determine the optimal concentration of generic eIF2α primary antibody to use, the membrane shown in Figure 3.4 was stripped of all antibodies (see section 2.6.5) and re-incubated using the generic eIF2α primary antibody in concentrations of 1:1000, 1:2000 and 1:3000. The secondary antibody was diluted to a concentration of 1:10000 before application according to manufacturer's directions.

The resulting exposure (Figure 3.5) showed that the expected band seen earlier at 37kDa was visible in all lanes containing bacterially expressed eIF2α (lanes 1, 5 and 9). The 28kDa band seen previously in protein extracted from *A. thaliana* when treated with phosphorylated eIF2α specific antibody was also detected when the generic eIF2α antibody was diluted 1:1000 (Figure 3.5, lanes 3 and 4) and 1:3000 (Figure 3.5, lanes 10 and 11) No protein extracted from *A. thaliana* was observed at the antibody concentration of 1:2000 (lanes 6-8).

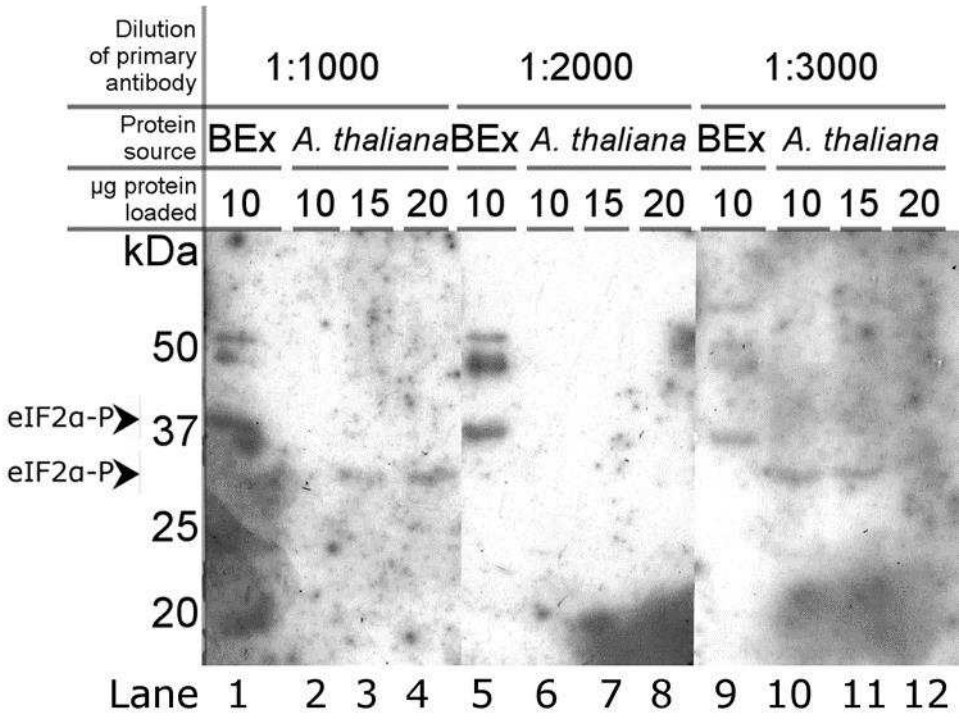

Figure 3.5: Exposure of membranes containing bacterially expressed in vitro *phosphorylated eIF2α and protein extracted from glyphosate treated* A. thaliana. *The membranes were incubated with varying dilutions of generic eIF2α primary antibody. BEx is a contraction of bacterially expressed eIF2α. As in Figure 3.4, the protein in lanes 2-4, 6-8 and 10-12 are from the extraction of a single sample of glyphosate treated* A. thaliana*, and phosphorylated eIF2α is detected at 37 kDa in lanes 1, 5 and 9, and at 28 kDa in lanes2- 4 and 10-12. Other bands are also visible which do not correspond with any known sizes of eIF2α, indicating binding of an antibody to nonspecific proteins.*

As well as the bands visible at the expected size of 37 kDa, samples containing bacterially expressed eIF2α showed two additional bands at approximately 50kDa (Figure 3.5, lanes 1, 5 and 9), while the membrane treated with a 1:3000 dilution of primary antibody, an additional band at approximately 70 kDa was also visible. These bands were not expected, as the bacterially expressed eIF2α had been purified, and when the membrane had previously been treated with phosphorylated eIF2α specific antibody, only one band at 37 kDa was visible. The only other known protein present in the lanes containing bacterially expressed eIF2α is bacterially expressed human PKR, which was added to phosphorylated eIF2α (see section 2.8). If the primary antibody bound to PKR, the band would appear at 68 kDa in size. Therefore, the unexpected bands are considered to be non-specific binding of the primary antibody to unknown proteins present on the membrane.

In order to confirm that the bands visible at 28 kDa and 37 kDa in Figure 3.5 were eIF2α, a second membrane which had previously been confirmed to contain phosphorylated eIF2α (Figure 3.3) was stripped of phosphorylated-specific eIF2α antibody and re-incubated with generic eIF2α antibody. In an attempt to increase sensitivity, the secondary antibody concentration was increased to 1:5000 from the previously used 1:10000.

As Figure 3.6 illustrates, no bands were visible at 30-37 kDa. The bands at 50kDa correspond to the protein band observable at this size on the Ponceau S-stained membrane (Figure 3.3), and are most likely ribulose-1,5-biphosphate carboxylase oxygenase (RuBisCo), a protein necessary for carbon fixation which is present in high concentrations in plant tissue (Badger and Andrews, 1974). The bands at approximately 110 kDa are of an unknown protein. All bands are therefore most likely due to non-specific binding of the antibody. Thus eIF2α was not detected on this membrane using the generic eIF2α antibody.

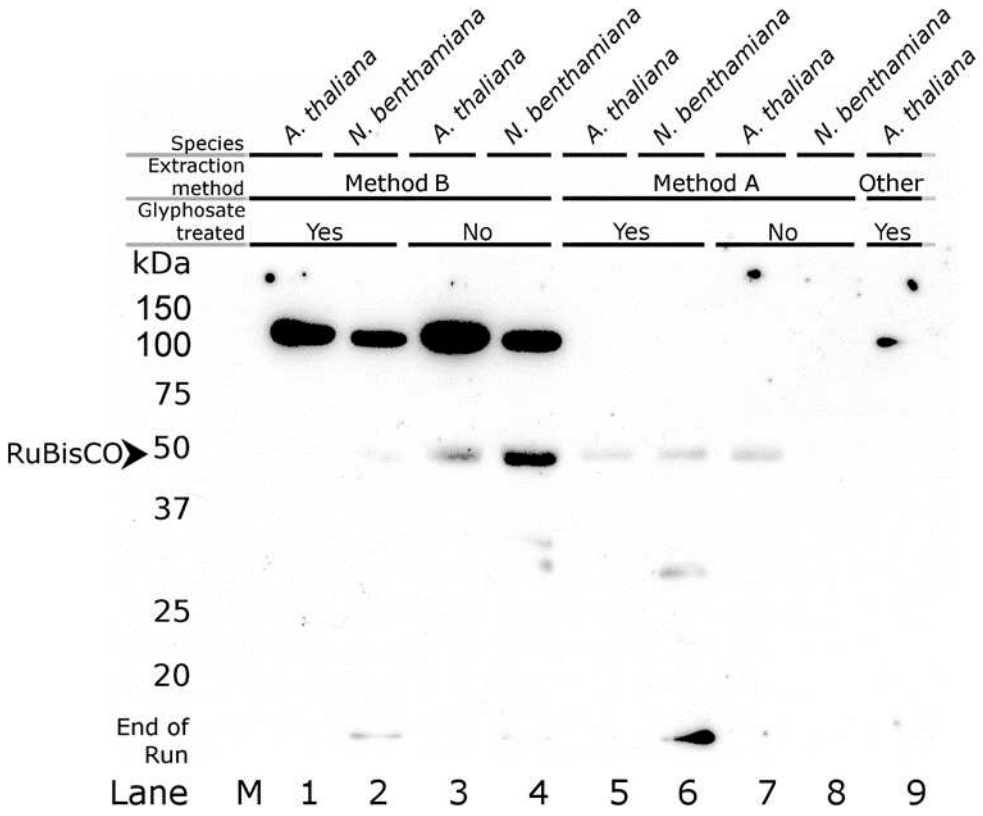

Figure 3.6: Exposure of membrane treated with the generic eIF2α antibody. No eIF2α is visible at 37 kDa, despite the fact that this membrane has previously been shown to contain phosphorylated eIF2α in all samples which were both extracted using Method A and treated with glyphosate. Phosphorylated eIF2α had also previously been shown to be present in the supplied A. thaliana protein sample in lane 9. Lane M contains 15 µl of Bio-Rad Precision Plus All Blue Protein™ marker, all other lanes contain 8µg of A. thaliana *protein*

It is possible that the non-specific binding of the generic eIF2α antibody interferes with its ability to bind to eIF2α when eIF2α is present in low concentrations in the lane. Therefore, it was thought that loading more total protein onto a gel may allow detection. To do this, total plant protein extracted from *A. thaliana* was concentrated via precipitation (see section 2.3) and 50 µg of plant protein was used in a western blot as described in sections 2.6and 2.6.1, as previous studies by Gallie et al (1998) required at least 40 µg of total plant protein to detect eIF2α. The concentration of primary antibody was also increased to 1:500 to improve sensitivity, and the secondary antibody remained at 1:10000 to prevent background noise.

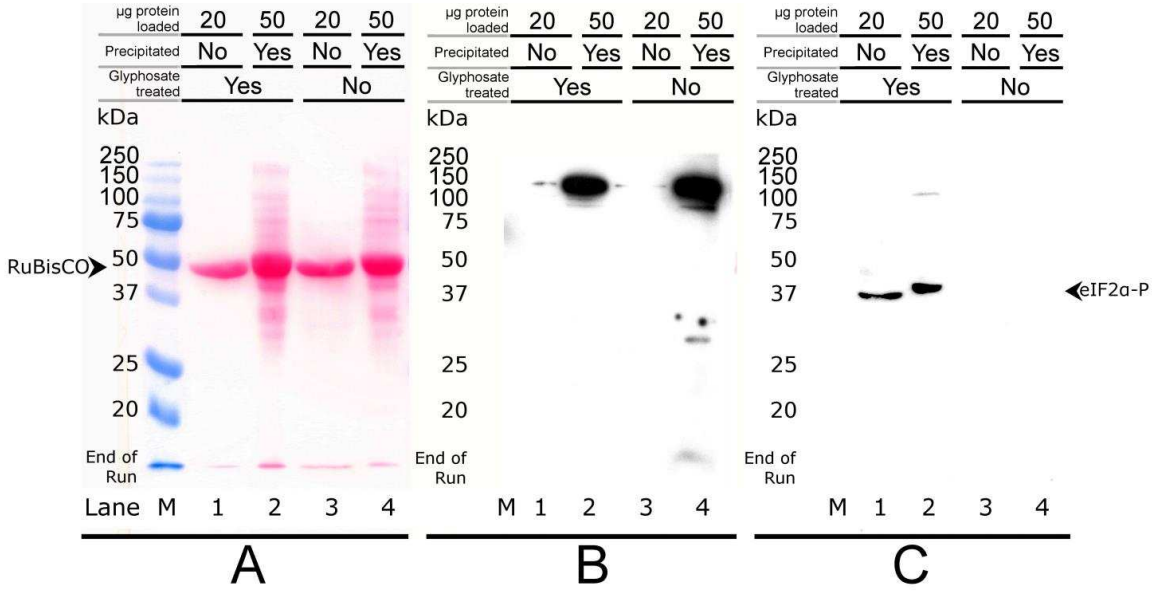

Figure 3.7: A comparison of the effect of increase protein concentration on the detection of eIF2α in a membrane containing high concentrations of A. thaliana *protein. The membrane was treated with generic (panel B) and phosphorylated specific (panel C) eIF2α antibodies in order to determine if the generic eIF2α antibody was detecting eIF2α at the same size at the phosphorylated-specific eIF2α antibody. Lane M contains 15 µl of Bio-Rad Precision Plus All Blue Protein™ marker. Lanes 1 and 3 contain 20 µg of protein from glyphosate treated (Lane 1) and untreated (Lane 3)* A. thaliana*, and Lanes 2 and 4 contain 50µg of precipitated protein from glyphosate treated (Lane 2) and untreated (Lane 4)* A. thaliana. *A) Ponceau S stain of a post-transfer membrane containing 20 and 50µg of protein from glyphosate treated and control* A. thaliana *plants. B) Exposure of the membrane in 7A after treatment with generic eIF2α antibody. C) Exposure of the membrane in panels A and B after the generic eIF2α antibody was removed and the membrane treated with the phosphorylated eIF2α specific antibody.*

Figure 3.7 shows that increasing the concentration of the generic eIF2α primary antibody to 1:500 did not allow detection of eIF2α at the expected size regardless of how much protein was loaded (Figure 3.7, panel B, lanes 1-4). A band of approximately 110 kDa was observed in all glyphosate and non-treated samples, as well as an additional band in the precipitated non-glyphosate treated protein at 28 kDa (Figure 3.7, panel B, lane 4).

It is possible that the eIF2α present in the plant tissue could have been bound to a larger protein, and therefore is present in the higher weight proteins, or that the band at 20 kDa is degraded eIF2α. However, upon stripping the generic eIF2α antibody from the membrane and re-incubating with the phosphorylated-specific antibody, bands were present within at the expected molecular weight of 37 kDa (Figure 3.7; panel C, lanes 1 and 2). An additional faint band was visible at approximately 110 kDa in the lane containing 50 µg of protein from glyphosate treated *A. thaliana* (Figure 3.7, panel C, lane 2). The band at 100 kDa may be from eIF2α that was, for an unknown reason, unable to pass through the gel, or it may be residual generic eIF2α primary antibody, or there may be a protein present in small quantities which is conformationally similar to non-phosphorylated eIF2α, and hence susceptible to generic eIF2α antibody binding. However, as eIF2α is present at 37 kDa when the membrane was treated with the phosphorylated eIF2α specific antibody, it is clear that eIF2α is not detected by the generic eIF2α primary antibody in the concentrated *A. thaliana* protein.

The failure of the generic eIF2α primary antibody to bind to eIF2α, even at high concentrations of both protein and antibody, combined with the non-specific binding to unknown proteins in bacterially expressed *A. thaliana* eIF2α seen in Figure 3.5 strongly suggests that the generic eIF2α primary antibody binds preferably to unknown proteins, and binds weakly or not at all to eIF2α. Therefore, the generic eIF2α antibody was deemed unsuitable for detecting plant eIF2α via western blot.

3.4. Quantification of phosphorylated eIF2α present in extracted *A. thaliana* protein for use as a positive control

As the generic eIF2α antibody proved to be unsuitable for plant eIF2α, an alternative method for quantifying the amount of phosphorylated eIF2α present in plant tissue upon virus infection had to be identified. A known quantity of eIF2α present on each membrane would serve as both a reference for quantification of phosphorylated eIF2α and as a positive control for detection. As bacterially expressed *A. thaliana* eIF2α was in limited supply, it was used as a standard to quantify the amount of phosphorylated eIF2α present in a protein extracted from glyphosate treated *A. thaliana*. The glyphosate treated *A. thaliana* protein was then used on each membrane as a reference.

Plant protein was extracted from a number of *A. thaliana* plants and the extractions pooled to provide a large volume of plant protein (see section 2.8.1). A western was performed on bacterially expressed, *in vitro* phosphorylated eIF2α which had been serially diluted in 1:4 concentrations ranging from 25.6 to 1.6 ng/µL. Of each dilution, 20µL was loaded into a lane of an SDS-PAGE gel. The other lanes in the gel contained 10, 7.5, 5, 2.5 and 1 µg of protein extracted from glyphosate treated *A. thaliana*. From a visual comparison of the resulting exposures, it was determined that 10 µg of the protein extracted from glyphosate treated *A. thaliana* contained roughly 32 ng of phosphorylated eIF2α (data not shown).

To more accurately estimate the concentration of phosphorylated eIF2α in the protein extracted from glyphosate treated *A. thaliana*, a second western was performed using the same amounts of *A. thaliana* protein and serial dilutions ranging from 152 to 0.6 ng of bacterially expressed, *in vitro* phosphorylated eIF2α. Figure 3.8 shows the Ponceau S stained membrane and western blot following incubation with the phosphorylated eIF2α specific antibody. Fading of the lane containing 10000 ng of *A. thaliana* is due to an error during the staining process caused by the vigorous addition of ddH_2O used to wash the superfluous Ponceau S stain off of the membrane. Upon detection of chemiluminescence it is obvious that the amount of protein is consistently diluted throughout all lanes, and overall there is no evidence of a lack of protein within the lane (Figure 3.8, panel B, lanes 1-5).

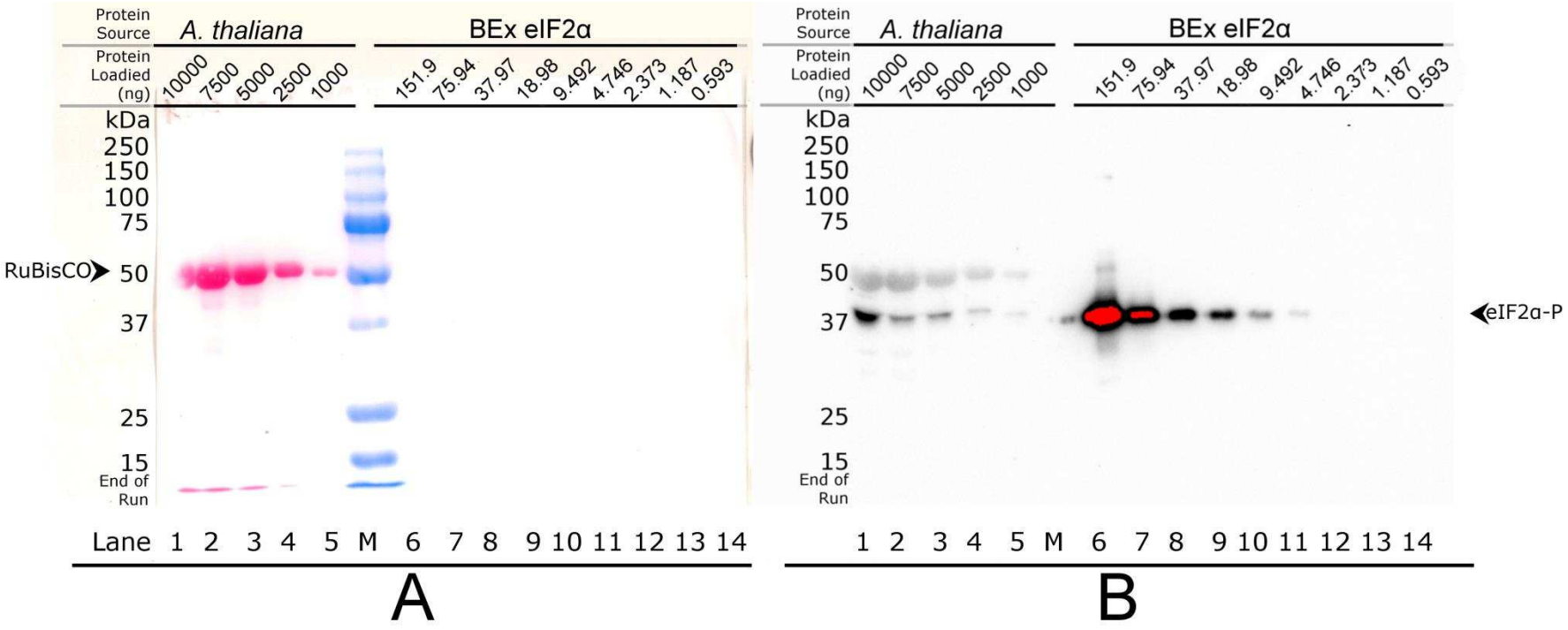

Figure 3.8: Ponceau S stain (A) and exposure of (B) a membrane comparing the amount of phosphorylated eIF2α present in protein extracted from glyphosate treated A. thaliana (Lanes 1-5) to serially diluted bacterially expressed in vitro *phosphorylated eIF2α (BEx, lanes 6-14). The lane containing 7500ng of A. thaliana protein was inaccurately loaded, and is not a valid representation of 7500 ng of protein. Areas of red within band in panel B indicate overexposure of the membrane. Rubisco is visible at 50 kDa, and eIF2α at 37 kDa, as indicated by arrows on the left and right hand sides, respectively. Lane M contains 15µL of Bio-Rad Precision Plus All Blue Protein™ marker.*

The intensity of chemiluminescence detected was determined as a percentage, with 0 being unexposed film and 100 the maximum chemiluminescence which could be detected before the image was considered overexposed using Bio-Rad Image Lab™ under the ChemiDoc® Hi-Sensitivity setting. The chemiluminescence produced by each band was then analysed using GIMP image manipulation software. When the chemiluminescence produced by a band is detected by the imager, the intensity of the chemiluminescence produced is displayed by darkening that area of the image. When the resulting image is analysed using the "cyan, yellow, magenta, key" (CYMK) model, the darkness of a pixel is represented by a key value between 0 (white) and 100 (black). Each band was deliniated using Bio-Rad Image Lab™, and the key value of each pixel in the band determined using GIMP software. The sum of the key values of each pixel in the image of the band was then divided by the number of pixels, giving the average key value of the band described as a value between 0 and 100. This allows the quantification of the chemiluminescence produced by each band on a scale of 1 to 100. Bands which contained areas which were over-exposed (Figure 3.8, lanes 6 and 7) were not included in the following calculations as degree of exposure in overexposed areas could not be reliably determined.

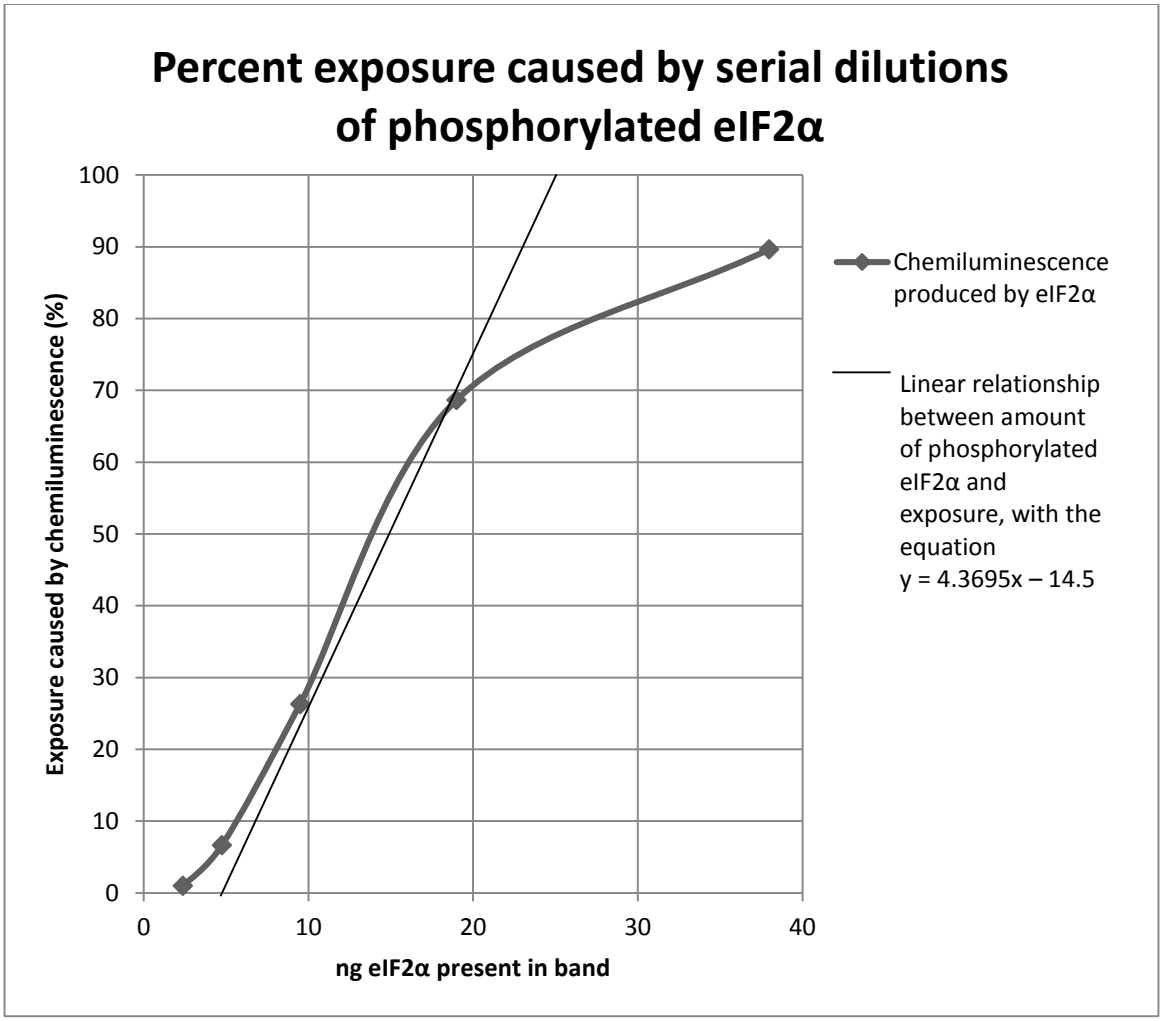

Figure 3.9: Relationship between concentration of phosphorylated eIF2α and chemiluminescence detected per band as seen in Figure 3.8 (panel B, lanes 8-12). Each datapoint is the amount of phosphorylated eIF2α present in a lane (x axis) plotted against the corresponding degree of exposure caused by that band (y axis). There is a strong linear relationship described by the equation y = 4.3695x – 14.5 between the amount of phosphorylated eIF2α present on the membrane and the amount of chemiluminescence produced between 0-20 ng eIF2α and 0-70 percent exposure, however at concentrations of higher that 20 ng phosphorylated eIF2α the relationship between the chemiluminescence produced and the amount of eIF2α present changes and the linear model deviates strongly from the observed results.

Figure 3.9 illustrates the relationship between the amount of bacterially expressed *in vitro* phosphorylated eIF2α present in each band and the chemiluminescence (quantified as a percentage as described above) produced by the sample. The data points corresponding to 4.746, 9.492 and 18.98 ng of phosphorylated eIF2α are approximately linear, with the equation y = 4.3695x - 14.5. In this equation, y is the percentage chemiluminescence and x is the nanograms of eIF2α present within the band. This is Equation 1, and was used to calculate the amount of phosphorylated eIF2α present on a membrane when the amount of phosphorylated eIF2α detected for that sample is between 4.5 and 19 ng. At concentrations higher than 20 ng of phosphorylated eIF2α, Equation 1 no longer accurately represents the relationship between the amount of phosphorylated eIF2α present and the amount of chemiluminescence detected, as the amount of chemiluminescence produced by amounts of phosphorylated eIF2α greater than 20 ng, when treated with the phosphorylated eIF2α specific antibody, is less than would be expected if the relationship followed the linear model.

Equation 1:

Percentage chemiluminescence detected = 4.3695[ng phosphorylated eIF2α present in band] – 14.5

When the amount of phosphorylated eIF2α present on the membrane is higher than 20 ng, Equation 1 is no longer accurate. In order to describe the relationship between the two factors accurately, when the amount of eIF2α present in a lane is greater than 20 ng, a logarithmic model is used. This provides the more accurate equation of y = 79.505x – 39.239 (see Figure 3.10). In this equation, x is the $\log_{10}$ of the nanograms of eIF2α present in

the band, and y is the percentage chemiluminescence produced by the corresponding band. By rearranging Equation 2, the amount of phosphorylated eIF2α present in a band can be calculated by quantifying the amount of chemiluminescence produced when the amount of phosphorylated eIF2α present in the lane is between 3.162 and 63.10 ng (Equation 2). Using Equation 2 to estimate 0 and 100% chemiluminescence produced, concentrations of eIF2α below 3.162 ng will not be able to be detected, and concentrations above 63.10 ng will cause over-exposure of the membrane. This matches the results obtained by western blot as shown in Figure 3.8, where 75.94 ng of bacterially expressed *in vitro* phosphorylated eIF2α has caused over-exposure (Figure 3.8, panel B, lane 8) and 2.373 ng is undetectable (Figure 3.8, panel B, lane 12).

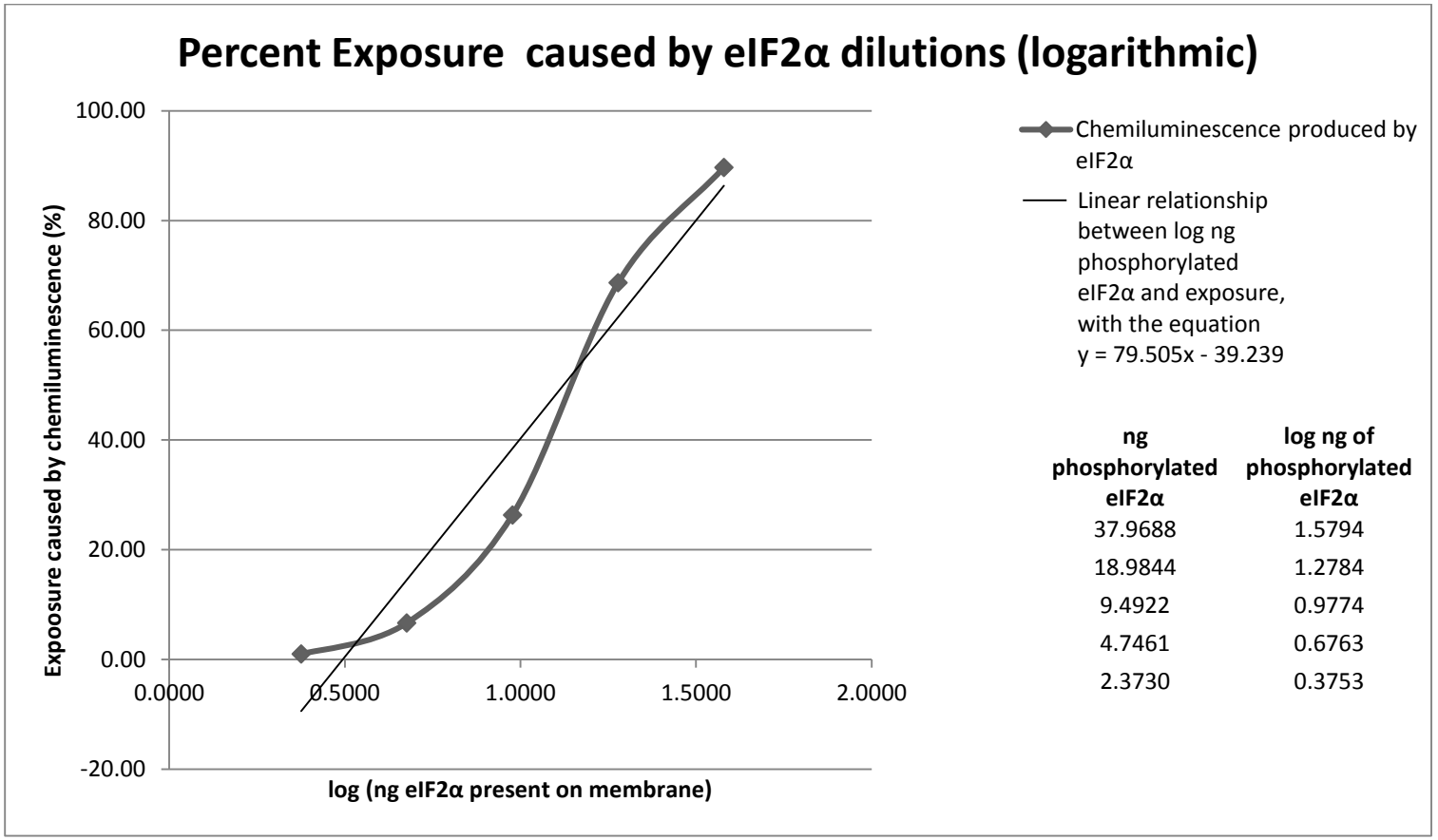

Figure 3.10: Relationship between concentration of phosphorylated eIF2α and amount of chemiluminescence detected in Figure 3.8, lanes 8-12. Each datapoint is log of the ng of phosphorylated eIF2α present in a lane (x axis) plotted against the corresponding degree of exposure caused by that band (y axis). The relationship describes an S curve, which only corresponds to a linear model (equation y = 79.505x - 39.239) at concentrations of phosphorylated eIF2α greater than 18.98 ng.

Equation 2:

$$\textit{Percentage chemiluminescence detected} = 79.505 \times \log_{10} [\textit{ng of phosphorylated eIF2}\alpha \textit{ in lane}] - 39.23$$

To calculate the amount of phosphorylated eIF2α present in the glyphosate sprayed *A. thaliana* control, the lane containing 5µg of total plant protein (Figure 3.8, panel B, lane 3) was used, as the amount of chemiluminescence detected was 24.3%. This fits within the limits for Equation 1. As the linear model Equation 1 is a better fit than that of Equation 2, a more accurate result will be gained where values are calculated using Equation 1, as long as the amount of phosphorylated eIF2α present on the membrane is within the accepted range. Rearranging Equation 1 gives the following:

[Percentage exposure of film] + 14.5 = [ng phosphorylated eIF2α] x 4.3695

Using this equation, 24.3% chemiluminescence gives an estimate of 8.825 ng of phosphorylated eIF2α present in the lane containing 5 µg of total plant protein. This provides a eIF2α concentration of 1.765 ng per µg of total glyphosate treated *A. thaliana* protein, or 0.1765% of this plant protein standard.

For additional accuracy, the amount of phosphorylated eIF2α in lanes containing 2.5 and 10 µg of total plant protein was also calculated using Equations 1 and 2, respectively. Using the rearranged Equation 1, to calculate the amount of eIF2α present in the lane containing 2.5 µg of plant protein, and the amount of chemiluminescence detected is 9.7% (Figure 3.8, panel B, lane 4), it is estimated that phosphorylated eIF2α content of the glyphosate treated *A. thaliana* protein standard is 1.950 ng/µL, or 0.195%.

The amount of chemiluminescence detected can be used to calculate the amount of phosphorylated eIF2α in the lane containing 10 µg of glyphosate treated *A. thaliana* protein (Figure 3.8, panel B, lane 1) by rearranging Equation 2 as follows:

$$[\text{ng phosphorylated eIF2}\alpha] = 10^{([\text{percentage chemiluminescence detected}+39.239]/79.505)}$$

The amount of chemiluminescence detected in the lane containing 10 µg of glyphosate treated *A. thaliana* plant protein was calculated as 81%. Using the rearranged Equation 2, this gives an estimated phosphorylated eIF2α content of 3.253 ng of phosphorylated eIF2α per µg of total protein, or 0.3253 %. Although the estimates generated using Equation 2 are likely to have some inaccuracies based on the poor fit of the linear equation to the observed results, the estimations of the amount of phosphorylated eIF2α present in each band match what was seen in Figure 3.8 where, visually, the intensity of the band created by 10 µg of *A. thaliana* protein is similar to the intensity of exposure caused by 37.97 ng of bacterially expressed eIF2α.

The estimated amounts of eIF2α present in the glyphosate treated *A. thaliana* positive control and their correlation with what can be observed in Figure 3.8 provide confidence that that the method of calculating the amount of chemiluminescence produced and the corresponding equations are appropriate. The amount of phosphorylated eIF2α present in protein extracted from *A. thaliana* can now be determined using the positive control (i.e. the protein extracted from glyphosate treated *A. thaliana*) as a reference, provided the unknown sample contains between 3.162 and 63.10 ng of phosphorylated eIF2α per lane.

3.5. Detection of phosphorylated eIF2α in time-point sampled TVCV and TYMV inoculated *A. thaliana*

In order to determine if eIF2α is phosphorylated upon infection with TVCV or TYMV, two experiments were carried out, each containing 48 wild-type and 48 IPK knockout *A. thaliana* plants. The 96 plants were inoculated with the target virus (see section 2.2.1), and the same number of *A. thaliana* plants mock-inoculated as a control to give a total count of 144 plants per virus.

3.5.1. Inoculation and confirmation of infection of *A. thaliana* with TVCV

To detect the phosphorylation of eIF2α at any stage of the infection process, samples of the inoculated leaves were taken immediately after inoculation and at 3 and 9 hours, 1, 2, 3, 5 and 7 days after inoculation. As the most recently developed leaf was produced after virus inoculation, presence of the virus in the most recently developed leaf indicated systemic infection of the host plant by the virus. At 28 dpi, samples were taken from the most recently developed, fully expanded leaf for confirmation of virus infection

via ELISA as described in section 2.2.4. Despite some issues with infection in nine of the uninoculated control plants (discussed in 3.7.2), all of the TVCV inoculated *A. thaliana* were infected (data not shown), even though all plants remained asymptomatic throughout the experiment. This may be due to a lower virus titre caused by a difference in temperature (Seo, 2001, Cowell, 2013) between the two experiments, as the initial experiment was performed in early spring, and the later performed in midsummer.

3.5.2. Quantification of phosphorylated eIF2α present in TVCV infected *A. thaliana* tissue

To detect any eIF2α phosphorylation in plants infected with TVCV, total plant protein was extracted from each sample using protein extraction method B and quantified using the Qubit® assay. A total of 8 µg of plant protein from each sample was loaded onto an SDS-PAGE gel for electrophoresis, followed by western blot analysis as described in sections 2.6, 2.6.1, 2.6.2 and 2.6.4. As shown in Figure 3.11, the expected 37 kDa band was detected in lanes containing 1, 5 and 10 µg of positive control protein extracted from glyphosate treated *A. thaliana* (described in section 3.4), indicating there were no issues with the experimental procedure. In contrast, phosphorylated eIF2α could not be detected in any of the TVCV infected samples at any stage following inoculation. Given that the plants were demonstrated to be virus infected, this indicates that eIF2α is not phosphorylated in *A. thaliana* in response to infection by TVCV.

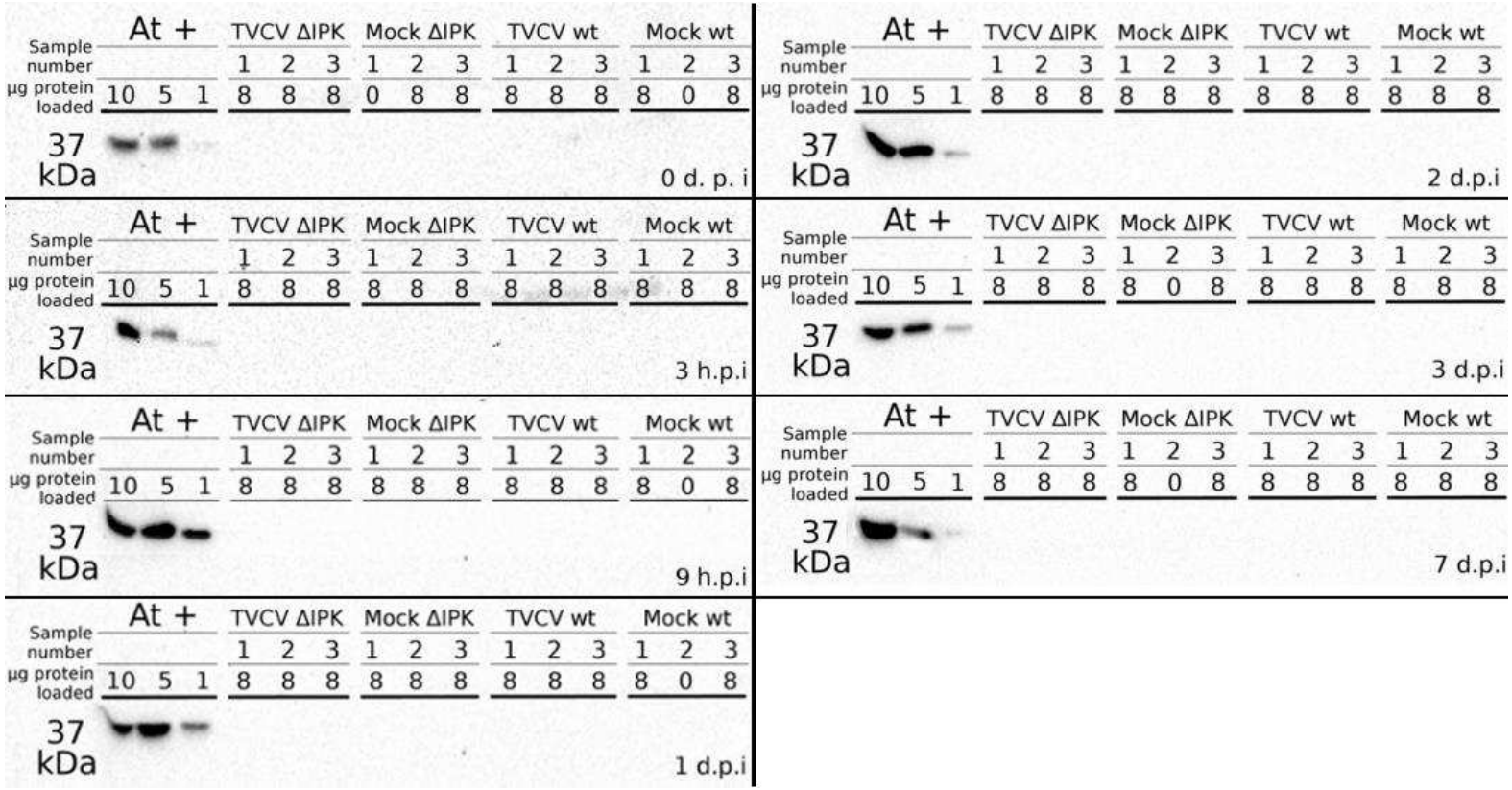

Figure 3.11: Western detection of phosphorylated eIF2α in wild-type (wt) and deficient (ΔIPK) A. thaliana either inoculated with TVCV or buffer (mock). Leaf samples were collected at 0 dpi, 3 and 9 hpi, and 1, 2, 3 and 7 dpi.

Although the glyphosate treated *A. thaliana* positive control samples are clearly visible in all of the exposures in Figure 3.11, in many cases there is not a clear gradient between the 5 and 10 µg amounts of total protein. This is likely due to the positioning of the lanes on the membrane, as there appears to be some loss of sample in the lane closest to the edge. In order to avoid this in future quantification, an empty lane was left between lanes containing protein used in the quantification process and the edge of the membrane. However, as there is no phosphorylated eIF2α present within the samples tested, there was nothing to quantify and so no phosphorylated eIF2α was quantified from these westerns.

3.5.3. Inoculation and confirmation of infection of *A. thaliana* with the virus TYMV

A similar experiment to that performed using TVCV was carried out using TYMV. Western analysis was used to determine phosphorylation of eIF2α in response to inoculation with TYMV in wild-type and ΔIPK mutant *A. thaliana*. Samples were taken at 0, 3, 6 and 9 hpi, 1, 3 5, 7 and 14 dpi; however, not all plants were sampled due to death of some plants from virus infection before samples could be taken. At 28 dpi, the remaining plants were inspected for signs of symptom development; all plants inoculated with TYMV displayed strong symptoms, including stunting, chlorosis, vein clearing, thin and/or limp inflorescences or plant death. None of the control plants showed any of these symptoms. From this and previous work described in section 3.1, it was determined that symptomology was sufficient to confirm TYMV infection. Consequently, TYMV was confirmed to have a 100% infection rate, all control plants were uninfected, and no further diagnostic tests were performed.

3.5.4. Quantification of phosphorylated eIF2α present in TYMV infected *A. thaliana* tissue

As with the TVCV infected tissue, protein was extracted from all infected leaves and run out on a western blot with proteins from the control glyphosate treated *A. thaliana*, then incubated with the phosphorylated eIF2α antibody as described in section 2.6.3. As is shown in Figure 3.1.2, the positive control glyphosate treated *A. thaliana* protein was clearly visible in all exposures, indicating no issues with experimental procedure. However, no phosphorylation of eIF2α is detected in protein extracted from plant tissue from wild-type or IPK mutant *A. thaliana* regardless of viral infection.

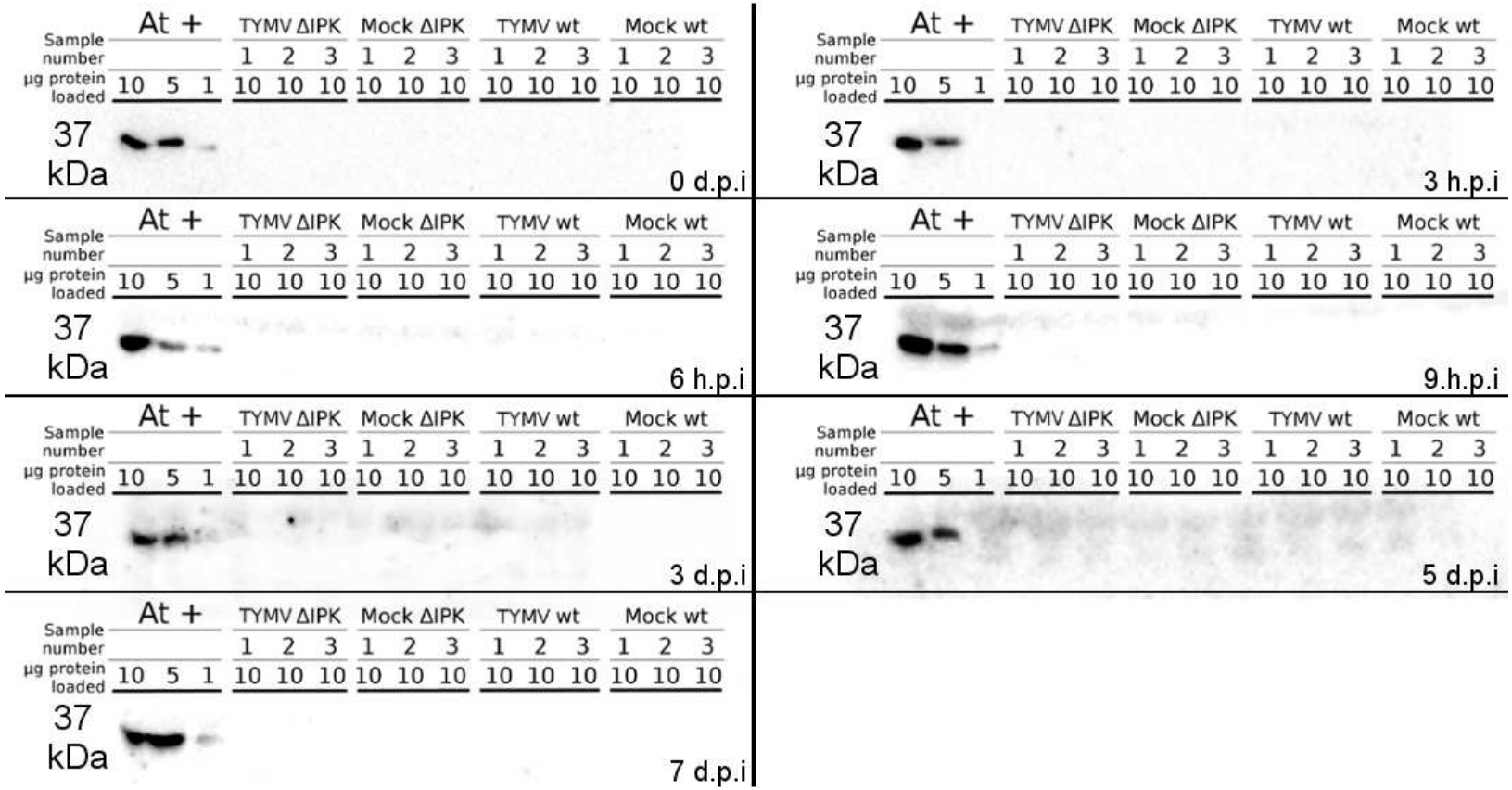

Figure 3.12: Detection of eIF2a phosphorylation in wild-type (wt) and ΔIPK mutant A. thaliana *either inoculated with TYMV or buffer (mock) by western blot using a phosphorylated eIF2α specific antibody. Leaf samples were collected at 0 dpi, 3, 6 and 9 hpi, and 3, 5 and 7 dpi.*

3.6. Summary of results

Few of the viruses tested were found to have a reliable rate of infection in *A. thaliana* under the experimental conditions available; however inoculation of *A. thaliana* with TVCV and TYMV appeared to give reliable infection rates. A generic eIF2α antibody was proven to be unsuitable for use on plant tissue, and a phosphorylated eIF2α antibody was optimised for use in western blot on total protein extracted from *A. thaliana*. The quantification of eIF2α in glyphosate treated *A. thaliana* allowed the quantification of phosphorylated eIF2α in unknown sample, showing that at least 3.162 ng of phosphorylated eIF2α must be present in a lane to detect phosphorylated eIF2α in a western blot. Western analysis of *A. thaliana* plants inoculated with either TVCV or TYMV and sampled over a two week period showed that infection by these viruses does not cause detectable phosphorylation of eIF2α between 3h post-infection and 7 dpi.

3.7. Discussion of results

3.7.1. Quantification of phosphorylated eIF2α in positive control *A. thaliana* protein

Bacterially expressed *in vitro* phosphorylated eIF2α was used as a reference to quantify the amount of phosphorylated eIF2α present in glyphosate treated *A. thaliana* (section 3.4). Due to the limited amount of bacterially expressed phosphorylated eIF2α, the quantification experiment contained a limited amount of samples and was only repeated once (data provided for only one duplicate).

To better quantify the amount of phosphorylated eIF2α present in the positive control, it would have been preferable to repeatedly measure protein concentration in the bacterially expressed eIF2α sample via Qubit® fluorometry in order to reduce any error caused by inaccuracies inherent to the measuring process. In order to more accurately quantify the amount of phosphorylated eIF2α present in the glyphosate treated *A. thaliana,* it would have been preferable to have had sufficient bacterially expressed *in vitro* phosphorylated eIF2α to prepare further western membranes quantifying the amount of phosphorylated eIF2α present in the control glyphosate treated *A. thaliana* against bacterially expressed *in vitro* phosphorylated eIF2α. Repeated lanes containing the same volume of glyphosate treated *A. thaliana* control and bacterially expressed *in vitro* phosphorylated eIF2α would allow the quantification of the range of error present in detection of phosphorylated eIF2α by western blot.

In addition to the margin of error caused by the low number of samples in westerns containing bacterially expressed *in vitro* phosphorylated eIF2α, the quantification of bacterially expressed eIF2α by Qubit® fluorometry assumed that the sample of bacterially expressed eIF2α contained no proteins other than eIF2α, which was not the case. The eIF2α generic antibody detected multiple bands at around 50 kDa (Figure 3.5), which did not correspond to the size of either eIF2α (37 kDa) or PKR (68 kDa, (Meurs et al., 1990)), indicating that eIF2α and PKR were not the only proteins present in the sample. Although the generic eIF2α antibody proved unsuitable for detection of plant eIF2α, in order for unknown bands to be visible in lanes containing only bacterially expressed eIF2α and PKR, additional proteins must have been present in the bacterially expressed eIF2α for the antibodies to bind to. The amount and identity of the protein is unknown, and therefore the

actual amount of eIF2α present in the bacterially expressed phosphorylated eIF2α will have been lower than expected. This means that the control protein extracted from glyphosate treated *A. thaliana*, and, subsequently, all samples where the phosphorylated eIF2α content was estimated using the control protein as a reference, may have contained less phosphorylated eIF2 than estimated.

If the above changes to the experimental procedure had been made and the amount of phosphorylated eIF2α present in both the bacterially expressed phosphorylated *in vitro* eIF2α and the glyphosate treated *A. thaliana* positive control, the outcome of this experiment would have remained the same as no eIF2α phosphorylation was detected upon infection with either TVCV or TYMV. However, it would have allowed a more accurate quantification of the changes in phosphorylated eIF2α produced upon glyphosate treated, VSR expressing, *N. benthamiana*, as described in section 5.8.1.

3.7.2. Detection of Tobamovirus infection in mock-inoculated *A. thaliana*

During the investigation into potential eIF2α phosphorylation upon infection of *A. thaliana* with TVCV (section 3.5.1), some mock-inoculated plants tested positive for TVCV. As a broad-spectrum Tobamovirus antibody was used to detect TVCV infection, it is possible that the mock inoculated *A. thaliana* which tested positive for TVCV were infected with another member of the Tobamovirus genus. Because the antibody used in the ELISA test is not species specific, if another Tobamovirus was present, some of the TVCV inoculated plants may have been infected with the unknown virus as well. As the mock inoculations were done before any handling of TVCV infected material, it is unlikely that the Tobamovirus detected in mock-inoculated plants was due to cross infection with TVCV.

A potential source of cross-contamination is TMV infected *A. thaliana*, which were grown in the same room. TMV is highly contagious and easily transmitted by contact between infected and healthy plants or via a fomite (Sacristán et al., 2011). Precautions taken to avoid cross contamination were the use of sterilized blades used to trim inflorescences and take samples, gloves were changed between working with one virus and another, mock-inoculated plants were handled before virus-inoculated plants, and a physical distance of 30 cm was kept between mock inoculated and virus inoculated plants. No known insect vectors of TMV were visible, although Sciarid flies were present, thus plants were treated with confidor insecticide at two weeks post inoculation. Despite these precautions, cross-contamination still appeared to have occurred, and some samples isolated from the mock control group were not able to be used in the final experiment. If time allowed, it would have been preferable to repeat the experiment to be certain that the TVCV inoculated plants did not also contain an unknown and undetected Tobamovirus, although the outcome of the experiment would not have altered as no phosphorylated of eIF2α was detected in any of the TVCV inoculated plants.

Chapter 4

Can VSRs affect eIF2α kinases outside of viral infection?

Methods and materials

4.1. Plants

Wild-type *N. benthamiana* were grown in Daltons Premium Seed Mix® and maintained at 22ºC, 16 hours light and 8 hours dark for the duration of the experiment. Seeds were initially sown in bulk, and the seedlings transferred into individual pots at two weeks post germination. The *N. benthamiana* plants were then left to mature for 3-10 days before infiltration, depending on the experiment.

4.2. Glyphosate treatment methods

Previous work by another researcher in the laboratory showed variation in the amount of phosphorylated eIF2α present in *N. benthamiana* treated with 150 μM glyphosate. In an attempt to reduce this variation, a range of glyphosate application methods were trialled. Two brands of glyphosate were used; RoundUp™ Concentrate and an unknown brand provided by a colleague. Both brands were diluted to the required concentration in ddH_2O directly before use. Depending on the experiment, plants were either sprayed with 150 or 1500 μM glyphosate, infiltrated with 150 or 300 μM glyphosate, or the areas of the plant above the soil immersed for one minute in 150, 300, 500, 1000 or 1500 μM glyphosate. Immersion in glyphosate was achieved by holding the pot in one hand in such a manner that fingers prevented the fall of soil, and then turning the pot and plant upside-down to allow immersion of the plant without saturating the soil with glyphosate.

4.3. Transformation of *A. tumefaciens*

4.3.1. Growth and maintenance of *A. tumefaciens*

The bacteria used for transformation and infiltration was electrocompetent *A.tumefaciens* strain GV3101, and was provided by The New Zealand Institute for Plant and Food Research. Cultures were in all cases grown either in LB broth or LB agar containing 50 µg/mL rifampicin and 50 µg/mL gentamycin, as well as other selective antibiotics where appropriate. Cultures were grown at 28ºC and stored at 4ºC for a maximum of two weeks, or if liquid, mixed with an equal volume glycerol and frozen at -80ºC. Cultures which were not frozen were transferred onto fresh media weekly.

4.3.2. Plasmids

Table 4.1 details plasmid information. All stock plasmids were provided by Robin MacDiarmid from Plant and Food Research, with the exception of plasmid p6p100, which was kindly provided by Professor Thomas Höhn (The Friedrich Miescher Institute for Biomedical Research, Basel, Switzerland

Table 4.1: Plasmids used for transformation of A. tumefaciens *and subsequent agroinfiltration of* N. benthamiana*. CMV: Cucumber mosaic virus, CaMV: Cauliflower mosaic virus, PVY: Potato virus Y, TBSV: Tomato bushy stunt virus.*

Plasmid Name	Insert	Backbone	Selective Antibiotic	Insert Size	Plasmid Reference	Gene Reference
2b241	2b gene from CMV strain 241 (Fny)	pGD	Kanamycin 100 µg/mL	333bp	(Goodin et al., 2002)	(Sulistyowati et al. 2004)
2b207	2b gene from CMV strain 207 (Fny)	pGD	Kanamycin 100 µg/mL	333bp	(Goodin et al., 2002)	(Sulistyowati et al. 2004)
P6p100	P6 gene from CaMV strain CM1841	pEarlyGate100	Kanamycin 100 µg/mL	1563bp	(Gleave, 1992)	(Gorden et al. 1988)
HC-ProPVY	HC-Pro gene from PVY (unknown strain)	pGD	Kanamycin 100 µg/mL	1380bp	(Goodin et al., 2002)	(Glais et al., 1998)
P19wt	P19 gene from TBSV	pART27	Spectinomycin 100 µg/mL	519bp	(Gleave, 1992)	(Hearne et al., 1990)
P19mut	P19 mutant gene from TBSV, point mutations at 71 and 72 bp	pART27	Spectinomycin 100 µg/mL	519bp	(Gleave, 1992)	Provided by Robin MacDiarmid, unknown origin
IPKpHEX	Human IPK	pHEX	Spectinomycin 100	1434bp	(Hellens et al., 2005)	(Barber et al., 1994)

4.3.2.1. Transformation of *Escherichia coli*

Plasmid DNA was diluted to between 2 and 20 pg/µL in ddH_2O and electroporated into competent *E. coli* cells in an Eppendorf Epoarator® set to 1710V. Cells were then allowed to recover for one hour in 1 mL LB broth at 37ºC under agitation. After recovery, 100 µL of culture was spread onto LB agar containing the appropriate selective antibiotic as described in Table 4.1. The remaining culture was centrifuged at 13000 rcf, the supernatant removed and the pellet resuspended in 100µL LB broth. This was then plated onto LB agar containing the appropriate antibiotic and grown for 24 hours at 37°C. Individual colonies from either plate were then screened using colony PCR to confirm presence of vector and insert as described in section 4.3.4 .

4.3.2.2. Plasmid extraction

Colonies which had been confirmed to contain the vector and insert from section 4.3.2.1 were used to inoculate 3 mL of LB broth containing the appropriate selective antibiotic and grown overnight under agitation at 37°C. Plasmids from the cell culture were then extracted using GenElute PureLink® Quick Plasmid Miniprep kit Sigma-Aldrich (St Louis, MO, USA) according to manufacturer's instructions.

For each plasmid, 2 mL of LB broth with the appropriate antibiotic was inoculated with transformed *E. coli* and grown overnight at 37ºC under agitation. The culture was then centrifuged at 12000 rcf for 2 minutes and the medium discarded. The *E.coli* cells were then resuspended in the provided resuspension buffer. The cells were then lysed and the cellular debris precipitated and removed via centrifugation. The plasmid DNA was then bound to the provided spin column and washed with both wash buffers provided, centrifuging at 12000 rcf in between each wash. Finally, plasmid DNA was eluted using ddH_2O instead of the provided elution buffer, as plasmids were later sequenced and the salts present in the elution buffer can interfere with sequencing (Macrogen, 2008). The final concentration of plasmid was measured using a Thermo-Fisher Nanodrop 1000 spectrophotometer at 260 nm

4.3.2.3. Confirmation of plasmid insert via Macrogen sequencing

In order to be certain that plasmids contain the correct insert, plasmids were sent for sequencing by Macrogen Standard Seq™ (Geumcheon-gu, Seoul, Korea). In order to be sequenced, plasmids were, where necessary, concentrated by centrifugation at 3000 rcf under vacuum overnight, and made up to 100 ng/µL using ddH_2O. Concentration of plasmid was measured using a Thermo-Fisher Nanodrop 1000 spectrophotometer at 260 nm. The sequence primer used binds to the 35S promoter, with the sequence 5´-ACAGTGGTGCCCAAAGATGGAC-3´ and annealing temperature of 57ºC. This was submitted for sequencing purposes with the plasmid at 10 pmol/µL.

All sequence data was analysed using Geneious 1.6.1 (Biomatters, 2013). In order to identify the insert sequence, the insert sequence was isolated from the promoter and terminator sequence. As the forward sequencing primers bound to an area within the 35S promoter sequence, it was necessary to remove the data belonging to the 35S promoter to prevent BLASTn search results from returning results related to the 35S promoter and not the insert. To do this, sequences were aligned with the 35S promoter sequence (Cooke and Penon, 1990) using the Geneious pairwise alignment tool. The sequence identical to the 35S promoter sequence was then removed from the beginning of the sequence. Any area of the sequence after the inserted gene identical to the terminator sequences from the octopine synthase (OCS) and nopaline synthase (NOS) genes was also removed in this manner.

Sequences similar to that of the trimmed sequences were then searched in the National Center for Biotechnology Information (NCBI), using the Geneious MegaBLAST (Morgulis et al., 2008) nr nucleotide search function and default search parameters.

4.3.2.4. Confirmation of plasmid insert via enzymatic digestion of plasmid

To determine if the plasmid p6p100 contained the inserted gene p6, the plasmid was digested using Invitrogen *Hin*dIII restriction enzyme. In a 1.5 mL tube, 15 U *Hin*dIII, 2 µL 10x REact®3 buffer, 500 ng p6100 and sufficient sterile ddH_2O to bring the total volume to 20 µL was mixed, then incubated at 37ºC for one hour. The solution was then mixed with 2 µL loading dye (as described in section 2.2.5.3) and mixed. From this, 15 µL was loaded into a 2% agarose 1 x TAE agarose gel (2% agarose, 40mM Tris-HCl [pH 8.4], 1mM EDTA, and 0.11% glacial acetic acid). One lane per gel contained 8-10 µg 1 Kb Plus DNA Ladder (Life Technologies, Carlsbad, CA, USA). The gel was run in 1 x TAE at 100 V for 60 minutes, then immersed in 0.01% ethidium bromide in 1x TAE for 20 minutes.

After staining with ethidium bromide, the gel was examined under UV light using a Bio-Rad GelDoc™ 1000 imager. Presence of a single band larger than 12000 bp indicates an empty vector (pEarleyGate), and presence of two bands, one at approximately 2500 bp and at sizes greater than 12000 bp indicates presence of both vector and insert.

4.3.3. Transformation of *A. tumefaciens*

In order to transform *A. tumefaciens* with the required plasmid, 2-20 ng of plasmid was added to 50 µL of electro-competent *A. tumefaciens* (provided by the New Zealand Institute for Plant and Food Research) and the mixture briefly vortexed. The *A. tumefaciens* was then placed into an Eppendorf Eporator® electroporation chamber and electroporated at 1440 V with an Eppendorf Eporator®. The chamber was removed from the machine and 1 mL of LB broth was added and mixed by pipetting up and down. The solution was then

incubated at 28ºC for four hours, after which 100 µL was plated onto LB agar containing 50 µg/mL rifampicin and 50 µg/mL gentamycin as well as the appropriate selective antibiotic for the plasmid used. The remaining cell culture was centrifuged, the supernatant removed and the pellet resuspended in 100 µl LB broth. This was also plated onto LB agar containing the appropriate antibiotics and the agar plates incubated at 28ºC for 48 hours. Individual colonies from either plate were then screened using colony PCR to confirm presence of vector and insert as described in section 4.3.4 .

4.3.4. Primer design

The primers p19 F and p19 R were kindly provided by the New Zealand Institute for Plant and Food Research. The primers CMV241-2b F, CMV241-2b R, HC-Pro Olliver1 F, HC-Pro Olliver2, p6 F and p6 R (Table 4.3) were designed using Primer 3 (Untergasser et al., 2012) from the sequences obtained in section 5.2.

4.3.5. Confirmation of successful transformation via colony PCR

Colony screening via PCR was undertaken by the addition of 0.2 µl of colony to 20 µL of PCR master mix, which consisted of 0.2 µM forward primer, 0.2 µM reverse primer, 0.25 µM dNTPs, 1x PCR buffer (10 mM Tris-HCl, 50 mM KCl [pH 6.8]), 2.5 mM$MgCl_2$ and 1 U *Taq* native DNA polymerase (Life Technologies, Carlsbad, CA, USA) in ddH_2O. When plasmid DNA was used as a positive control, 5ng of plasmid DNA was added to the mix instead of 0.2 µL of *A. tumefaciens* colony. The PCR products were then examined via agarose gel electrophoresis as described in section 2.2.5.3. Presence of a band the same size as the amplified area of vector and insert (see Table 4.2 for primer details) was used as confirmation of successful transformation.

Table 4.2: Primers used for confirmation of successful transformation of A. tumefaciens *and* E.coli *via PCR, including sequence, primer target and amplicon size. All primers anneal at 55ºC.*

Primer	**Sequence (5´-3´)**	**Target**	**Expected product size**	
			Plasmid	**Amplicon size**
277 F	CGCACAATCCCACTATCCTT	35S promoter in pART27,	pART27	116 bp
			P19wt	635 bp
			P19mut	635 bp
277 R	AGGCGTCTGCGCATATCTCAT	OCS terminator in pART27	pHEX	120 bp
			IPKpHEX	1554 bp
			p100	Approx. 100 bp
			P6p100	Approx. 1650 bp
277 F	CGCACAATCCCACTATCCTT	35S promoter in PGD	pGD	Approx. 600 bp
			2b241	Approx. 933 bp
NOS R	TTATCCTAGTTTGCGCGCTA[1]	NOS terminator in pGD	2b207	Approx. 933 bp
			HC-ProPVY	Approx 1980 bp

[1](Hardegger et al., 1999)

4.4. Infiltration of *N. benthamiana*

4.4.1. Preparation of *A. tumefaciens*

In order to introduce the largest number of actively growing and replicating transformed bacterial cells to the *N. benthamiana* plants, the cultures of *A. tumefaciens* were grown into larger volumes in a series of steps. First, colonies of transformed *A. tumefaciens* on LB agar were replated onto LB agar containing 50 µg/mL rifampicin, 50 µg/mL gentamycin and 100µg/mL of the selective antibiotic and were incubated at 28ºC overnight. Tubes containing 4 mL of LB broth to which the same antibiotic cocktail had been added were then inoculated with the overnight culture and grown for a further 16 hours under agitation at 28ºC. Fresh LB broth (10 mL) was then prepared using the antibiotics as described above, to which acetosyringone was added to a final concentration of 150 µm. This was then inoculated with 50 µL of the overnight liquid culture and incubated overnight under agitation at 28ºC.

The cells were then collected by centrifugation at 4000 rcf for 15 minutes and resuspended in infiltration buffer (10 mM $MgCl_2$, 10 mM MES [pH 5.7, autoclaved], 500 µM acetosyringone) to an optical density of 1.00 when read using a spectrophotometer set to 600 nm and blanked using uninoculated infiltration buffer. The culture was then left to incubate for four hours at room temperature.

4.4.2. Infiltration of *N. benthamiana*

The leaves of three to four week old *N. benthamiana* were infiltrated with *A. tumefaciens* which had been treated as described in section 4.4.1. This was done by filling a 1 mL syringe without needle with the desired culture and applying the nozzle of the syringe to the underside of the leaf. Gentle counter pressure was applied to the other side of the leaf with a fingertip. Pressure was then applied to the syringe in order to force the culture into the air gaps inside the leaf until the entire leaf was fully infiltrated with the desired culture. Only one leaf was infiltrated per plant, and the leaf chosen varied between experiments. The plants were then left for four to five days to allow full expression of the gene of interest. The plants were then treated with glyphosate in one of the ways described in section 4.2, and allowed to rest for a further 24 hours before sampling. Two samples were taken from each side of the midrib, in the centre of the infiltrated leaf, and were 1 cm^2 in size. Samples were then placed into two separate 1.5 mL tubes, sealed, frozen in liquid nitrogen and stored at -80ºC until use.

4.5. Confirmation of expression of gene of interest

Confirmation of expression of the gene introduced to *N. benthamiana* plants via agroinfiltration was done by RT-PCR of RNA extracted from infiltrated tissue five days post-infiltration. RNA was extracted from the infiltrated tissue as described in section 2.2.5.1, with the additional step of the addition of 10 µL DNase I and 70 µL of Sigma DNase II (Sigma Aldrich, St Louis, MO, USA) to the column after binding. The RNA was then used as a template for cDNA synthesis (section 2.2.5.2), with the exception that the primers used bound to the inserted gene specifically, as detailed in Table 4.3.

The cDNA was then examined via agarose gel electrophoresis as described in section 2.2.5.3. It was assumed that presence of a band of the correct size indicated the inserted gene was being successfully transcribed into mRNA, and then expressed as a protein.

Table 4.3: Primers used for confirmation of expression of the gene of interest in infiltrated N. benthamiana *tissue, including sequence, primer target, annealing temperature and amplicon size.*

Primer	Sequence (5´-3´)	Target	Annealing temp	Amplicon size
P19 F	ATTTCTCGAGCCATGGAACGAGCTATA	P19 from TBSV	61°C	518 bp
P19 R	CCCTTCTAGATTACTCGCTTTCTTTTTCGA			
HC-ProGlias F	CGAAGGGGTGATAGTGGAGT[1]	HC-Pro from PVY (multiple strains)	57ºC	1.8 kb
HC-ProGlias R	GTTTCTGCCGCTGACACTCG[1]			
HC-ProOlliver1 F	TGCCGGTTAGCGATCTGTTT	HC-Pro insert in plasmid HC-ProPVY	63ºC	235 bp
HC-ProOlliver1 R	ATGAATGGCAGGTGGCTCAA			
CMV241-2b F	CTCCACCTAGCCCATTTGCA	2b insert in plasmid 2b241	56ºC	168 bp
CMV241-2b R	ACGGGATCTACTCCGTGGAA			
P6p100 F	CTCTTCGCAACAAGGAGACC	P6 gene from CaMV	64ºC	173 bp
P6p100 R	GGCTTTACGGGCCTAATTTC			

[1] (Glais et al., 2002)

4.6. Protein extraction

Protein extraction was undertaken as described in section 2.2.5.3 using protein extraction method B, and total protein extracted quantified using Qubit® fluorometry.

4.7. Quantification of phosphorylated eIF2α in infiltrated *N. benthamiana*

Presence, absence and quantification of eIF2α was undertaken as described in sections 2.6, 2.6.1, 2.6.2 and 2.6.4, using the positive control developed as described in section 3.5.2.

Chapter 5

Can VSRs affect eIF2α kinases outside of viral infection?

Results

To complete Aim 2 of this research, to determine if plant VSRs alter eIF2α kinase activity, *N. benthamiana* plants transiently expressing the VSRs 2b, HC-Pro, p6, p19 or no VSR were treated with glyphosate and the amount of phosphorylated eIF2α produced measured via western blot. In order to do this, *A. tumefaciens* was transformed (section 4.3.3) using a number of binary vectors capable of expressing plant virus VSRs within plant tissue (Table 4.1). The transformed *A. tumefaciens* was infiltrated into the one leaf of each of six healthy *N. benthamiana* (section 4.4), where the VSR was expressed by the plant cells. After four days to allow the transient expression of the VSR, the leaves of three of the six plants were infiltrated with glyphosate (section 4.2) and left for 24 hours to allow eIF2α phosphorylation. To determine if the expression of a VSR had an effect on the amount of phosphorylated eIF2α present, the amount of phosphorylated eIF2α in the leaf tissue was determined via western blot (as described in section 2.6).

5.1. Induction of eIF2α phosphorylation in *N. benthamiana*

Initial attempts to induce eIF2α phosphorylation by the spraying of plants with 150 μM glyphosate caused a low and variable amount of eIF2α phosphorylation (Figure 5.1). Thus, although the application of 150 μM glyphosate via aerosol was a suitable method for inducing eIF2α phosphorylation in *A. thaliana,* it proved unsuitable for use with *N. benthamiana*. Neither increasing the concentration of glyphosate (Figure 5.1), nor changing the method of application (Figure 5.2, see section 4.2 for method), significantly improved the amount and reliability of eIF2α phosphorylation in plant tissue. Increasing the concentration of glyphosate to 300 μM and applying the glyphosate by infiltration of the leaf tissue did provide some minor improvement (Figures 5.1 and 5.2).

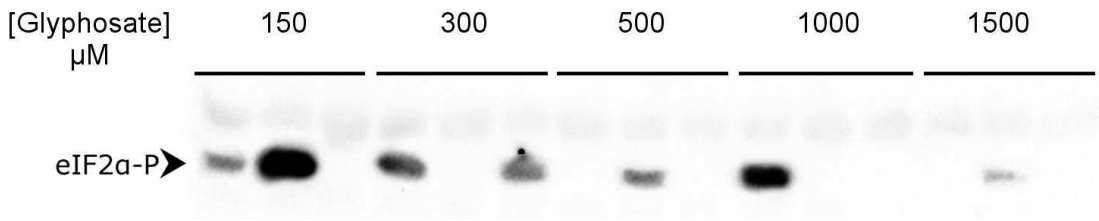

Figure 5.1: Western blot detection of phosphorylated eIF2α. Each lane contains 10 µg of total protein extracted from N. benthamiana *leaves sprayed with varying concentrations of glyphosate. Three leaves, each taken from a different plant 24 hours after glyphosate treatment, were tested. Increasing glyphosate concentration does not appear to increase the amount or reliability of phosphorylated eIF2α present within the leaf tissue.*

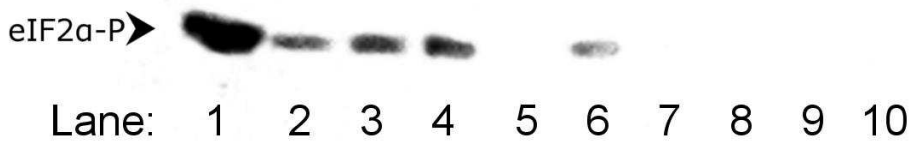

Figure 5.2: Detection of phosphorylated eIF2α in plant tissue by western blot. All lanes contain 10 µg of protein. Lane 1 contains positive control glyphosate sprayed A. thaliana*. Lanes 2 – 10 show phosphorylation in* N. benthamiana infiltrated *with 150 µM glyphosate (lanes 2 and 3); sprayed with 150 µM glyphosate (lanes 4-7) and immersed in 150 µM glyphosate for one minute (lanes 8-10). All samples were collected 24 hours after treatment. Topical application of glyphosate produces weak and intermittent phosphorylation of eIF2α, whereas infiltration of glyphosate into the air gap within the leaf produces weak but consistent phosphorylation of eIF2α.*

As eIF2α is also phosphorylated during germination as part of the developmental process (Le et al., 1998), it was suspected that the low and sporadic concentration of phosphorylated eIF2α in glyphosate treated *N. benthamiana* may be due to the age of the leaf sampled. In order to determine whether or not this was the case, three week old *N. benthamiana* seedlings of the same developmental state had each leaf labelled in order of age, where "1" was the newest emerging leaf and "3" the third oldest leaf. All plants had all leaves excluding the cotyledons fully infiltrated with 300 µM glyphosate. After 24 hours, each leaf was sampled, the protein extracted, and the phosphorylated eIF2α content examined via western blot with the phosphorylated specific eIF2α antibody (section 2.6).

As shown in Figure 5.3, the less developed the leaf, the higher the concentration of phosphorylated eIF2α present in glyphosate treated leaf tissue. As leaves aged, the quantity of phosphorylated eIF2α present per gram of protein within the leaf tissue decreased. Therefore, it was concluded that the older age of the leaves sampled was the cause of the intermittent and low levels of eIF2α phosphorylation in *N. benthamiana* leaves treated with glyphosate. In all subsequent experiments the newest emerging leaf large enough to be infiltrated (greater than 5mm^2) was used.

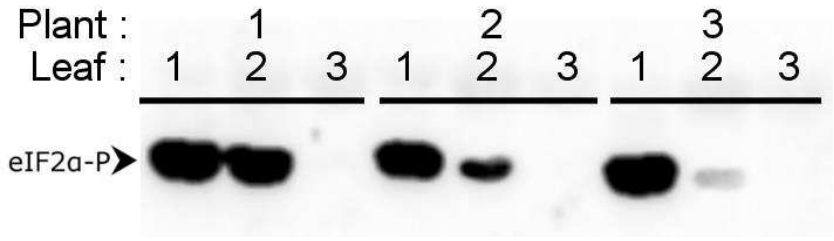

Figure 5.3: Western blot detection of phosphorylated eIF2α present in protein extracted from the tissue of emerging (leaf 1, unfolding (leaf 2) and expanded (leaf 3) leaves) from three individual plants, all of which were treated with 300 µM glyphosate. Samples were collected 24 hours after treatment.

5.2. Confirmation of the presence of plasmid inserts via sequencing

In order to be confident that the VSR of interest would be expressed in *N. benthamiana* tissue upon agroinfiltration, the integrity of the binary vector containing the gene of interest had to be confirmed. To do this, the plasmids to be used for transformation of *A. tumefaciens* were partially sequenced. Plasmids extracted from transformed *E. coli* (described in section 4.3.2.2) were sent to Macrogen for sequencing as described in section 4.3.2.3.

The identity of the plasmid sequences is given in Table 5.1. The sequences from the plasmids 2b241, HC-ProPVY, p19wt, p19mut and IPKpHEX all returned results matching the gene of interest, and with exceptionally low E values in all cases, indicating high confidence in the identity of the sequence. However, the sequenced area of plasmids 2b207 and p6p100 did not contain sequences which matched the gene of interest for each plasmid, and BLAST searches of the sequences against the CMV and CaMV genomes did not return any matches. This was likely due to errors during sample preparation which damaged or contaminated the sample, preventing the sequence from being correctly determined. In order to determine if the plasmids 2b207 and p6p100 did contain the intended genes 2b and p6, further analysis of the plasmid insert was required.

Table 5.1 Megablast results of trimmed sequences from plasmids extracted from transformed E.coli.

Plasmid	Insert	Top Megablast match by E value	Pairwise identity	E value
2b241	2b gene from CMV strain 241 (Fny)	CMV 2a protein and 2b protein mRNAs, complete cds	100%	1.78^{-154}
2b207	2b gene from CMV strain 207 (Fny)	Plant transit expression vector pSAT6-EGFP-Ca, complete sequence	100%	1.13^{-87}
P6p100	P6 gene from CaMV strain CM1841	Site-specific excision vector pCRE3, complete sequence	99.6%	0
HC-ProPVY	HC-Pro gene from PVY	PVY mRNA for polyprotein (pol gene), isolate SCRI-O	95.7%	0
P19wt	P19 gene from TBSV	TBSV partial p19 gene for 19 kDa protein, isolate L8C, genomic RNA	99.2%	0
P19mut	P19 mutant gene from TBSV, point mutations at 71 and 72 bp	TBSV mRNA for a 22kDa and a 19kDa protein	94.2%	0
IPKpHEX	IPK from *Homo sapiens*	*N. benthamiana* P58IPK mRNA, complete cds	96.7%	0

5.2.1. Detection of the inserted gene in the plasmid 2b207

In order to determine whether or not the lack of sequence identity in plasmid 2b207 with the gene 2b was due to an error during sequencing or absence of the gene insert, a PCR was performed. The original aliquot of plasmid provided was used as a template along with primers which bracketed the insertion site of the plasmid (Table 4.2). As the binary vector pGD does not have a publically available sequence, the precise size of the amplicon was unknown. However, the 2b gene in both plasmids 2b241 (confirmed sequence, section 5.2) and 2b207 (no sequence) should be the same size, therefore the PCR was undertaken with 2b241 as a positive control, and empty pGD as a negative control (section 4.3.4).

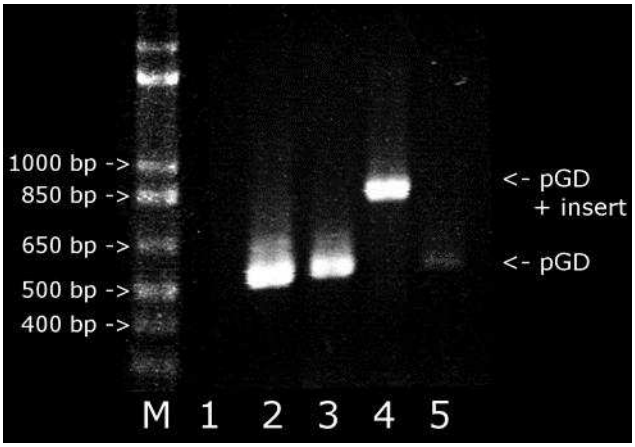

Figure 5.4: PCR amplification of plasmid DNA using the 277F and 277R primers. Lane M: 1 Kb Plus DNA Ladder. Templates used were as follows: No template control (lane 1), empty pGD plasmid (lane 2), stock 2b207 plasmid (lane 3), sequenced 2b241 plasmid (lane 4) and E. coli *transformed with stock 2b207 (lane 5).*

As shown in Figure 5.4, the amplicon from of 2b207 was the same size as that from an empty pGD plasmid. The PCR product from plasmid 2b241 under the same conditions is approximately 350 bp larger than that amplified from the empty pGD. The increase of approximately 350 bp corresponds to the size (333 bp) of the 2b gene. Therefore, it was concluded that the plasmid 2b207 did not contain the gene 2b, and was not suitable for further research

5.2.2. Detection of the gene p6 in the plasmid p6p100

In order to determine whether or not the gene p6 was present in the plasmid p6p100, the plasmid was digested using *Hin*dIII (see section 4.3.2.4) and the number of restriction sites determined using Geneious (Biomatters, 2013). The sequence and size of the vector pEarleyGate and the insert p6 are both publicly available, and both contain a *Hin*dIII restriction enzyme digest site. Therefore, when digested using *Hin*dIII, pEarleyGate was cut once and should produce a single band, whereas p6p100 should be cut once in the plasmid and once in the insert, producing two bands. The distance between the two restriction sites in p6p100 is 2386 bp. As Figure 5.5 shows, when p6p100 was digested using *Hin*dIII (lane 2), two bands were formed; one band of 2.3 kb in size, and one larger band which consists of the remaining uncut plasmid. This provides evidence that the insert p6 is present in the plasmid p6p100.

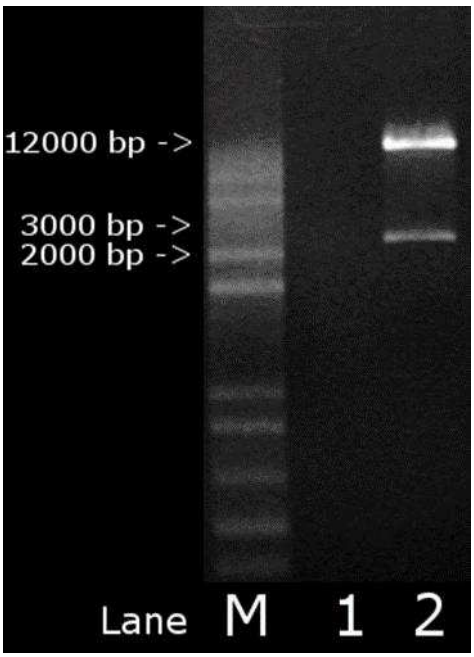

Figure 5.5: Digestion of the plasmid p6p100 with Hin*dIII. Two bands are visible, one at 2300 bp (lane 1), and one at greater than 12000 bp (lane 2). Lane M contain 1 Kb Plus DNA Ladder. Lane 1 contains an* H_2O *control containing only dd*H_2O *and* Hin*dIII. Lane 2 contains 300 ng of digested p6p100.*

5.3. Confirmation of successful transformation of bacteria

To ensure that *E. coli* or *A. tumefaciens* were successfully transformed with the intended plasmid, colonies to be used for plasmid extraction or agroinfiltration were screened for the presence of vector and insert by PCR amplification. In order to determine the size and presence of the insert within the transformed colony, forward and reverse primers which bracket the insertion site of the plasmid were used to amplify the insert via PCR, which was then sized by agarose gel electrophoresis and compared to the expected size of amplicon (section 4.3.4). Colonies transformed with an empty plasmid produced a smaller band than those colonies which had been transformed with a plasmid containing the insert.

Figure 5.6 shows the PCR amplicons produced from successfully transformed *A.* tumefaciens containing the plasmids p19wt, p19mut, p6p100, 2b241, IPKpHEX and HC-ProPVY (panels A to F, respectively). In all cases, the size of the PCR product matched the expected size of the amplicon (Table 4.3), confirming each *A. tumefaciens* colony contains the correct plasmid.

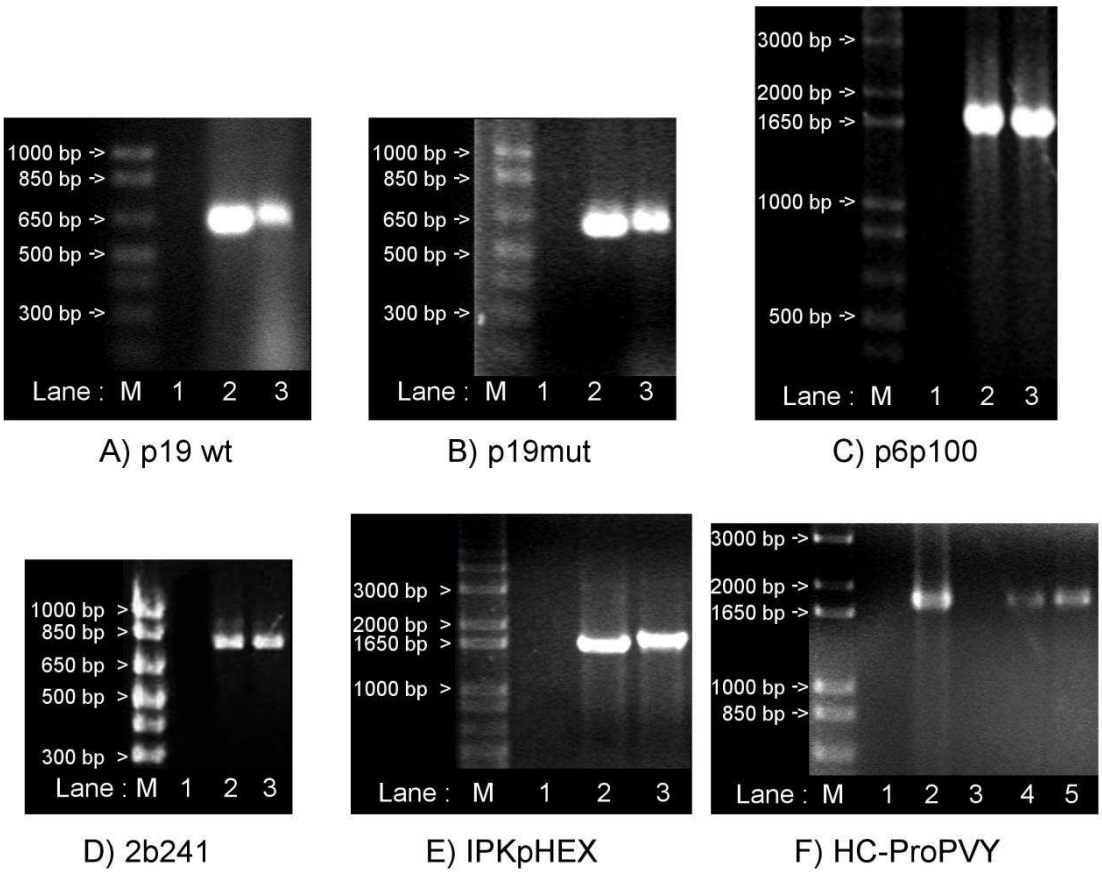

Figure 5.6: PCR products resulting from the amplification of transformed A. tumefaciens colonies. Lane M contain 1 Kb Plus DNA Ladder. Lane 1 contains no template. Lane 2 contains plasmid DNA amplified with the primer pairs 277F and 227R (Panels A, B, C and E) or 277F and NOS R (Panels D and F).Lanes 3, 4 and 5 contain transformed A. tumefaciens *colonies amplified using the primer pairs 277F and 227R (Panels A, B, C and E) or 277F and NOS R (Panels D and F). Only the areas of each gel containing bands are shown.*

5.4. Infiltration of *N. benthamiana* in order to determine if VSR expression alters eIF2α kinase ability

In order to achieve transient expression of a VSR within *N. benthamiana* tissue, transformed *A. tumefaciens* containing the genes 2b, p6, HC-Pro and p19 were cultured to 1 OD, then infiltrated into the leaf tissue of six three-week old *N. benthamiana* plants (see sections 4.4.1 and 4.4.2). To determine if the expression of human IPK in plant tissue altered the ability of a VSR to interfere with eIF2α phosphorylation, an equal number of plants were co-infiltrated with both IPK and VSR encoding *A. tumefaciens*. The plants were then grown in the glasshouse for four days to allow full expression of the gene(s) of interest (Johansen and Carrington, 2001) before infiltration of half of the plants with 300 μM glyphosate. The remaining, and equal, number of *A. tumefaciens* infiltrated plants were not treated with glyphosate, as a control to determine whether or not eIF2α phosphorylation was triggered by the expression of the VSR. All plants were then left for a further 24 hours before the infiltrated leaves were harvested and the phosphorylated eIF2α content determined by western blot.

5.5. Detection of VSR mRNA in *N. benthamiana*

In order to confirm that the VSR was expressed upon introduction of the binary vector to *N. benthamiana* tissue, the RNA was extracted from several leaves infiltrated with *A. tumefaciens*, but not treated with glyphosate, as described in section 5.5.1. All DNA was removed by DNases, and the RNA used as a template for RT-PCR amplification using primers specific to the gene of interest (Table 4.3).

5.5.1. Detection of VSR mRNA via RT-PCR

No anti-VSR antibodies were available in the laboratory, as so in order to have confidence that the VSRs were being produced, VSR mRNA was detected via RT-PCR. To do this, RNA was extracted from *N. benthamiana* leaves five days after infiltration. As part of the RNA extraction process, the DNA within the sample was digested by application of a DNase (see section 4.5). This destroyed all plasmid DNA present within the leaf tissue, including the plasmid DNA, leaving only those sequences which were successfully transcribed to RNA remaining in the sample. The RNA was then used as a template for RT-PCR using the primers detailed in Table 4.3.

Each sample was amplified using both the NAD5 primer pair and the primer pair specific to the infiltrated VSR. Amplification of the NAD5 gene served two purposes; firstly as a positive control to confirm that the RNA was of good quality and the RT-PCR was set up correctly, and secondly, that no genomic DNA was present in the sample. The NAD5 primers border an intron in the NAD5 DNA, which is removed during the production of mRNA. If both RNA and genomic DNA were present in the sample, two bands would be visible in the RT-PCR. The presence of a single band at 180 bp in all lanes amplified with the NAD5 primer pair indicates that no genomic DNA was present in the samples.

Figure 5.7 shows the results of RT-PCR amplification of RNA extracted from *N. benthamiana* infiltrated with wild-type or 2b241 transformed *A. tumefaciens*. A single band is visible at 180 bp in lanes containing RNA amplified with the NAD5 primer pair (Figure 5.7, lanes 2 and (faintly) 3). No band is visible at 112 bp in lane 3, which contains RNA extracted from wild-type *A. tumefaciens* infiltrated *N. benthamiana*. In contrast to this, a single band is visible at 122 bp in lane 5, which contains RNA extracted from *N. benthamiana* which had been infiltrated with 2b241 transformed *A. tumefaciens*, and lane 6, which contains the product of amplification of the plasmid 2b241. The template in both lanes 5 and 6 were amplified using the primer pair CMV241-2b. This shows that the primer pair CMV241-2b is specific to the 2b gene and mRNA encoding the 2b gene is being produced in *N. benthamiana* leaf tissue infiltrated with 2b241 transformed *A. tumefaciens*.

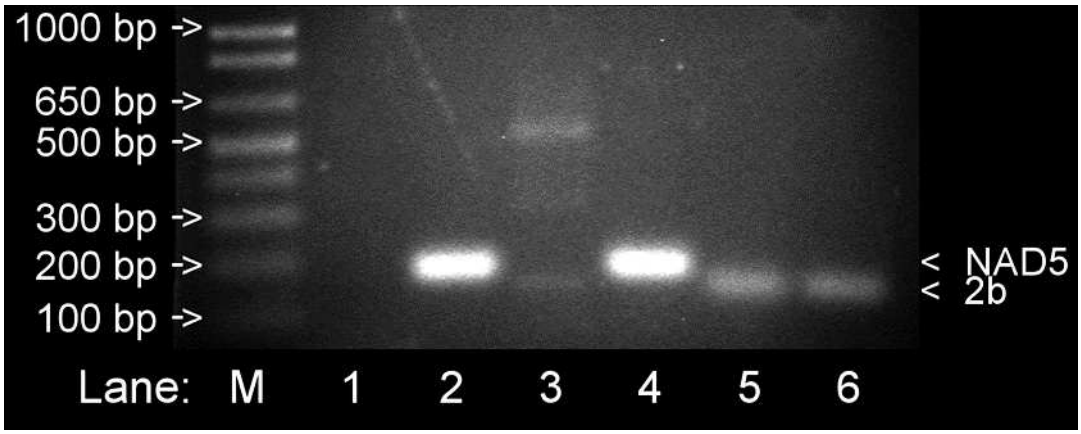

Figure 5.7: RT-PCR products amplified from RNA extracted from N. benthamiana *tissue infiltrated with wild-type or 2b241 transformed* A. tumefaciens*. Lane M contains 1 Kb Plus DNA Ladder. Lane 1 contains no template DNA. Lanes 2 and 3 contain RNA extracted from* N. benthamiana *infiltrated with wild-type A.* tumefaciens *and amplified using the NAD5 and CMV241-2b primer pairs respectively. Lanes 4 and 5 contain RNA extracted from* N. benthamiana *imfiltrated with 2b241 and amplified using the NAD5 and CMV241-2b primer pairs respectively. Lane 6 contains 2b241 plasmid DNA amplified using the CMV241-2b primer pair.*

Figure 5.8 shows the products of RT-PCR amplification of RNA extracted from *N. benthamiana* infiltrated with wild-type or p19wt transformed *A. tumefaciens*. As in Figure 5.7, the presence of a 180 bp band in all lanes containing RNA amplified with the NAD5 primer pair (Figure 5.8, lanes 4 and 6) indicates that the RNA is of good quality and is not contaminated with DNA. The presence of a band at approximately 550 bp in lanes 2 and 3 is near the expected amplicon size of 540 bp and is not present in lanes containing template RNA from wild-type *A. tumefaciens* infiltrated *N. benthamiana* (Figure 5.8, lane 5). Because of this, it can be assumed that the band indicates the presence of p19wt RNA in *N. benthamiana* infiltrated with p19wt transformed *A. tumefaciens*.

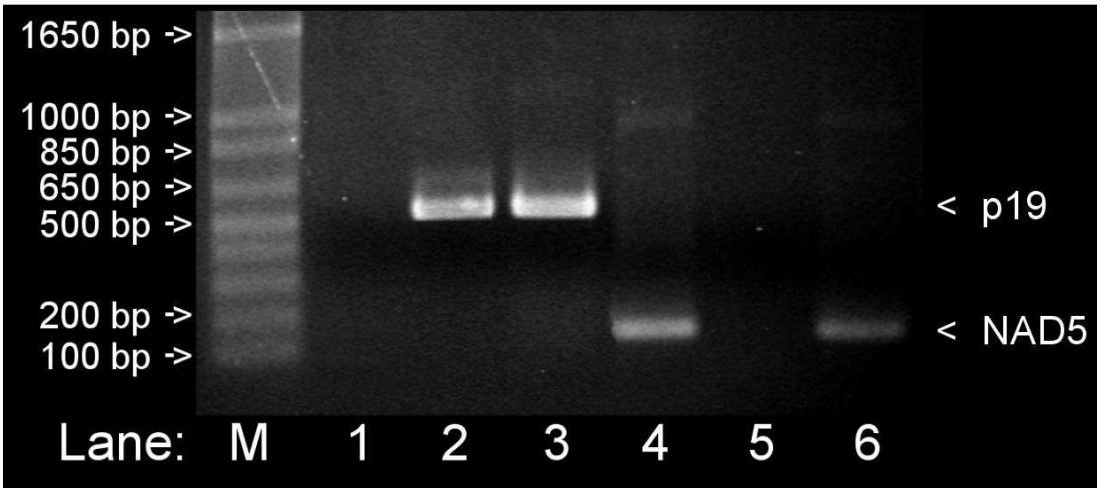

Figure 5.8: RT-PCR products amplified from RNA extracted from N. benthamiana *tissue infiltrated with wild-type or 2b241 transformed* A. tumefaciens*. Lane M contains 1 Kb Plus DNA Ladder. Lane 1 contains no template with the NAD5 primers. Lane 2 contains p19wt plasmid DNA amplified with the p19 primer pair. Lanes 3 and 4 contain RNA extracted from* N. benthamiana *agroinfiltrated with p19wt and amplified using the p19 and NAD5 primer pairs respectively. Lane 6 contains the products of the amplification using the NAD5 primer pair on RNA from N. benthamiana infiltrated with wild-type A. tumefaciens.*

The detection of mRNA from *N. benthamiana* infiltrated with *A. tumefaciens* containing the HC-Pro, p6 and IPK genes was not possible due to an inability to locate primers which bound reliably and specifically to the VSR of interest. In all cases, multiple primers were trialled and were found to be either non-specific, or did not produce a product. Both of these issues were present in primers designed to amplify the gene HC-Pro, as both generic potyvirus HC-Pro primers developed by Glias et al (2002) and primers designed in this study against the sequence obtained in section 5.2 failed to produce the desired product.

As Figure 5.9 and 5.6 show, the primers HC-ProGlias F and HC-ProGlias R did not produce a band of the expected 1.8 kb size. A product of the expect size of 235 bp was visible upon amplification of RNA extracted from *N. benthamiana* which had been agroinfiltrated with HC-ProPVY using the primers HC-ProOlliver1 F and HC-ProOlliver1 R (Figure 5.10). This band, as well as many others, was also visible in *N. benthamiana* tissue infiltrated with wild-type *A. tumefaciens*, and was not indicative of the presence of the HC-Pro gene. Increasing or decreasing the annealing temperature or amount of $MgCl_2$ present in the amplification buffer from those described in 4.3.5 did not improve binding of either primer pair (data not shown). As neither primer pair bound reliably or specifically, neither was suitable for the detection of HC-Pro RNA.

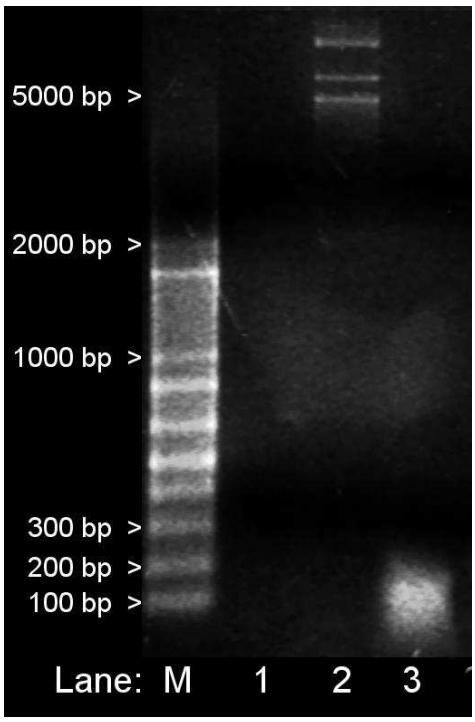

Figure 5.9: PCR products resulting from the amplification of the plasmid HC-ProPVY (lane 2) and DNA extracted from A. tumefaciens *transformed with the plasmid HC-ProPVY (lane 3) using the primer pair HC-ProGlias F and HC-ProGlias R. Lane M contains 1 Kb Plus DNA Ladder. Lane 1 contains no template. No bands are visible in either lane at the expected size of 1.8 kb. No bands of the same size are visible in either lane 2 or lane 3.*

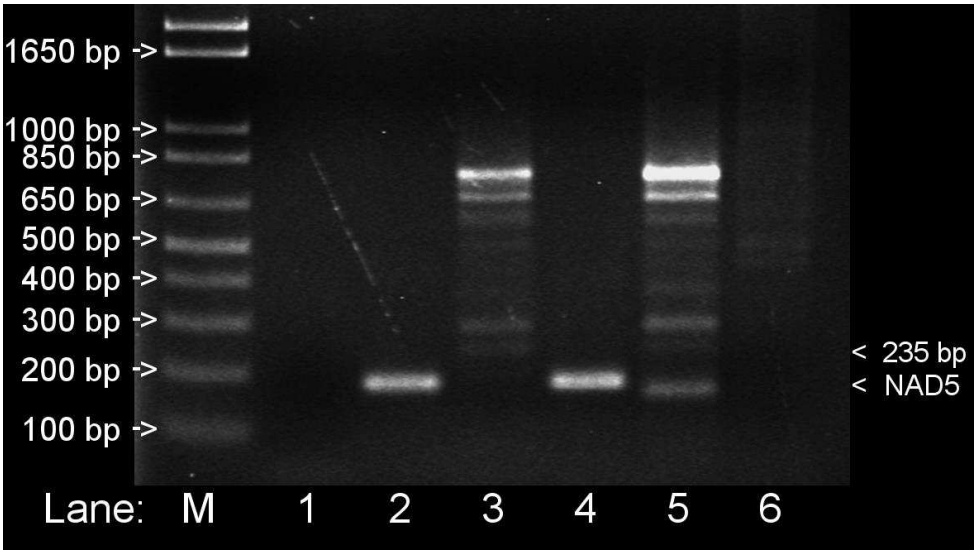

Figure 5.10: RT-PCR products amplified from RNA extracted from N. benthamiana *tissue argoinfiltrated with HC-ProPVY or wild-type* A. tumefaciens*. Lane M contains 1 Kb Plus DNA Ladder. Lane 1 contains no template. Lanes 2 and 3 contain RNA extracted from wild-type* A. tumefaciens *infiltrated* N. benthamiana *amplified using the NAD5 and HC-ProOlliver1 primers respectively. Lanes 4 and 5 contain RNA extracted from* N. benthamiana *agroinfiltrated with HC-ProPVY and amplified using the NAD5 and HC-ProOlliver1 primer pairs respectively. Lane 6 contains the PCR product of the HC-ProPVY plasmid amplified with the HC-ProOlliver1 primer pair.*

5.6. Detection of phosphorylated eIF2α in VSR expressing *N. benthamiana*

As all plasmids had been confirmed to contain the gene of interest, and transcription of the genes p19 and 2b had been confirmed in agroinfiltrated *N. benthamiana* tissue, the next step in determining whether or not VSRs alter the ability of plant eIF2α kinases to phosphorylate eIF2α could be taken. Experiments were conducted to determine if a) expression of a VSR in *N. benthamiana* alters the ability of the plant to phosphorylate eIF2α upon exposure to glyphosate, and b) if the expression of IPK influences the ability of the VSR to alter eIF2α phosphorylation levels. To do this, VSRs, IPK and a combination of both VSR and IPK were transiently expressed in three week old *N. benthamiana* plants, some of which were then treated with 300 μM glyphosate.

For each plasmid, six plants had the newest leaf infiltrated with transformed *A. tumefaciens* containing that plasmid. A further six plants for each plasmid were infiltrated with both the VSR and IPKpHEX *A. tumefaciens*. As a control, six plants were infiltrated with wild-type, untransformed *A. tumefaciens*, and six with infiltration buffer, to ensure that neither agroinfiltration or infiltration alone influenced the ability of plant eIF2α kinases to phosphorylate eIF2α. At four days post-infiltration, three of the six plants in each group were then infiltrated with 300 μM glyphosate. After 24 hours, all infiltrated leaves were harvested, the protein extracted using extraction method B (see section 2.3) and the amount of phosphorylated eIF2α present in the plant tissue determined by western blot using a phosphorylated eIF2α specific antibody (see section 2.6). The resulting exposure is shown in Figure 5.11.

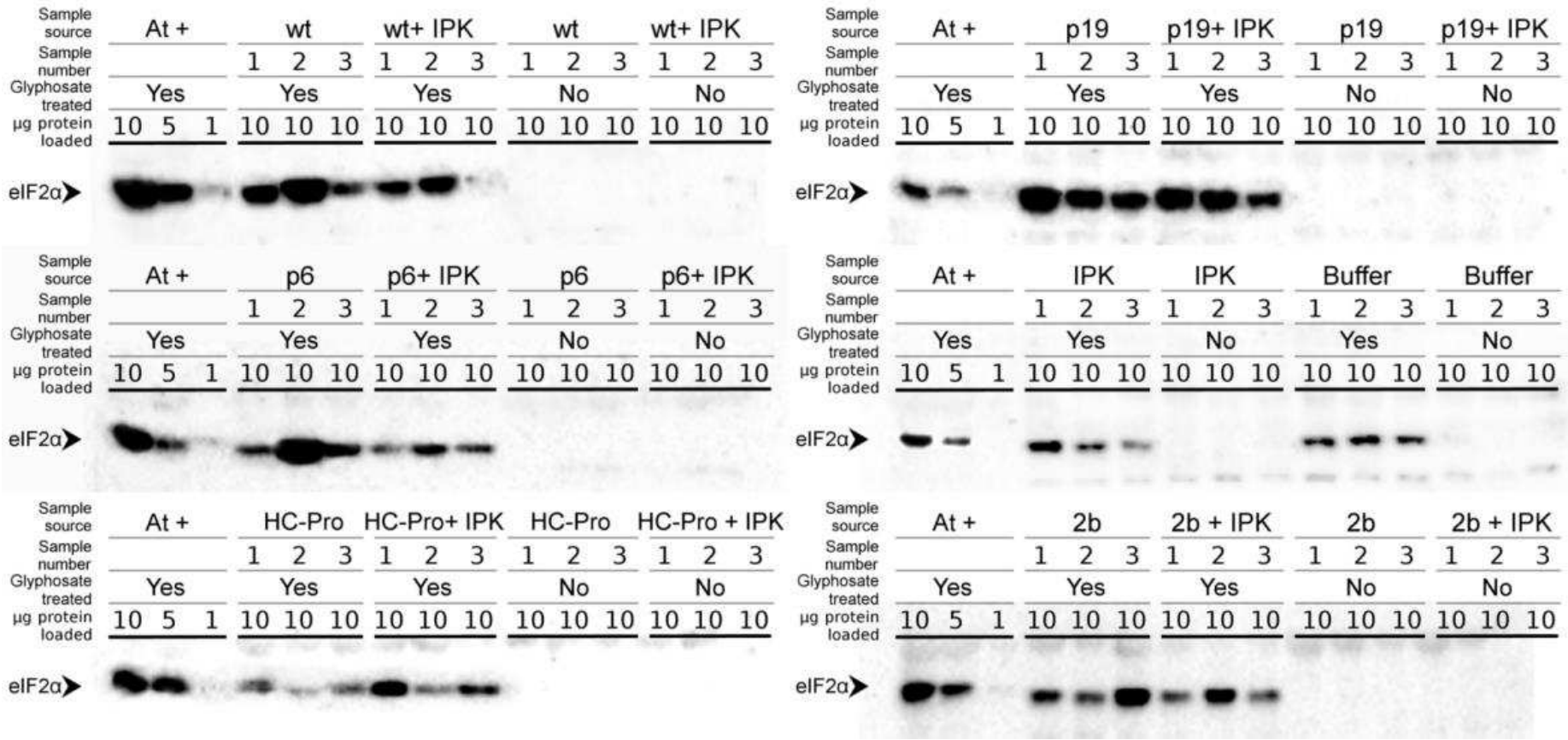

Figure 5.11: Detection of phosphorylated eIF2α in VSR and/or IPK expressing N. benthamiana *tissue by western blot using a phosphorylated eIF2α specific antibody. All positive control lanes (At+) contain aliquots of the same positive control. Differences in the size and darkness of sample bands relative to the positive control is due to a difference in the amount of phosphorylated eIF2α present between the positive control and the sample. Detection of chemiluminescence was achieved using the BioRad ChemiDoc MP™ System and ImageLab™ Software.*

In order to determine the amount of phosphorylated eIF2α per µg of protein in each group, the amount of chemiluminescence produced by each lane was determined as a key value as described in section 3.4. The amount of phosphorylated eIF2α for each group was determined using Equation 1 (section 3.4), as the amount of chemiluminescence detected falls within, or close to the range for which this equation is most accurate. It was necessary to first convert the amount of chemiluminescence detected to the amount of eIF2α present in the lane, as the relationship between the amount of phosphorylated eIF2α in the lane and the degree of exposure is not a 1:1 relationship.

In order to reduce the impact of any variation between individual samples within a group, each group's data was averaged (i.e, the phosphorylated eIF2α content in ng/µg of phosphorylated protein present in lanes containing 10 and 5 µg glyphosate treated *A. thaliana* positive control (sections 2.8.2 and 3.4), the phosphorylated eIF2α content of all lanes containing the VSR, or the phosphorylated eIF2α content of all lanes containing the VSR + IPK, was averaged. Although this may have helped reduce any error, it also causes the results to be skewed by any outliers. It would have been preferable to repeat the experiment and include further data.

The amount of phosphorylated eIF2α present per µg of plant protein in each sample group was compared to the amount of phosphorylated eIF2α present in the positive control as detected by the amount of chemiluminescence emitted. The standard curve in section 3.4 shows that the amount of chemiluminescence in 1µg of positive control *A. thaliana* protein is equivalent to 3.253 ng phosphorylated eIF2α; $1/307^{th}$ of the protein in the *A. thaliana* control is phosphorylated eIF2α. Thus, the average amount of phosphorylated eIF2α present in each group could be determined by comparison to the positive control. For example, if the average phosphorylated eIF2α content of the positive control was calculated to be 2 ng/µg of phosphorylated eIF2α in each lane and sample X gave an average of 1 ng/µg of phosphorylated eIF2α present in each lane, we know that sample X contains half as much phosphorylated eIF2α as the positive control. As we know that the positive control actually contains 3.253 ng/µg of phosphorylated eIF2α to total protein, it can be determined that sample X contains 1.627 ng of phosphorylated eIF2α per µg of sample. In this manner the amount of phosphorylated eIF2α present in each group was calculated.

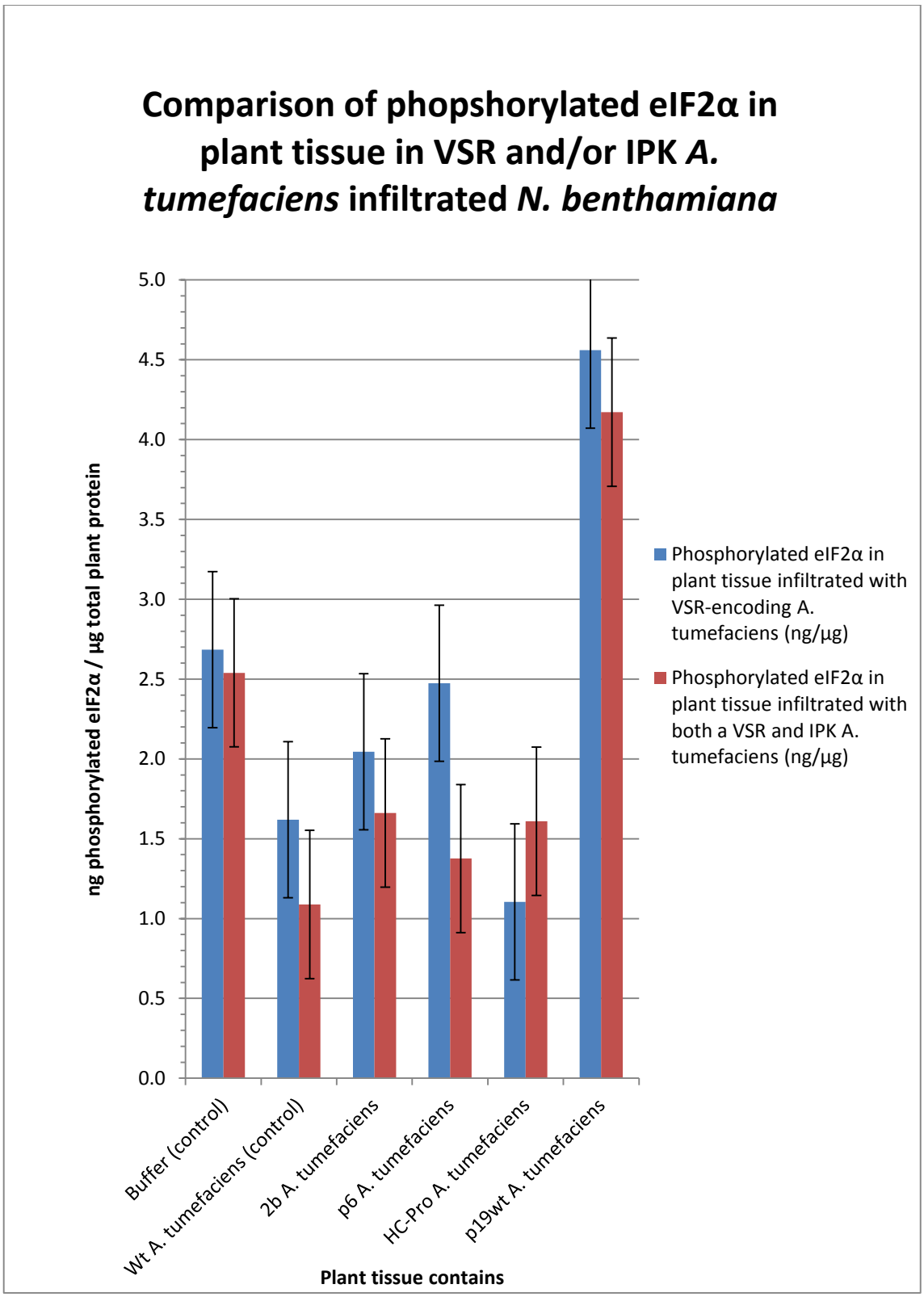

Figure 5.12: A comparison of the average amount of phosphorylated eIF2α present per µg of total plant protein in glyphosate treated N. benthamiana *expressing a VSR or a VSR+IPK. Error bars show the standard error of each sample group.*

Table 5.2: The amount of phosphorylated eIF2α present in protein extracted from glyphosate treated N. benthamiana *tissue expressing a variety of VSRs and/or IPK. Quantification of eIF2α was done by comparison to a control sample with a known concentration of phosphorylated eIF2α.*

Infiltrated with	**Phosphorylated eIF2A per µg total plant protein (ng/µg)**
Infiltration buffer (mock)	2.685
Wild-type *A. tumefaciens*	1.619
Wild-type *A. tumefaciens,* IPKpHEX *A. tumefaciens*	1.088
2b241 *A. tumefaciens*	2.044
2b241 *A. tumefaciens,* IPKpHEX *A. tumefaciens*	1.661
p6p100 *A. tumefaciens*	2.474
p6p100 *A. tumefaciens,* IPKpHEX *A. tumefaciens*	1.376
HC-ProPVY *A. tumefaciens*	1.104
HC-ProPVY *A. tumefaciens,* IPKpHEX *A. tumefaciens*	1.610
p19wt *A. tumefaciens*	4.561
p19wt *A. tumefaciens,* IPKpHEX *A. tumefaciens*	4.172
IPKpHEX *A. tumefaciens*	2.540

Leaf tissue assumed to be expressing the VSRs 2b, p6 and HC-Pro did not appear to have any significant difference in phosphorylated eIF2α content when compared to the positive control. Although less phosphorylated eIF2α is detected in glyphosate treated tissue infiltrated with wild-type *A. tumefaciens* alone or *A. tumefaciens* carrying the plasmids 2b241, p6p100 and HC-ProPVY than is detected in tissue infiltrated only with buffer or *A. tumefaciens* expressing IPK, the difference is not pronounced and may be due to natural variation within plants. In contrast to this, the protein extracted from glyphosate treated leaf tissue expressing p19 or both p19 and IPK contained almost twice as much phosphorylated eIF2α (4.561 ng/µg, 4.172 ng/µg) as leaf tissue infiltrated with wild-type *A. tumefaciens* (1.619 ng/µg) or IPK encoding *A. tumefaciens* (2.540 ng/µg). This was well beyond any variation encountered between the samples from tissue not expressing p19. No phosphorylated eIF2α was detected in leaf tissue expressing p19 which was not treated with glyphosate, indicating that p19 enhances the effect of glyphosate on plant tissue, but does not trigger eIF2α phosphorylation itself.

5.7. Summary of results

The plasmids provided were sequenced to confirm the presence of the intended gene and all plasmid were found to contain the correct sequence except the plasmids 2b207 and p6p100, which returned sequences which were not similar to the genes 2b or p6. Plasmid 2b207 was analysed by PCR and found to not contain the gene 2b, in contrast the plasmid p6p100, which was digested with the enzyme *Hin*dIII and found to contain the gene p6.

Transformed *A. tumefaciens* with the plasmids 2b241, p19wt, HC-Pro, p6p100 and IPKpHEX was confirmed by colony PCR using primers which bracketed the insertion site of each plasmid. Transformed and wild-type *A. tumefaciens* were infiltrated into *N. benthamiana* leaves. RNA was extracted from leaves infiltrated with 2b241 and p19wt containing *A. tumefaciens,* and mRNA encoding the VSRs 2b and p19 detected by RT-PCR. Infiltrated *N. benthamiana* leaves were harvested and the total plant protein extracted. This protein was analysed by western blot using the phosphorylated eIF2α antibody and the amount of phosphorylated eIF2α was compared between plants treated and untreated with glyphosate. No eIF2α phosphorylation was detecting in VSR or IPK expressing plants which were not treated with glyphosate, and the expression of a VSR or IPK did not appear to inhibit eIF2α phosphorylation. In contrast to the expected outcome, increased levels of eIF2α phosphorylation were detected in glyphosate treated *N. benthamiana* which were expressing the VSR p19.

5.8. Discussion of results

5.8.1. Variation in the amount of phosphorylated eIF2α detected in agroinfiltrated *N. benthamiana*

As is visible in Figure 5.11, there is considerable variation in the amount of phosphorylated eIF2α present in glyphosate treated *N. benthamiana*, regardless of VSR expression. Although the average phosphorylated eIF2α content of three plants was taken for each sample, there is enough variation within the results that only the significant increase in phosphorylated eIF2α seen upon glyphosate treatment of p19 expressing *N. benthamiana* is obvious, and less apparent changes in the amount of phosphorylated eIF2α produced upon glyphosate treatment may have been overlooked. It would have been preferable to repeat the experiment with a greater number of plants in each group, as well as further defining the amount of phosphorylated eIF2α present in the positive control as described in section 3.7.1. These changes would have allowed the more accurate measurement of the amount of phosphorylated eIF2α present in plant samples, allowing the detection of smaller increases or decreases in the amount of phosphorylated eIF2α present in agroinfiltrated *N. benthamiana* which may not have been noticed due to the natural variability in phosphorylated eIF2α content in glyphosate treated plants.

5.8.2. Expression of VSRs and IPK in agroinfiltrated *N. benthamiana*

Although 2b and p19 mRNAs were detected in agroinfiltrated *N. benthamiana*, the proteins 2b and p19 were not directly detected. Although the production of mRNA indicates that the gene is being transcribed, it does not prove that the gene is being translated into a protein. In order to be certain that the introduced gene is being translated into protein, immunological testing is required. Due to time and budget limitations, antibodies for each of the VSRs expressed in *N. benthamiana* in chapters 4 and 5 were not available to detect the presence of an introduced VSR in *N. benthamiana* tissue by western blot. Consequently, it is uncertain if the target VSRs were produced in agroinfiltrated *N. benthamiana* tissue. However, given the significant increase in the concentration of phosphorylated eIF2α seen in *N. benthamiana* tissue expressing p19 mRNA, it is likely that the VSR p19 was being produced, and that it influences the amount of phosphorylated eIF2α being produced in glyphosate treated *N. benthamiana*.

5.8.3. Increased phosphorylation of eIF2α upon glyphosate treatment of p19 expressing *N. benthamiana*

No previous studies on the ability of p19 to trigger or enhance eIF2α phosphorylation appear to exist, and studies regarding the effects p19 may have other than RNA silencing are sparse. As it is possible for both the protein and the RNA of a gene to have an affect on the host systems, investigation into how expression of the gene p19 in *N. benthamiana* increases eIF2α phosphorylation upon glyphosate treatment would first need to determine if it is the protein or the RNA that is causing the change in eIF2α phosphorylation levels. In TBSV, the genes p22 and p19 are encoded by overlapping ORFs

on the same subgenomic RNA molecule (Scholthof et al., 1995) and if the increase in eIF2α phosphorylation upon glyphosate treatment is due to a property of the RNA, it is likely this would also be observable in plants expressing the gene p22.

TBSV RNA has previously been shown to bind to a large number of host proteins, including the delta subunit of eIF2β. In yeasts, many other proteins involved in translation have also been shown to bind to TBSV RNA (Li et al., 2009), including RNA binding proteins which are required for maturation of tRNA precursors (Yoo and Wolin, 1994), the protein DPS1, an enzyme which participates in aminoacyl-tRNA biosynthesis (Gangloff and Dirheimer, 1973), and the protein ARC1, which associates with tRNA and aminoacyl-tRNA synthetases and may be required for efficient aminoacylation *in vivo* (Simos et al., 1996). Disruption of any of these proteins could result in an accumulation of uncharged tRNAs, which would trigger the eIF2α kinase GCN2 and cause an increase eIF2α phosphorylation.

However, no phosphorylated eIF2α was detected in p19 expressing *N. benthamiana* which were not treated with glyphosate, indicating that under normal conditions the effect of p19 is not sufficient to trigger eIF2α phosphorylation.

The VSR p19 functions by binding to small dsRNA, protecting it from enzymes involved in the RNAi pathway. Therefore, it was expected that the presence of the p19 protein would inhibit eIF2α phosphorylation. As noted in section 1.2.1.2, any disruption of the RNAi pathway can have implications that act beyond the inhibition of the antiviral defence aspect of RNAi. As RNAi is a necessary part of the developmental system, and eIF2α is phosphorylated as part of the developmental process, it is possible that the disruption to the RNAi pathway caused by the expression of p19 could increase the amount and ease of phosphorylation of eIF2α.

Further work on the effect of p19 expression in plant tissue on eIF2α phosphorylation is required to determine if the increased level of eIF2α phosphorylation in *N. benthamiana* upon glyphosate treatment is caused by the p19 RNA or the p19 protein itself, the method by which it occurs, and if other stresses on p19 expressing *N. benthamiana* result in increased eIF2α phosphorylation.

Chapter 6

General discussion

6.1. Viruses and VSRs used in this research

The overall aim of this research was to determine if VSRs encoded by plant viruses are also capable of suppression of eIF2α kinases, as has been seen in some animal viruses. In this study, two different methods were used to examine the effects that VSRs have on the phosphorylation of eIF2α; firstly, whether or not infection of *A. thaliana* with the viruses TYMV and TVCV triggers eIF2α phosphorylation, and secondly, if the expression of a VSR in *N. benthamiana* inhibits eIF2α phosphorylation. Previous studies investigating the properties of viral genes have compared the infection of a plant by the virus with binary vector-mediated expression of the gene in a separate experiment (Wang et al., 2012, Duan et al., 2012, Kasschau et al., 2003, Elmer et al., 1988). This allows confirmation that it is the gene of interest is/is not responsible for any results seen in virus-infected plants, and not other genes encoded by the virus. In addition to this, vector-mediated expression of a gene allows for the gene of interest to be reliably expressed in higher quantities than may be seen in viral infection alone, amplifying any effect on the host system and in some cases exaggerating subtle changes in the host plant, allowing otherwise subtle changes to be more easily detected.

Unfortunately, in this study where both the virus and VSR were available, CaMV/p6 and CMV/2b, the infection rate of the virus was so low as to be impossible to reliably infect sufficient plants for any experiments. Although *A. thaliana* is a known host of both CaMV (Leisner et al., 1993) and CMV (Takahashi et al., 1994), the infection rate and severity varies with both the strain of virus and host plant (Takahashi et al., 1994, Takahashi, 2008, Tang and Leisner, 1997).

Although twelve different isolates of CMV collected from environmental samples and provided by the Ministry of Primary Industries were investigated for the ability to infect *A. thaliana*, the strains of the isolates were not known, and no isolate was able to consistently cause infection. Therefore, the study did not include a comparison of the effects of virus infection and vector-mediated expression of the corresponding VSR. However, the broad range viruses and VSRs used in these experiments allowed a comparison of the mechanisms of action used by VSRs and the potential effects they had on the host plant. Specifically, it was of interest that the VSR p19, which functions by binding to siRNAs (Ye et al., 2003, Vargason et al., 2003, Silhavy et al., 2002b) caused an increase in the amount of phosphorylated eIF2α produced upon glyphosate treatment. In contrast to this, other small-dsRNA binding VSRs such as the 2b and coat proteins of CMV and TVCV, did not cause any detectable change in the amount of phosphorylated eIF2α produced upon virus infection. This suggests it is not the ability of p19 to act as a suppressor of RNA silencing by binding to dsRNA which caused the increased levels of eIF2α phosphorylation upon glyphosate treatment.

6.2. Lack of phosphorylation of eIF2α upon infection or wounding of *A. thaliana* or *N. benthamiana*

Previous literature has shown that upon virus infection of IPK-deficient mice cells, a significant increase in eIF2α phosphorylation levels occurs (Kash et al., 2006). A similar finding, that TVCV infection of IPK-deficient *N. benthamiana* and *A. thaliana* results in eIF2α phosphorylation occurring to such an extent as to cause plant death, has also been found. This suggests that both animal and plant cells require IPK to regulate eIF2α phosphorylation, and in cells with non-functional IPK, increased levels of eIF2α

phosphorylation occur upon virus infection. However, no increase in eIF2α phosphorylation was seen in IPK deficient *A. thaliana* upon infection with either TVCV or TYMV, and the expression of human IPK did not appear to have any effect on the phosphorylation of eIF2α in *N. benthamiana* leaves. This is in direct contrast with the results of Bilgin et at (2003), who reported plant death by 18-20 dpi upon infection of IPK deficient *A. thaliana* with TVCV. This research found that at 28 dpi, TVCV infected IPK deficient *A. thaliana* and wild-type *A. thaliana* appeared equally healthy, with no evidence of eIF2α phosphorylation.

The cause of this difference in results between those seen by Bilgin et al (2003) and those seen in this research is so far unknown, but may be due to the difference between *A. thaliana* ecotypes and TVCV strains used in experiments. As the symptomology and presumably response of the host plant vary depending on the strain of virus and cultivar of host (Takahashi, 2008, Takahashi et al., 1994), it could be that the strain of TVCV used in this research did not contain the trigger necessary for the phosphorylation of eIF2α, or that *A. thaliana* ecotype Col-0 contains an additional protein which is capable of substituting for IPK when IPK is inactivated. In order to determine if the lack of eIF2α phosphorylation in *A. thaliana* upon infection with TVCV is due to the ecotype, an experiment comparing the amount of phosphorylated eIF2α present in plant tissue upon TVCV infection of the *A. thaliana* ecotype used by Bilgin et al (2003), Ws-0, and the ecotype used in this research, Col-0, could be undertaken. Unfortunately, ecotype Ws-0 *A. thaliana* were not available for this research.

In addition to the lack of phosphorylated eIF2α present in TVCV infected IPK-deficient *A. thaliana*, phosphorylation of eIF2α was also not detected in plants after inoculation with mock or virus containing inoculum. As the inoculation process damages the leaf in order to allow the virus to enter the leaf tissue, and in *A. thaliana* GCN2 has been reported to phosphorylate eIF2α upon wounding, it was expected that eIF2α phosphorylation would be visible at 4-12 hours post-inoculation (Lageix et al., 2008). However, no phosphorylated eIF2α was visible in either wild-type or IPK deficient *A. thaliana* at any time point. This was not due to a failure to detect phosphorylated eIF2α by western blot; as the positive controls were clearly visible in all cases, indicating that the transfer of sample proteins to the membrane and subsequent detection of any phosphorylated eIF2α present was successful.

The lack of detection of phosphorylated eIF2α upon either wounding or TVCV infection may be indicative of issues with the extraction and preparation of plant protein. The addition of a control group of plants that were glyphosate treated 24 hours before sampling would have allowed a greater degree of confidence that any phosphorylated eIF2α present in the plant tissue was being detected. However, given the consistency with which no phosphorylated eIF2α was detected, and the fact that other researchers present in the lab also failed to detect eIF2α phosphorylation in IPK deficient *A. thaliana* or IPK knockout *N. benthamiana* upon TVCV infection, it is likely that eIF2α was not phosphorylated upon virus infection.

6.3. Do virus-encoded suppressors of RNA silencing reduce plant eIF2α kinase activity and thereby increase susceptibility to infection?

As no phosphorylation of eIF2α was detected in wild-type or IPK deficient *A. thaliana* upon viral infection, this suggests that the plant viruses TVCV and TYMV do not utilise the host encoded inhibitor of eIF2α kinases, IPK, to reduce eIF2α phosphorylation upon virus infection. In addition to this, no reduction in phosphorylated eIF2α was detected upon glyphosate treatment of *N. benthamiana* expressing the VSRs 2b, p6, p19 and HC-Pro. This suggests that the expression of these VSRs in plant tissue does not significantly reduce the ability of the eIF2α kinase GCN2 to phosphorylate eIF2α. However, as the expression of p6 and HC-Pro in *N. benthamiana* was not confirmed by PCR or Western blot, it is possible that HC-Pro and p6 were not expressed in the leaf tissue sampled. In order to be certain that the expression of HC-Pro and p6 do not reduce the ability of *N. benthamiana* to phosphorylate eIF2α in response to glyphosate treatment, further work is needed to confirm that the proteins HC-Pro and p6 were in fact expressed.

In conclusion, no evidence was found to suggest that the plant viruses or VSRs used in this experiment are capable of reducing plant eIF2α kinase activity in *A. thaliana* or *N. benthamiana*. Further research involving a greater range of *A. thaliana* ecotypes, viruses and VSRs is necessary to determine if this is representative of virus infection in *A. thaliana*.

References:

ATREYA, P. L., ATREYA, C. D. & PIRONE, T. P. 1991. Amino acid substitutions in the coat protein result in loss of insect transmissibility of a plant virus. *Proceedings of the National Academy of Sciences of the United States of America,* 88**,** 7887-7891.

BADGER, M. R. & ANDREWS, T. J. 1974. Effects of CO2, O2 and temperature on a high-affinity form of ribulose diphosphate carboxylase-oxygenase from spinach. *Biochemical and Biophysical Research Communications,* 60**,** 204-210.

BALACHANDRAN, S., KIM, C. N., YEH, W.-C., MAK, T. W., BHALLA, K. & BARBER, G. N. 1998. Activation of the dsRNA-dependent protein kinase, PKR, induces apoptosis through FADD-mediated death signaling. *The EMBO Journal,* 17**,** 6888-6902.

BALACHANDRAN, S., ROBERTS, P. C., BROWN, L. E., TRUONG, H., PATTNAIK, A. K., ARCHER, D. R. & BARBER, G. N. 2000. Essential Role for the dsRNA-Dependent Protein Kinase PKR in Innate Immunity to Viral Infection. *Immunity,* 13**,** 129-141.

BANCHEREAU, J. & STEINMAN, R. M. 1998. Dendritic cells and the control of immunity. *Nature,* 392**,** 245-252.

BARBER, G., THOMPSON, S., LEE, T., STROM, T., JAGUE, R., DARVEAU, A., KATZE, M. 1994. The 58-kilodalton inhibitor of the interferon-induced double-stranded RNA-activated protein kinase is a tertratricopeptide repeat protein with oncogenic properties. *Proceedings of the National Academy of Sciences of the Unitied States America,* 91, 4278-4282.

BERLANGA, J. J., VENTOSO, I., HARDING, H. P., DENG, J., RON, D., SONENBERG, N., CARRASCO, L. & DE HARO, C. 2006. Antiviral effect of the mammalian translation initiation factor 2α kinase GCN2 against RNA viruses. *The EMBO Journal,* 25**,** 1730-1740.

BERNSTEIN, E., CAUDY, A. A., HAMMOND, S. M. & HANNON, G. J. 2001. Role for a bidentate ribonuclease in the initiation step of RNA interference. *Nature,* 409**,** 363-366.

BILGIN, D. D., LIU, Y., SCHIFF, M. & DINESH-KUMAR, S. P. 2003. $p58^{IPK}$, a Plant Orthologue of Double-Stranded RNA-Dependant Protein Kinase PKR Inhibitor, Functions in Viral Pathogenesis. *Developmental Cell,* 4**,** 651-661.

BIOMATTERS 2013. Geneious. 1.6.1 ed.

BLEVINS, T., RAJESWARAN, R., AREGGER, M., BORAH, B., SCHEPETILNIKOV, M., BAERLOCHER, L., FARINELLI, L., MEINS, F., HOHN, T., POOGGIN, M. 2011. Massive production of small RNAs from a non-coding region of *Cauliflower mosaic virus* in plant defense and viral counter-defense. *Nucl. Acids. Res.*, 39, 5003-5014.

CAÑIZARES, C., NAVAS-CASTILLO, J. & MORIONES, E. 2008. Multiple suppressors of RNA silencing encoded by both genomic RNAs of the crinivirus, Tomato chlorosis virus. *Virology,* 379**,** 168-174.

CHAN, S. W.-L., ZILBERMAN, D., XIE, Z., JOHANSEN, L. K., CARRINGTON, J. C. & JACOBSEN, S. E. 2004. RNA Silencing Genes Control de Novo DNA Methylation. *Science,* 303**,** 1336.

CHANG, H. W., WATSON, J. C. & JACOBS, B. L. 1992. The E3L gene of vaccinia virus encodes an inhibitor of the interferon-induced, double-stranded RNA-dependent protein kinase. *Proceedings of the National Academy of Sciences,* 89**,** 4825-4829.

CHAPNIK, E., SASSON, V., BLELLOCH, R. & HORNSTEIN, E. 2011. Dgcr8 controls neural crest cells survival in cardiovascular development. *Developmental Biology,* 362**,** 50-56.

CLARKE, P. A., SHARP, N. A. & CLEMENS, M. J. 1990. Translational control by the Epstein-Barr virus small RNA EBER-1. *European Journal of Biochemistry,* 193**,** 635-641.

COOKE, R. & PENON, P. 1990. In vitro transcription from cauliflower mosaic virus promoters by a cell-free extract from tobacco cells. *Plant Molecular Biology,* 14**,** 391-405.

COWELL, S. J. 2013. *Virus elimination from Actinidia germplasm.* Doctor of Science, University of Auckland.

CSORBA, T., BOVI, A., DALMAY, T. & BURGYAN, J. 2007. The p122 Subunit of *Tobacco Mosaic Virus* Replicase Is a Potent Silencing Suppressor and Compromises both Small Interfering RNA- and MicroRNA-Mediated Pathways. *Journal of Virology,* 81**,** 11768-11780.

CULLEN, B. R. 2011. RNA Interference does not Function as an Innate Antiviral Response in Mammalian Somatic Cells. *Future Virology,* 6**,** 1381-1384.

DENZLER, K. L. & JACOBS, B. L. 1994. Site-Directed Mutagenic Analysis of Reovirus σ3 Protein Binding to dsRNA. *Virology,* 204**,** 190-199.

DEVER, T. E., FENG, L., WEK, R. C., CIGAN, A. M., DONAHUE, T. F. & HINNEBUSCH, A. G. 1992. Phosphorylation of initiation factor 2α by protein kinase GCN2 mediates gene-specific translational control of GCN4 in yeast. *Cell,* 68**,** 585-596.

DIAZ-PENDON, J. A., LI, F., LI, W.-X. & DING, S.-W. 2007. Suppression of Antiviral Silencing by Cucumber Mosaic Virus 2b Protein in Arabidopsis Is Associated with Drastically Reduced Accumulation of Three Classes of Viral Small Interfering RNAs. *The Plant Cell,* 19**,** 2053-2063.

DING, X. S., LIU, J., CHENG, N.-H., FOLIMONOV, A., HOU, T.-M., BAO, Y., KATAGI, C., CARTER, S. A. & NELSON, R. S. 2004. The *Tobacco mosaic virus* 126-kDa Protein Associated with Virus Replication and Movement Suppresses RNA Silencing. *Molecular plant-microbe interactions,* 17**,** 583-592.

DUAN, C.-G., FANG, Y.-Y., ZHOU, B.-J., ZHAO, J.-H., HOU, W.-N., ZHU, H., DING, S.-W. & GUO, H.-S. 2012. Suppression of Arabidopsis ARGONAUTE1-Mediated Slicing, Transgene-Induced RNA Silencing, and DNA Methylation by Distinct Domains of the Cucumber mosaic virus 2b Protein. *The Plant Cell Online,* 24**,** 259-274.

EBHARDT, H. A., THI, E. P., WANG, M.-B. & UNRAU, P. J. 2005. Extensive 3′ modification of plant small RNAs is modulated by helper component-proteinase expression. *Proceedings of the National Academy of Sciences of the United States of America,* 102**,** 13398-13403.

ECKE, W., SCHMITZ, U. & MICHAELIS, G. 1990. The mitochondrial nad5 gene of sugar beet (Beta vulgaris) encoding a subunit of the respiratory NADH dehydrogenase. *Current Genetics,* 18**,** 133-139.

ELMER, J. S., BRAND, L., SUNTER, G., GARDINER, W. E., BISARO, D. M. & ROGERS, S. G. 1988. Genetic analysis of the tomato golden mosaic virus II. The product of the AL1 coding sequence is required for replication. *Nucleic Acids Research,* 16**,** 7043-7060.

ENDO-MUNOZ, L., WARBY, T., HARRICH, D. & MCMILLAN, N. 2005.

Phosphorylation of HIV Tat by PKR increases interaction with TAR RNA and enhances transcription. *Virology Journal,* 2**,** 17.
FARRELL, P. J., BALKOW, K., HUNT, T., JACKSON, R. J. & TRACHSEL, H. 1977. Phosphorylation of initiation factor eIF-2 and the control of reticulocyte protein synthesis. *Cell,* 11**,** 187-200.
FÉNELON, K., MUKAI, J., XU, B., HSU, P.-K., DREW, L. J., KARAYIORGOU, M., FISCHBACHE, G. D., MACDERMOTTA, A. B. & GOGOS, J. A. 2011. Deficiency of Dgcr8, a gene disrupted by the 22q11.2 microdeletion, results in altered short-term plasticity in the prefrontal cortex *Proceedings of the National Academy of Sciences of the United States of America*.
FIERRO-MONTI, I. & MATHEWS, M. B. 2000. Proteins binding to duplexed RNA: one motif, multiple functions. *Trends in Biochemical Sciences,* 25**,** 241-246.
FIRE, A., ALBERTSON, D., HARRISON, S. W. & MOERMAN, D. G. 1991. Production of antisense RNA leads to effective and specific inhibition of gene expression in C. elegans muscle. *Development,* 113**,** 503-514.
FUJII, H., CHIOU, T.-J., LIN, S.-I., AUNG, K. & ZHU, J.-K. 2005. A miRNA Involved in Phosphate-Starvation Response in Arabidopsis. *Current Biology,* 15**,** 2038-2043.
GALE JR, M. & KATZE, M. G. 1998. Molecular Mechanisms of Interferon Resistance Mediated by Viral-Directed Inhibition of PKR, the Interferon-Induced Protein Kinase. *Pharmacology & Therapeutics,* 78**,** 29-46.
GALLIE, D. R., LE, H., TANGUAY, R. L. & BROWNING, K. S. 1998. Translation initiation factors are differentially regulated in cereals during development and following heat shock. *The Plant Journal,* 14**,** 715-722.
GANGLOFF, J. & DIRHEIMER, G. 1973. Studies on aspartyl-tRNA synthetase from baker's yeast I. Purification and properties of the enzyme. *Biochimica et Biophysica Acta (BBA) - Nucleic Acids and Protein Synthesis,* 294**,** 263-272.
GATTO, E. M., RIOBÓ, N. A., CARRERAS, M. C., CHERÑAVSKY, A., RUBIO, A., SATZ, M. L. & PODEROSO, J. J. 2000. Overexpression of Neutrophil Neuronal Nitric Oxide Synthase in Parkinson's Disease. *Nitric Oxide,* 4**,** 534-539.
GERGERICH, R. C. & DOLJA, V. V. 2006. Introduction to Plant Viruses, the Invisible Foe. *The Plant Health Instructor* [Online].
GLAIS, L., TRIBODET, M., GAUTHIER, J. P., ASTIER-MANIFACIER, C., ROBAGLIA, C., KERLAN, C. 1998. RFLP mapping of the whole genome of ten viral isolates representative of different biological groups of potato virus Y. *Archives of Virology,* 143, 2077-2091.
GLAIS, L., TRIBODET, M. & KERLAN, C. 2002. Genomic variability in Potato potyvirus Y (PVY): evidence that PVYNW and PVYNTN variants are single to multiple recombinants between PVYO and PVYN isolates. *Archives of Virology,* 147**,** 363-378.
GLEAVE, A. 1992. A versatile binary vector system with a T-DNA organisational structure conducive to efficient integration of cloned DNA into the plant genome. *Plant Molecular Biology,* 20**,** 1203-1207.
GORDON, K., PFEIFFER, P., FUTTERER, J., HOHN, T. 1988. In vitro expression of cauliflower mosaic virus genes. *The EMBO Journal,* 7, 309-317.
GONSKY, R., LEBENDIKER, M. A., HARARY, R., BANAI, Y. & KAEMPFER, R. 1990. Binding of ATP to eukaryotic initiation factor 2. Differential modulation of mRNA-binding activity and GTP-dependent binding of methionyl-tRNAMetf. *Journal of Biological Chemistry,* 265**,** 9083-9089.

GOODIN, M. M., DIETZGEN, R. G., SCHICHNES, D., RUZIN, S. & JACKSON, A. O. 2002. pGD vectors: versatile tools for the expression of green and red fluorescent protein fusions in agroinfiltrated plant leaves. *The Plant Journal,* 31**,** 375-383.

HAAS, G., AZEVEDO, J., MOISSIARD, G., GELDREICH, A., HIMBER, C., BUREAU, M., FUKUHARA, T., KELLER, M. & VOINNET, O. 2008. Nuclear import of CaMV P6 is required for infection and suppression of the RNA silencing factor DRB4. *The EMBO Journal,* 27.

HAASE, A., JASKIEWICZ, L., ZHANG, H., LAINE, S., SACK, R., GATIGNOL, A. & FILIPOWICZ, W. 2005. TRBP, a regulator of cellular PKR and HIV-1 virus expression, interacts with Dicer and functions in RNA silencing. *The EMBO Journal,* 6.

HAMMOND, S. M., BERNSTEIN, E., BEACH, D. & HANNON, G. J. 2000. An RNA-directed nuclease mediates post-transcriptional gene silencing in Drosophila cells. *Nature,* 404**,** 293-296.

HAN, A.-P., YU, C., LU, L., FUJIWARA, Y., BROWNE, C., CHIN, G., FLEMING, M., LEBOULCH, P., ORKIN, S. H. & CHEN, J.-J. 2001. Heme-regulated eIF2[alpha] kinase (HRI) is required for translational regulation and survival of erythroid precursors in iron deficiency. *EMBO J,* 20**,** 6909-6918.

HARDEGGER, M., BRODMANN, P. & HERRMANN, A. 1999. Quantitative detection of the 35S promoter and the NOS terminator using quantitative competitive PCR. *European Food Research and Technology,* 209**,** 83-87.

HARDING, H. P., ZHANG, Y. & RON, D. 1999. Protein translation and folding are coupled by an endoplasmic-reticulum-resident kinase. *Nature,* 397**,** 271-274.

HEARNE, P., KNORR, D., HILLMAN, B. & MORRIS, T. 1990. The complete genome structure and synthesis of infection RNA from clones of tomato bushy stunt virus. *Virology.* 177, 141-151

HELLENS, R., ALLAN, A., FRIEL, E., BOLITHO, K., GRAFTON, K., TEMPLETON, M., KARUNAIRETNAM, S., GLEAVE, A. & LAING, W. 2005. Transient expression vectors for functional genomics, quantification of promoter activity and RNA silencing in plants. *Plant Methods,* 1**,** 13.

HOFMANN, S., CHERKASOVA, V., BANKHEAD, P., BUKAU, B. & STOECKLIN, G. 2012. Translation suppression promotes stress granule formation and cell survival in response to cold shock. *Molecular Biology of the Cell,* 23**,** 3786-3800.

HUTVÁGNER, G. & ZAMORE, P. D. 2002. RNAi: nature abhors a double-strand. *Current Opinion in Genetics and Development,* 12**,** 225-232.

INVITROGEN 2010. Qubit Protein Assay Kits. *In:* INVITROGEN (ed.).

JIANG, H.-Y. & WEK, R. C. 2005. GCN2 phosphorylation of eIF2alpha activates NF-kappaB in response to UV irradiation. *Biochem. J.,* 385**,** 371-380.

JIANG, H.-Y., WEK, S. A., MCGRATH, B. C., SCHEUNER, D., KAUFMAN, R. J., CAVENER, D. R. & WEK, R. C. 2003. Phosphorylation of the α Subunit of Eukaryotic Initiation Factor 2 Is Required for Activation of NF-κB in Response to Diverse Cellular Stresses. *Molecular and Cellular Biology,* 23**,** 5651-5663.

JOHANSEN, L. K. & CARRINGTON, J. C. 2001. Silencing on the Spot. Induction and Suppression of RNA Silencing in the Agrobacterium-Mediated Transient Expression System. *Plant Physiology,* 126**,** 930-938.

KASH, J. C., GOODMAN, A. G., KORTH, M. J. & KATZE, M. G. 2006. Hijacking of the host-cell response and translational control during influenza virus infection. *Virus Research,* 119**,** 111-120.

KASSCHAU, K. D. & CARRINGTON, J. C. 1998. A Counterdefensive Strategy of Plant Viruses: Suppression of Posttranscriptional Gene Silencing *Cell,* 95**,** 461-470.
KASSCHAU, K. D. & CARRINGTON, J. C. 2001. Long-Distance Movement and Replication Maintenance Functions Correlate with Silencing Suppression Activity of Potyviral HC-Pro. *Virology,* 285**,** 71-81.
KASSCHAU, K. D., XIE, Z., ALLEN, E., LLAVE, C., CHAPMAN, E. J., KRIZAN, K. A. & CARRINGTON, J. C. 2003. P1/HC-Pro, a viral suppressor of RNA silencing, interferes with Arabidopsis development and miRNA function. *Developmental Cell,* 4**,** 205-217.
LAGEIX, S., LANET, E., POUCH-PELISSIER, M.-N., ESPAGNOL, M.-C., ROBAGLIA, C., DERAGON, J.-M. & PELISSIER, T. 2008. Arabidopsis eIF2alpha kinase GCN2 is essential for growth in stress conditions and is activated by wounding. *BMC Plant Biology,* 8**,** 134.
LAGOS-QUINTANA, M., RAUHUT, R., LENDECKEL, W. & TUSCHL, T. 2001. Identification of Novel Genes Coding for Small Expressed RNAs. *Science,* 294**,** 853-858.
LAU, N. C., LIM, L. P., WEINSTEIN, E. G. & BARTEL, D. P. 2001. An Abundant Class of Tiny RNAs with Probable Regulatory Roles in Caenorhabditis elegans. *Science,* 294**,** 858-862.
LE, H., BROWNING, K. S. & GALLIE, D. R. 1998. The Phosphorylation State of the Wheat Translation Initiation Factors eIF4B, eIF4A, and eIF2 Is Differentially Regulated during Seed Development and Germination. *Journal of Biological Chemistry,* 273**,** 20084-20089.
LEE, R. C. & AMBROS, V. 2001. An Extensive Class of Small RNAs in Caenorhabditis elegans. *Science,* 294**,** 862-864.
LEE, R. C., FEINBAUM, R. L. & AMBROS, V. 1993. The C. elegans heterochronic gene lin-4 encodes small RNAs with antisense complementarity to lin-14. *Cell,* 75**,** 843-854.
LEISNER, S. M., TURGEON, R. & HOWELL, S. H. 1993. Effects of host plant development and genetic determinants on the long-distance movement of cauliflower mosaic virus in Arabidopsis. *The Plant Cell Online,* 5**,** 191-202.
LI, F. & DING, S.-W. 2006. Virus Counterdefense: Diverse Strategies for Evading the RNA-Silencing Immunity. *Annual Reveiw of Microbiology,* 60**,** 503-531.
LI, H., LI, W. X. & DING, S. W. 2002. Induction and Suppression of RNA Silencing by an Animal Virus. *Science,* 296**,** 1319-1321.
LI, Y., LU, J., HAN, Y., FAN, X. & DING, S.-W. 2013. RNA Interference Functions as an Antiviral Immunity Mechanism in Mammals. *Science,* 342**,** 231-234.
LI, Z., POGANY, J., PANAVAS, T., XU, K., ESPOSITO, A. M., KINZY, T. G. & NAGY, P. D. 2009. Translation elongation factor 1A is a component of the tombusvirus replicase complex and affects the stability of the p33 replication co-factor. *Virology,* 385**,** 245-260.
LICHNER, Z., SILHAVY, D. & BURGYAN, J. 2002. Double-stranded RNA-binding proteins could suppress RNA interference-mediated antiviral defences. *Journal of General Virology,* 84 (4), 975-980.
LINDBO, J. A., SILVA-ROSALES, L., PROEBSTING, W. M. & DOUGHERTY, W. G. 1993. Induction of a Highly Specific Antiviral State in Transgenic Plants: Implications for Regulation of Gene Expression and Virus Resistance. *The Plant Cell,* 5**,** 1749-1759.

LIU, H., REAVY, B., SWANSON, M. & MACFARLANE, S. A. 2002. Functional Replacement of the Tobacco rattle virus Cysteine-rich Protein by Pathogenicity Proteins from Unrelated Plant Viruses. *Virology,* 298**,** 232-239.

LOVE, A. J., LAIRD, J., HOLT, J., HAMILTON, A. J., SADANANDOM, A. & MILNER, J. J. 2007. Cauliflower mosaic virus protein P6 is a suppressor of RNA silencing. *Journal of General Virology,* 88**,** 3439-3444.

LU, R., FOLIMONOV, A., SHINTAKU, M., LI, W.-X., FALK, B. W., DAWSON, W. O. & DING, S.-W. 2004. Three distinct suppressors of RNA silencing encoded by a 20-kb viral RNA genome. *Proceedings of the National Academy of Sciences of the United States of America,* 101.

MACROGEN 2008. Macrogen Sample Submission Guide. Online.

MAILLARD, P. V., CIAUDO, C., MARCHAIS, A., LI, Y., JAY, F., DING, S. W. & VOINNET, O. 2013. Antiviral RNA Interference in Mammalian Cells. *Science,* 342**,** 235-238.

MATTHEWS, R. E. F. 1992. *Fundamentals of Plant Virology,* San Diego, Academic Press Inc.

MATTS, R. L. & LONDON, I. M. 1984. The regulation of initiation of protein synthesis by phosphorylation of eIF-2(alpha) and the role of reversing factor in the recycling of eIF-2. *Journal of Biological Chemistry,* 259**,** 6708-6711.

MENZEL, W., JELKMANN, W. & MAISS, E. 2002. Detection of four apple viruses by multiplex RT-PCR assays with coamplification of plant mRNA as internal control. *Journal of Virological Methods,* 99**,** 81-92.

MEURS, E., CHONG, K., GALABRU, J., THOMAS, N. S. B., KERR, I. M., WILLIAMS, B. R. G. & HOVANESSIAN, A. G. 1990. Molecular cloning and characterization of the human double-stranded RNA-activated protein kinase induced by interferon. *Cell,* 62**,** 379-390.

MORGULIS, A., COULOURIS, G., RAYTSELIS, Y., MADDEN, T. L., AGARWALA, R. & SCHÄFFER, A. A. 2008. Database indexing for production MegaBLAST searches. *Bioinformatics,* 24**,** 1757-1764.

NAPOLI, C., LEMIEUX, C. & JORGENSEN, R. 1990. Introduction of a Chimeric Chalcone Synthase Gene into Petunia Results in Reversible Co-Suppression of Homologous Genes in trans. *The Plant Cell,* 2**,** 279-289.

O'NEILL, R. E. & RACANIELLO, V. R. 1989. Inhibition of translation in cells infected with a poliovirus 2Apro mutant correlates with phosphorylation of the alpha subunit of eucaryotic initiation factor 2. *Journal of Virology,* 63**,** 5069-5075.

OLLAND, A. M., JANE-VALBUENA, J., SCHIFF, L. A., NIBERT, M. L. & HARRISON, S. C. 2001. Structure of the reovirus outer capsid and dsRNA-binding protein [sigma]3 at 1.8 A resolution. *EMBO J,* 20**,** 979-989.

OLSEN, D. S., JORDAN, B., CHEN, D., WEK, R. C. & CAVENER, D. R. 1998. Isolation of the Gene Encoding the Drosophila melanogaster Homolog of the Saccharomyces cerevisiae GCN2 eIF-2α Kinase. *Genetics,* 149**,** 1495-1509.

PRUSS, G., GE, X., SHI, X. M., CARRINGTON, J. C. & VANCE, V. B. 1997. Plant Viral Synergism: The Potyviral Genome Encodes a Broad-Range Pathogenicity Enhancer That Transactivates Replication of Heterologous Viruses. *The Plant Cell,* 9**,** 859-868.

QIU, H., DONG, J., HU, C., FRANCKLYN, C. S. & HINNEBUSCH, A. G. 2001. The tRNA-binding moiety in GCN2 contains a dimerization domain that interacts with the kinase domain and is required for tRNA binding and kinase activation. *The*

EMBO Journal, 20**,** 1425-1438.
QIU, W., PARK, J.-W. & SCHOLTHOF, H. B. 2002. Tombusvirus P19-Mediated Suppression of Virus-Induced Gene Silencing Is Controlled by Genetic and Dosage Features That Influence Pathogenicity. *Molecular plant-microbe interactions,* 15**,** 269-280.
RATCLIFF, F., HARRISON, B. D. & BAULCOMBE, D. C. 1997. A Similarity Between Viral Defense and Gene Silencing in Plants. *Science,* 276**,** 1558-1560.
RATCLIFF, F. G., MACFARLANE, S. A. & BAULCOMBE, D. C. 1999. Gene Silencing without DNA: RNA-Mediated Cross-Protection between Viruses. *The Plant Cell Online,* 11**,** 1207-1215.
REDONDO, N., SANZ, M. A., WELNOWSKA, E. & CARRASCO, L. 2011. Translation without eIF2 Promoted by Poliovirus 2A Protease. *PLoS ONE,* 6**,** e25699.
RICE, G., TANG, L., STEDMAN, K., ROBERTO, F., SPUHLER, J., GILLITZER, E., JOHNSON, J. E., DOUGLAS, T. & YOUNG, M. 2004. The structure of a thermophilic archaeal virus shows a double-stranded DNA viral capsid type that spans all domains of life. *Proceedings of the National Academy of Sciences of the United States of America,* 101**,** 7716-7720.
ROMANO, N. & MACINO, G. 1992. Quelling: transient inactivation of gene expression in Neurospora crassa by transformation with homologous sequences. *Molecular Microbiology,* 6**,** 3343-3353.
ROTH, B. M., PRUSS, G. J. & VANCE, V. B. 2004. Plant viral suppressors of RNA silencing. *Virus Research,* 102**,** 97-108.
RYABOVA, L. A. & HOHN, T. 2000. Ribosome shunting in the cauliflower mosaic virus 35S RNA leader is a special case of reinitiation of translation functioning in plant and animal systems. *Genes and Development,* 14**,** 817-829.
SACRISTÁN, S., DÍAZ, M., FRAILE, A. & GARCÍA-ARENAL, F. 2011. Contact Transmission of Tobacco Mosaic Virus: a Quantitative Analysis of Parameters Relevant for Virus Evolution. *Journal of Virology,* 85**,** 4974-4981.
SAFER, B., ADAMS, S. L., ANDERSON, W. F. & MERRICK, W. C. 1975. Binding of MET-TRNAf and GTP to homogeneous initiation factor MP. *Journal of Biological Chemistry,* 250**,** 9076-9082.
SCHOLTHOF, H. B., SCHOLTHOF, K.-B. G., KIKKERT, M. & JACKSON, A. O. 1995. Tomato Bushy Stunt Virus Spread Is Regulated by Two Nested Genes That Function in Cell-to-Cell Movement and Host-Dependent Systemic Invasion. *Virology,* 213**,** 425-438.
SHARP, T. V., WITZEL, J. E. & JAGUS, R. 1997. Homologous Regions of the α Subunit of Eukaryotic Translational Initiation Factor 2 (eIF2α) and the Vaccinia Virus K3L Gene Product Interact with the Same Domain within the dsRNA-Activated Protein Kinase (PKR). *European Journal of Biochemistry,* 250**,** 85-91.
SEO, S., SETO, H., YAMAKAWA, H. & OHASHI, Y. 2001. Transient accumulation of jasmonic acid during the synchronised hypersensitive cell death in *Tobacco Mosaic Virus*-infected tobacco leaves. *The American Phytopathological Society,* 14, 261-254.
SILHAVY, D., MOLNAR, A., LUCIOLI, A., SZITTYA, G., HORNYIK, C., TAVAZZA, M. & BURGYAN, J. 2002a. A viral protein suppresses RNA silencing and binds silencing-generated, 21- to 25-nucleotide double-stranded RNAs. *EMBO J,* 21**,** 3070-3080.
SILHAVY, D., MOLNÁR, A., LUCIOLI, A., SZITTYA, G., HORNYIK, C., TAVAZZA,

M. & BURGYÁN, J. 2002b. A viral protein suppresses RNA silencing and binds silencing generated, 21 to 25 nucleotide double stranded RNAs. *The EMBO Journal,* 21**,** 3070-3080.
SIMOS, G., SEGREF, A., FASIOLO, F., HELLMUTH, K., SHEVCHENKO, A., MANN, M. & HURT, E. C. 1996. The yeast protein Arc1p binds to tRNA and functions as a cofactor for the methionyl- and glutamyl-tRNA synthetases. *The EMBO journal,* 15**,** 5437-5448.
TAKAHASHI, H. 2008. Study on interaction between Cucumber mosaic virus and host plants at a molecular level. *Journal of General Plant Pathology,* 74**,** 454-456.
TAKAHASHI, H., GOTO, N. & EHARA, Y. 1994. Hypersensitive response in cucumber mosaic virus-inoculated Arabidopsis thaliana. *The Plant Journal,* 6**,** 369-377.
TAKEDA, A., SUGIYAMA, K., NAGANO, H., MORI, M., KAIDO, M., MISE, K., TSUDA, S. & OKUNO, T. 2002. Identification of a novel RNA silencing suppressor, NSs protein of Tomato spotted wilt virus. *FEBS Letters,* 532.
TANG, G., REINHART, B. J., BARTEL, D. P. & ZAMORE, P. D. 2003. A biochemical framework for RNA silencing in plants. *Genes & Development,* 17**,** 49-63.
TANG, J. Z. B. 2006. *Is Protein Kinase R Involved in RNA silencing?* Master of Science, University of Auckland.
TANG, W. & LEISNER, S. M. 1997. Cauliflower Mosaic Virus Isolate NY8153 Breaks Resistance in Arabidopsis Ecotype En-2. *Phytopathology,* 87**,** 792-798.
THIMMAPPAYA, B., WEINBERGER, C., SCHNEIDER, R. J. & SHENK, T. 1982. Adenovirus VAI RNA is required for efficient translation of viral mRNAs at late times after infection. *Cell,* 31**,** 543-551.
TOMARI, Y., MATRANGA, C., HALEY, B., MARTINEZ, N. & ZAMORE, P. D. 2004. A Protein Sensor for siRNA Asymmetry. *Science,* 306**,** 1377-1380.
UNTERGASSER, A., CUTCUTACHE, I., KORESSAAR, T., YE, J., FAIRCLOTH, B. C., REMM, M. & ROZEN, S. G. 2012. Primer3—new capabilities and interfaces. *Nucleic Acids Research,* 40**,** e115.
VANCE, V. & VAUCHERET, H. 2001. RNA Silencing in Plants-Defense and Counterdefense. *Science,* 292**,** 2277-2280.
VARGASON, J. M., SZITTYA, G., BURGYÁN, J. & HALL, T. M. T. 2003. Size Selective Recognition of siRNA by an RNA Silencing Suppressor. *Cell,* 115**,** 799-811.
VAZQUEZ, F., VAUCHERET, H., RAJAGOPALAN, R., LEPERS, C., GASCIOLLI, V., MALLORY, A. C., HILBERT, J.-L., BARTEL, D. P. & CRETE, P. 2004. Endogenous *trans*-Acting siRNAs Regulate the Accumulation of *Arabidopsis* mRNAs *Molecular Cell,* 16**,** 69-79.
VOGLER, H., AKBERGENOV, R., SHIVAPRASAD, P. V., DANG, V., FASLER, M., KWON, M.-O., ZHANYBEKOVA, S., HOHN, T. & HEINLEIN, M. 2007. Modification of Small RNAs Associated with Suppression of RNA Silencing by Tobamovirus Replicase Protein. *Journal of Virology,* 81**,** 10379-10388.
VOINNET, O. 2001. RNA silencing as a plant immune system against viruses. *Trends in Genetics,* 17**,** 449-459.
VOINNET, O., LEDERER, C. & BAULCOMBE, D. C. 2000. A Viral Movement Protein Prevents Spread of the Gene Silencing Signal in Nicotiana benthamiana. *Cell,* 103**,** 157-167.
VOINNET, O., PINTO, Y. M. & BAULCOMBE, D. C. 1999. Suppression of gene silencing: A general strategy used by diverse DNA and RNA viruses of plants. *Proceedings of the National Academy of Sciences,* 96**,** 14147-14152.

WANG, L.-Y., LIN, S.-S., HUNG, T.-H., LI, T.-K., LIN, N.-C. & SHEN, T.-L. 2012. Multiple Domains of the Tobacco mosaic virus p126 Protein Can Independently Suppress Local and Systemic RNA Silencing. *Molecular Plant-Microbe Interactions,* 25**,** 648-657.

WARGELIUS, A., ELLINGSEN, S. & FJOSE, A. 1999. Double–Stranded RNA Induces Specific Developmental Defects in Zebrafish Embryos. *Biochemical and Biophysical Research Communications,* 263**,** 156-161.

WOOD, E. J. 1992. Molecular biology labfax: Edited by T A Brown. pp 322. Bios Scientific/Blackwells, Oxford. 1991. £21.95 (spiral, layflat) ISBN 1-872748-00-7. *Biochemical Education,* 20**,** 29-29.

WU, S. & KAUFMAN, R. J. 1997. A Model for the Double-stranded RNA (dsRNA)-dependent Dimerization and Activation of the dsRNA-activated Protein Kinase PKR. *Journal of Biological Chemistry,* 272**,** 1291-1296.

YAMAMOTO, M., MARUYAMA, D., ENDO, T. & NISHIKAWA, S.-I. 2008. Arabidopsis thaliana Has a Set of J Proteins in the Endoplasmic Reticulum that are Conserved from Yeast to Animals and Plants. *Plant and Cell Physiology,* 49**,** 1547-1562.

YANG, W. & HINNEBUSCH, A. G. 1996. Identification of a regulatory subcomplex in the guanine nucleotide exchange factor eIF2B that mediates inhibition by phosphorylated eIF2. *Molecular and Cellular Biology,* 16**,** 6603-16.

YE, K., MALININA, L. & PATEL, D. J. 2003. Recognition of small interfering RNA by a viral suppressor of RNA silencing. *Nature,* 426**,** 874-878.

YELINA, N. E., SAVENKOV, E. I., SOLOVYEV, A. G., MOROZOV, S. Y. & VALKONEN, J. P. T. 2002. Long-Distance Movement, Virulence, and RNA Silencing Suppression Controlled by a Single Protein in Hordei- and Potyviruses: Complementary Functions between Virus Families. *Journal of Virology,* 76**,** 12981-12991.

YOO, C. J. & WOLIN, S. L. 1994. La proteins from Drosophila melanogaster and Saccharomyces cerevisiae: a yeast homolog of the La autoantigen is dispensable for growth. *Molecular and Cellular Biology,* 14**,** 5412-5424.

ZAMORE, P. D., TUSCHL, T., SHARP, P. A. & BARTEL, D. P. 2000. RNAi: Double-Stranded RNA Directs the ATP-Dependent Cleavage of mRNA at 21 to 23 Nucleotide Intervals. *Cell,* 101**,** 25-33.